Norwegian University of Life Sciences
Department of mathematical sciences and technology (IMT)

Master Thesis 2014
30 credits

PV system design and production simulations for Mully Children´s Family Yatta, Kenya

Ragnhild Tjore

Preface

Several years of studying is coming to an end. It has been a rollercoaster of emotions!

When getting the opportunity to take part in this project I never hesitated about my decision. After years of studying, the possibility to get hands on experience seemed like both an exciting, and challenging opportunity. A months field work is not a long time, but it thought me much about the process of implementing new technologies, especially the importance of using a bottom-up approach, meaning that solutions has to be found by listening to the users, and develop a project together instead of presenting an already finished proposal. I would like to thank Eirik Eid Hohle at Energigården for letting me be part of this project, and for arranging a field trip to Kenya. I also would especially like to thank my supervisor Petter H. Heyerdahl who introduced me to the topic in the first place. Thank you for your support and guidance during the work with this thesis.

Further I want to thank Andreas Tutturen, Ioannis Georgiadis and Petter D. Jenssen for their good company and support during the field trip to Kenya.

A big thanks to all the people that helped us during our stay: To Joshua Nyalita at Mully´s Children Family for providing us with all the information about Yatta. To Paul Mbole and Kirsten Engebakk at the Norwegian Church Aid in Nairobi for their valuable inputs on our work, and for arranging meetings and workshops. Further I want to thank Dr. Charles M. Mulli for letting us stay at and learn to know MCF and the great work they are doing.

Finally I want to thank all my fellow students who made the years of studying so enjoyable.

A special thanks goes to my mum, dad and Anders for your invaluable support, corrections, and discussions during this period. I couldn't have done this without you.

Bergen, 22.12.2014

Ragnhild Tjore

Abstract

The purpose of this thesis is to evaluate the potential and economic feasibility of the establishment of a grid-connected photovoltaic system (PV system) at Mully Children´s Family, Kenya. The energy demand of the farm is estimated to be around 230 MWh per year, with an average power load of about 30kW. This is currently covered with electricity supplied from the grid, and a diesel generator that is used during power outages. The last few years, grid-connected PV systems have become more attractive due to reduced costs and increased electricity prices.

The system is sized by power, with a system production that is kept below the local consumption due to the lack of purchase agreements for feeding surplus energy to the grid. Because of the farm´s size, the PV system´s required area has not been considered a limitation.

The available solar resources have been investigated using six different databases with solar irradiance data based on satellite measurements. Yearly global irradiation is assumed to be between 1482-2033 kWh/m^2. The meteorological data is the most uncertain factor affecting the expected yearly system production.

A base case was used to perform a sensitivity analysis for the system by changing the input parameters during simulations. The irradiation data and the orientation of the array had the greatest impact on the system output. The greatest system losses were caused by high temperatures (array losses between 3.8-6,7%). The CIS thin-film module gave the highest nominal production, at 4.44kWh/kWp pr. day, while the lowest production was estimated at 3.61 kWh/kWp pr.day. A PV system with an installed power of 50kWp (peak power) will thus have an expected nominal production of about 65.9-81.0 MWh per year. This accounts to around 29-35% of the yearly energy consumption at the farm. If the system is oriented both east- and westward the daily production will even out, and the probability of producing excess energy reduced. To reduce the vulnerability of the PV system due to shading or damaged modules it is recommended to use either string or multi-string inverters although this will increase the cost of the system. This will also make the system easier to expand in the future when systems for net-metering are put in use.

According to the performed economic analysis, the levelized cost of energy (LCOE) for a system of 50kWp is between 0.16-0.24 euro/kWh depending on installation costs. The installation costs and the type of financing are crucial for the profitability of the system.

Samandrag

Formålet med denne masteroppgåva er å undersøkje potensialet og lønsemda ved å dekke delar av dagens energiforbruk på Mully Children´s Family, Kenya ved å etablere eit fotovoltaisk anlegg (PV anlegg) tilknytt det eksisterande nettet. Energibruken per i dag er estimert til om lag 230 MWh årleg, og det gjennomsnittlege effektbehovet er estimert til om lag 30kW. Dette blir i dag dekka av elektrisitet frå det lokale nettet og ein dieselgenerator som er nytta ved straumbrot.

Dei siste åra har nettilknytte PV anlegg blitt meir attraktive grunna reduserte kostnader og auka elektrisitetsprisar i Kenya. Det er ikkje sett eit avgrensing på arealbruken til anlegget, og anlegget er dimensjonert ut i frå forbruk. På grunn av manglande ordningar for innmating av elektrisitet på nettet, er anlegget dimensjonert slik at produksjonen er mindre enn forbruket.

Ressursgrunnlag er undersøkt frå seks ulike databasar med solinnstrålingsverdiar kalkulert frå satellittdata. Årleg global innstråling er venta å vere i området 1482-2033 kWh/m^2 pr år. Estimeterte meteorologiske data er og den mest usikre faktoren knytt til årleg forventa produksjon frå eit PV anlegget.

Eit «base case» med faste variablar vart nytta for å utføre ei sensitivitetsanalyse for systemet ved endring av dei ulike parametrane. Dei simuleringsvariablane som hadde størst påverknad på systemet, var strålingdataene og orienteringa til panela. Det største systemtapet var tap i panela ved høge temperaturar (tap mellom 3.8-6,7%). Simulering med CIS tynn-film modular gav den høgste spesifikke produksjonen. Resultata viser at forventa årleg spesifikk produksjon er mellom 3.61-4.44 kWh/kWp per dag. Eit anlegg med ein installert effekt på 50kWp vil produsere mellom 65.9-81.0 MWh årleg. Dette tilsvarer om lag 29-35% av det årleg forbruket. Ved å ha ei aust- og vestvendt orientering av PV systemet vil den daglege produksjonen jamnast ut, og sannsynet for å produsere overskotssenergi vert redusert. For enkelt å kunne utvide systemet, og for å avgrense effekten av tap på grunn av skugging eller øydelagte modular er det tilrådd å nytte anten streng- eller multistrengvekselrettarar. Dette vil auke kostnaden, men gjere det enklare å gjennomføre ei framtidig utviding av systemet når ordninga for bruk av nettmålarar (net metering) startar opp.

Det er og utført ei kostnads- og lønnsemdsanalyse for systemet. LCOE-berekningar (Levelized Cost of Energy) viser at eit system på 50kWp har ein LCOE mellom 0.16-0.24 euro/kWh, avhengig av installasjonskosnadane. Desse, saman med finansieringa av systemet, vil vere avgjerande for om systemet er lønsamt eller ikkje.

Table of contents

List of figures

List of tables

Abbreviations

Notation	Meaning
ASTM	American Society for Testing and Materials
AM	Air Mass ratio
DHI	Diffuse Horizontal Irradiation
DLR	Deutsches Zentrum für Luft- und Raumfahrt
DNI	Direct Normal Irradiation
FIT	Feed-in tariff
GHI	Global Horizontal Irradiation
GTZ (now GIZ)	Deutsche Gesellschaft für Technische Zusammenarbeit
GIZ	Deutsche Gesellschaft für Internationale Zusammenarbeit
HRA	Hour Angle
IEC	International Electrotechnical Commission
ITCZ	Inter Tropical Convergence Zone
LCOE	Levelized Cost Of Energy
MPP	Maximum power point
RES	Renewable Energy Source
RES-E	Renewable Energy Sources Generated Electricity
SHS	Solar home system
SWERA	Solar and Wind Energy Resource Assessment
PV	Photovoltaic
STC	Standard Test Conditions (1000W/m2, 25, AM1.5)
UNEP	United Nations Environment Programme

Nomenclature

Letter	Description	Unit
B	Direct beam radiation on a horizontal plane	W/m^2
D	Diffuse radiation on a horizontal plane	W/m^2
R	Reflected radiation on a horizontal plane	W/m^2
S	Solar constant	W/m^2
β	Panel inclination to the horizontal plane	°
α	Solar elevation	°
δ	Solar declination	°
φ	Geographical latitude	°
ω	Hour angle	°
γ	Azimuth angle	°
θ_z	Zenith angle	°
A	Albedo	
h	Planck´s constant	eVs
v	Frequency of light	s^{-1}
λ	wavelength	μm

1 Introduction

1.1 Background

The world population recently exceeded 7 billion people. In 2011, out of these 7 billion, nearly 1.3 billion people were without access to electricity, and more than 2.6 billion lacked other options for cooking than the use of traditional biomass. Over 95% of these people live in areas in either sub-Saharan Africa or in Asia, and 84% live in rural, remote areas. The last 30 years the growth in access to electricity has been more or less equal to population growth [1].

Electricity is one of the driving forces for economic development. The challenge to meet the growing demand is difficult for both developed and developing countries alike. For people in rural areas the cost of electricity is often high and inaccessible due to the high cost of energy infrastructure[2]. Decentralized energy systems are often based on renewable energy sources, can operate both on- and off-grid, and focuses on meeting the local demand [3]. A grid connected system can feed the surplus power to the grid, eliminating the need of batteries for storage.

Access to energy is more than just having an electrical connection. It is about the quality and reliability of the service, and the economical availability of the system. An even greater barrier to overcome can be the changing of people's habits. An essential question to arise in the study of potential substitutes is therefore how one can accommodate the changes so that people are willing to change their known energy patterns, both on the household and agricultural level [4].

Renewable energy resources that are locally available can reduce the amount of imported oil and gas, making a country less vulnerable to changes in oil prices. There is without doubt a global urgency for social and technological changes to reduce poverty, adapt to climate change and create a clean energy future.

In Kenya, the majority of the rural energy household need is covered by biomass. Around 15- 20% of the population has access to electricity, with a rural rate of only 5-10%. Out of the population without access, 83% rely on traditional biomass for cooking [5, 6].

Solar energy is the most abundant energy resource on earth. The total energy reaching the surface each year is well over 1000 times higher than the total global energy consumption [7]. In Kenya, according to a study conducted by DLR [8] the average daily insolation is about 4-6 kWh/m^2. Figure 1.1 shows the geographical distribution of average daily horizontal irradiation in Kenya in for the year 2002.

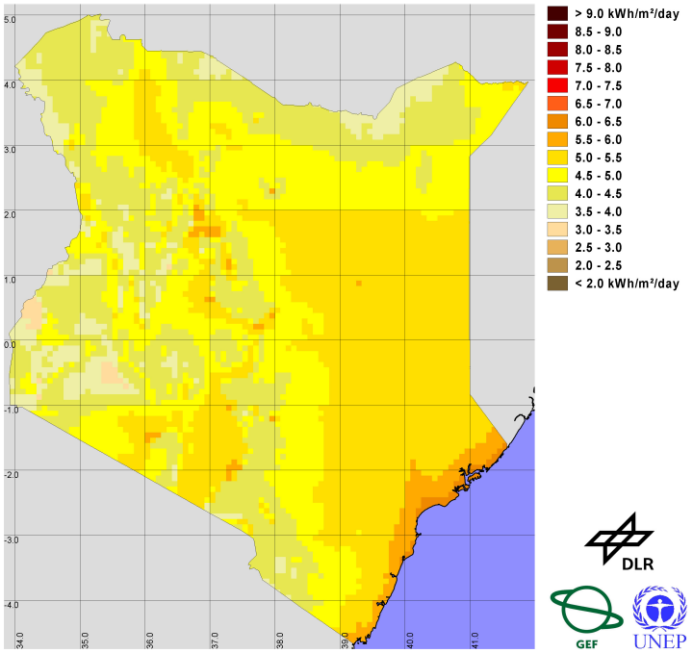

Figure 1.1 Average daily sum of global horizontal irradiance for Kenya, 2002. From [8].

One of the main challenges with the use of solar energy is its variability. There is often a mismatch between the incoming irradiance and energy need, both on a daily and seasonal basis. On a daily basis this can be solved using temporary storage, or grid connected systems feeding the excess energy into the grid.

Good resource data is essential to make better use of variable, renewable energy resources. This is important both for the dimensioning of the solar system, and to evaluate if a project is economically feasible. In Kenya, it has turned out to be difficult to retrieve data from the meteorological ground stations on irradiance. While temperature data was available for a short period of time, the irradiance data was incomplete and difficult to make use of. The solution was to use estimated data based on satellite images.

The world solar energy market is fast expanding. In the last four years, the new added photovoltaic (PV) capacity has been greater than in the previous four decades. Prices of PV systems have been reduced by a factor of three during the last six years, and modules by a factor of five. Several countries, such as Germany, Italy and Australia reached grid parity in 2013 [9]. Solar PV development in Kenya has mainly been driven by efforts of the government to increase rural electrification, and while solar home systems (SHS) and small pico-systems (solar chargers, lanterns etc.) are common in Kenya, grid connected PV systems are not [10]. In 2013, according to Tobias Gossen of GIZ, the total installed solar capacity was 20MWp (divided between off- and on-grid systems) [11].However, recent studies suggest that grid-connected PV systems are becoming more attractive and may already have price levels competitive with the more expensive conventional power plants and can be a feasible option for small-scale power production in developing countries [11, 12].

1.2 Earlier studies

The Solar and Wind Energy Resource Assessment project (SWERA) is a study supported by UNEP, in among other countries Kenya, based on data from the geostationary satellite Meteosat 7 [8, 13]. Meteosat 7 is located at an orbit at 0° latitude and 0° longitude. A high resolution study for the years 2000-2002 have estimated an average daily global horizontal irradiation (GHI) of between 4-6 kWh/m^2, and an average daily direct normal irradiation (DNI) around 4 kWh/m^2. The DNI and GHI data are given at a 10km spatial resolution. The project also provides hourly time series of irradiation for several locations in Kenya. Among these is Thika weather station, located at a distance roughly 50 km from Yatta (and with an altitude difference of around 250m).

There is limited available information on grid-connected PV systems in Kenya. Three similar plants have been used to gain knowledge, and serves as examples and for comparison with the simulated system [14-17]. The plants are

- 60 kWp plant at SOS Children´s village in Mombasa
- 515 kWp plant at UNEP in Nairobi
- 10 kWp plant at Strathmore University in Nairobi
- 72 kWp plant at Uhuru flower farm

where kWp stands for the peak production of the PV system

Ondraczek [12] presents the economics of PV systems in developing countries and argues that the Levelized Cost of Energy (LCOE) of grid-connected PV may already be competitive compared to costly power plants such as diesel generators. Details and hands-on experiences from this study and the plants above are useful for both the design and investment analysis of a potential PV system at Yatta. The report by Georg Hille et al. [6] studies the implementation of a net metering system in Kenya.

A previous master thesis by Tutturen [18] on the use of biomass for charcoal production and power generation at MCF Yatta. The thesis by Tutturen shares much of the same results as this paper regarding the estimated energy demand due to the shared fieldwork.

1.3 Scope

In 2011, the Norwegian Church Aid Kenya finalized a project proposal together with Mully's Children Family (MCF) Yatta, Kenya and Energigården (EG), Norway. The project goal is to "Promote learning and enable replication of 'Best Practices' in the area of renewable energy, energy efficiency and adaptation to climate change for energy poor and climate vulnerable communities in Kenya and beyond." This thesis is part of the ongoing collaboration and in February 2013, a field study was conducted together with two fellow students that focused on the biogas and biomass potential at the farm. This thesis is a feasibility study of the solar energy potential at MCF Yatta, with a focus on grid-connected PV systems.

Today, MCF Yatta is connected to the national electricity grid. A local, decentralized production of electricity will substitute part of today´s electricity purchase. In addition to the solar resource base and potential technologies and use, it is therefore relevant to look at the cost of a potential solar energy system compared to today's cost of electricity.

Being introduced to this project has been a great opportunity to study and analyze the possibility to implement a renewable energy system in a defined area. The focus of the field work, in addition to and equally important as mapping the available resources and current energy use was to get to know the organization, the farm and those who live and

work there. Keeping the social aspect in mind, this thesis will of course have a more technical approach.

Questions that will be attempted answered are: “What are the available solar irradiation data for the location, and what is the potential energy resource?” “What is the potential energy production from an optimized PV system?” “How can the production best fit the current consumption?” and “How is the economic feasibility of the system”?

1.4 Structure

Chapter 1 gives the necessary background and scope for the thesis. In chapter 2 the data collected during the field study is described and analyzed. Current demand of electric energy at MCF Yatta is evaluated.

Chapter 3 describes the theory and method behind the evaluation of available solar resources and climatic conditions in Kenya in general and at MCF Yatta specifically. In chapter 4, appropriate solar cell technologies and components of a PV system are presented.

Chapter 5 explains the theory and method behind the evaluation of the climatic data, the simulation of a PV system and the economic analysis. The assumptions and methods used for the dimensioning and simulation using PVsyst are described.

Chapter 6 presents the results and discussion of the simulated systems, the climate data and the economic cost. Chapter 7 discusses different options, and presents a possible PV system based on the previous chapters. The last chapter also recommends further work.

2 Field study

2.1 Current energy situation in Kenya

Kenya being astride the equator receives a considerable amount of solar radiation, but only a small rate of the country's electricity production comes from solar energy.

In 2012 the total electricity production in Kenya was divided as shown in the figure 2.1 below [19]. As illustrated almost ¾ of the total production was from renewable energy sources, mainly hydro and geothermal power. The country is also heavily dependent on imported petroleum for industrial need. From 2011 to 2012 there was a reduction in power generated by fossil fuels from 36,5% to 26,9% due to an increase in the hydro electric power production. Included in the electricity price is an inflation rate and a fuel cost charge, making the rate depend on current oil prices. As a result, when the hydroelectric production is low, a greater share of the power production is from fossil power plants thus increasing the fuel cost. In 2013, according to Tobias Gossen of GIZ, the total installed solar capacity was 20MWp [11].

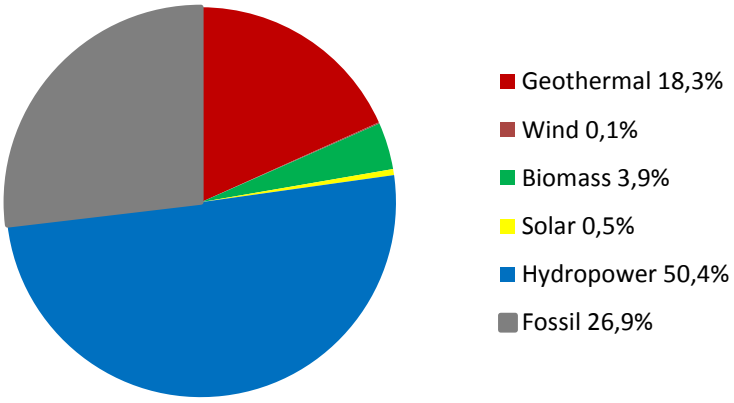

Figure 2.1 Share of total electricity production in Kenya in 2012.Based on data from Observ'ER [19]

Several policies and strategies have been introduced to promote the use of renewable energy resources in the later years, but literature regarding the effects is lacking. Feed in tariffs (FITs) were first introduced in Kenya in March 2008, and a first revision was carried out in January 2010. New tariffs for Solar energy was then included, but at this moment the FIT only applies to "individual solar power plants whose effective generation

capacity are equal to or more than 500kW and does not exceed 10MW" [20]. There is also tax rebates on solar panels and equipment, and it is also mandatory for all new buildings to install solar heaters [21]. Net metering was introduced in the end of 2012, but the regulatory framework has not been completed[11]. For Kenya, increasing the use of renewable energy sources such as solar, hydro and geothermal will reduce the dependence on imported fuel, enhance energy security and give more stable electricity prices.

2.2 Field study in Kenya

As part of this thesis, a field study was carried out in Kenya in February, 2013.

The field trip lasted four weeks and its objective can roughly be divided in two,

1) To get to know the organization and its actors. This was crucial to achieve a better understanding of their work, and to learn about their needs and interests concerning the implementation of new energy technologies at the farm. During our stay we had several meetings with key people from both MCF and NCA. Other relevant agencies and local sites were also visited.

2) Collection of data, both of the current energy use and mapping of the resource base. Available meteorological data from nearby stations was gathered.

The first week of the trip was spent getting to know key people in both MCF and NCA, and how MCF carries out its work. At Yatta we gathered information through the collection of raw data and through discussions with the head of the agricultural department, Joshua Nyalita. He also contributed with valuable inputs to our project, and with possible solutions. Towards the end of our stay a seminar was held to discuss different solutions with the partners, and to together discuss possible project outcomes.

Since the aim of this thesis is to analysis the potential use of solar energy at MCF Yatta, the daily use of firewood for cooking is not included in the energy demand analysis. One can argue that this could be covered by either solar cookers or electricity from a PV system, but the impression we were left with after our field study was that the wish was to continue to use biomass for cooking, but with more efficient stoves. Fuel used for

transportation is left out as it is not realistic to cover this using solar energy. For this reason the energy use is divided between the consumption of electricity and hot water.

During the field work we experienced some smaller issues due to cultural differences. A small experiment was set up to do electricity readings during several days to map how the power load varies throughout the day. But because of misunderstandings between the electrician and us, we ended up doing the reading ourselves, and only managed to get readings for one day. We also got the impression that people would rather give a wrong answer than no answer at all. As a result we had to ask several times for the same numbers to validate our numbers.

2.2.1 A socio-technological approach

According to a research by Ulsrud [22] on solar mini-grids in India, the importance of using a combined social and technical approach is crucial when it comes to creating good, lasting energy systems. The social and technical sides of the systems are mutually dependent, and equally important. According to this study the technology cannot be seen without its social context; meaning for instance the social values, its institutions, the expected usefulness of the system, and the competences of the society.

Some common barriers for the implementation of rural energy systems has been summarized in an analysis by Hirmer and Cruickshank [23] and are;

- Financial: High upfront cost; lack of capital; dependency on subsidies.
- Infrastructure: Remote locations lacking infrastructure and other market-based factors (e.g. competition).
- Technical: Low technical skill levels and access to quality materials/products
- Social: Lack of local ownership and acceptance

This study also underlines the importance of local ownership to enhance the sustainability of community operated rural electrification schemes. The local ownership is influenced by (amongst other) user training, financial contributions, and community involvement.

Barriers also exists at the institutional- and policy levels. The national policies and strategies for the implementation of rural, renewable energy services are crucial both when it comes to the financing and the management of the projects[4]

In their research, Müggenburg et al. [24] states that the approach should be human-oriented, and technology should be chosen from peoples need, and not simply from a technical point of view. Therefore it is important to involve the end users early on in the processes. Using this socio-technological approach the social acceptance can be divided into two contributing parts; the technological functioning and the societal impact and needs of the user.

Since this is a master thesis within the natural sciences, a technological approach is used. However, during the meetings with the cooperating organizations (MCF and NCA) the social context was discussed, and the socio-technological approach was highly relevant during the field study.

2.3 MCF Yatta

MCF Yatta is located in the Yatta district in Machakos County in Kenya (coordinates -1.11, 37.36) and the altitude is 1300m. There are currently 350 girls and children residing at MCF Yatta. In total there are 80 staff members working with the children. Out of these, 60 also live at the farm. In addition, 15 people work in the office building. There are also seasonal agricultural workers (varying in number). There are two workers camps. One with 15-20 residents and the other has 50 residents. Only the first camp has a grid connection.

MCF is a children's charity that manages residential homes for orphaned and vulnerable children. MCF was founded in 1989 by Ev. Dr. Charles M. Mulli, and is a non-governmental organization. MCF provides the children the necessary education to be active, contributing members in the community. The programs at MCF consist of registered learning and training centers, sustainability agricultural projects, environmental conservation and development projects especially in relation to climate change mitigation and adaptation. They also support community education and development initiatives [25].

Figure 2.2 MCF Yatta Photo: A. Tutturen

The environmental conservation and development projects include the establishment of an Eco-Village and Environmental development programme focusing on the implementation of green energy technology and the promotion of renewable energy infrastructure, both within MCF and at community level. At MCF Yatta the plan is to establish a learning, research and demonstration center focusing on the development of various renewable energy resources such as solar, biomass and biogas.

Figure 2.3 presents a map of the site with a possible location for a solar power plant. The building A (with a flat roof) could also serve as a good alternative.

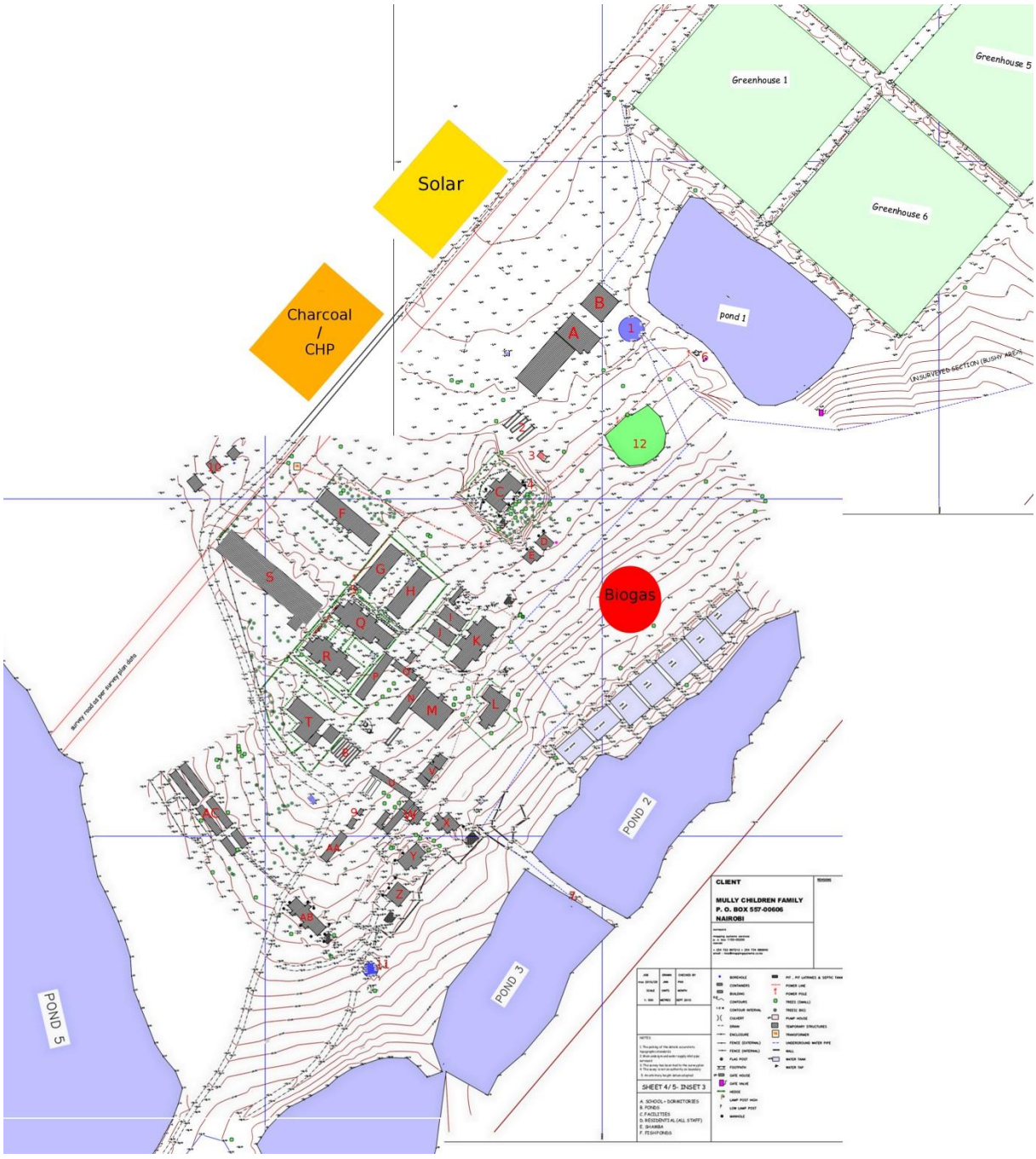

Figure 2.3 Map of MCF Yatta From Tutturen [18]

2.4 Electricity demand

For the current energy use at MCF Yatta, data was gathered on all the major electrical components in use at the farm such as pumps, cooling systems, etc. Also, from discussions with operating personnel, data was collected of when and for how long the different machinery was in use every day. This, of course, also varies throughout the year;

therefore previous electricity bills were collected to try to make an overview of when the electricity consumption is at its highest.

Initially the plan was to make detailed power load curves for the different buildings, but since the use is fairly irregular this was not possible. As mentioned, ideally this should have been based on readings from several days, but it still gives a realistic picture of the daily load. Also, a day without a black out would have been preferred.

All equipment below a limit of around 1kW was not considered individually but as part of the total load from electricity readings. It is important to bear in mind that these numbers are *estimates* based on collected data, interviews and literature, and *not* exact numbers.

2.4.1 Estimated energy demand

There are three meters that measure the consumption at MCF Yatta; the north, middle and south meter. A list of the main equipment connected to each meter is shown in table 2.1. Estimates of consumed kWh/day are based on our own measurements, data collection and conversations with residents. Roughly divided the north meter measure the electricity consumption related to irrigation, the middle meter the cold room, and the south meter measure the electricity consumed by the pump located at the fish dam, transporting water from the dam to the tank. Connected to the south meter is also the tools used by the students in the workshops.

The consumption in the dormitories, staff housing and dispensary are not included due to the inaccuracy of the mapping of smaller equipment. The water pump located at the south meter is also used for irrigating a small field, and to pump water to the poultry house. Also note that only one pump is used at a time for irrigation purposes.

Table 2.1 Overview of the different electricity meters and estimated daily consumption and power load (electricity consuming equipment)

	Equipment	Number	Power (kW)	Max power (kW)	Running hours/day	kWh /day
MIDDLE METER						
Cold room	Compressor	1	10,8	10,8	4,8	51,8
	Indoor and outdoor fans	9	0,62-0,7	6,0	4,8	28,7
Pack room	Fans	11	0,1	1,1	24,0	26,4
NORTH METER						
Offices	Computer, lighting, etc.		NA	NA		NA
Irrigation room	Irrigation pump	2	18,5	18,5		
	Misty pump	1	7,5	7,5		
	Fertilizer mixer	3	0,75	2,3	10,0	94,2
Borehole north		1	2,0	2,0	12,0	24,0
SOUTH METER						
Computer lab & practical training	Computer	19	0,3-0,5	9,5	4,0	38,0
	Hairblower	5	1,0	5,0	4,0	20,0
	Welder	2	26,0 & 8,2	34,2	4,0	136,8
	Drill	1	6,5	6,5	4,0	26,0
Borehole south		1	2,0	2,0		NA
Pump house	Pump	1	15,0	15,0	4,0-8,0	90,0
GRAND TOTAL						***536 kWh/day***

Using estimated running times the daily consumption is 536 kWh, giving an annual consumption of 195604 kWh, not including lights, computers, water heaters etc. (as mentioned above).

The power consumption at MCF Yatta based on meter readings and electricity bills between 02.05.2011 – 01.03.2013 is summarized in table 2.2. From these, the average annual and daily consumption is estimated. The middle meter lacked data before 14.02.2013. An electricity bill from 25.05.2012 suggests that the meter has been replaced; therefore no values are available prior to this date.

Table 2.2 Power Energy consumption based on meter readings and electricity bills.

Date	South meter (kWh)	Middle meter (kWh)	North meter (kWh)
02.05.2011		NA	
30.05.2011	17887	NA	5668
25.06.2011	23302	NA	10363
27.07.2011	28717	NA	15058
25.08.2011	37215	NA	20854
30.09.2011	42315	NA	25662
29.10.2011	50352	NA	32516
01.12.2011	56649	NA	NA
25.05.2012	93588	914	76039
30.08.2012	109345	914	91888
27.09.2012	123640	NA	105461
14.02.2013	150099	30400	135432
01.03.2013	153354	32331	140437
	267,3 kWh/day	**128,7 kWh/day**	**227,6 kWh/day**

Table 2.2 gives an average daily consumption of 624 kWh. The period between 02.05.2011 – 01.03.2013 yields an annual average around 227600 kWh. Compared to table 2.1, the meter readings yield a higher consumption corresponding well with the fact that table 2.1 has left out part of the electric equipment in use.

It is likely to assume that the consumption of electricity will be somewhat higher during the dry season (mid-June to early October) because of increased need of irrigation.

Based on table 2.3, the average power load is calculated for the farm. Studying this table one notes that the average power load rarely exceeds 30 kW.

Table 2.3 Average estimated power load based on meter readings and electricity bills

	South meter	Middle meter	North meter
Date	kW	kW	kW
30.05.2011	26,6	NA	8,4
25.06.2011	8,7	NA	7,5
27.07.2011	7,1	NA	6,1
25.08.2011	12,2	NA	8,3
30.09.2011	5,9	NA	5,6
29.10.2011	11,5	NA	9,8
01.12.2011	8,0	NA	NA
25.05.2012	8,7	NA	8,7
30.08.2012	6,8	NA	6,8
27.09.2012	21,3	NA	20,2
14.02.2013	7,9	7,3	8,9
01.03.2013	9,0	5,4	13,9
Average kW	11,1	6,3	9,5

In addition to electricity supplied from the grid, there is a diesel generator in use for whenever a blackout occurs. According to the manager this is likely to happen several times a month.

2.4.2 Daily variation

During the field study electricity readings was carried out. The result is presented in figure 2.4. Due to a blackout in the middle of the day the figure makes a dip around 14:00. Missing data has been interpolated, and figure 2.5 shows how the day is assumed to look like without a blackout.

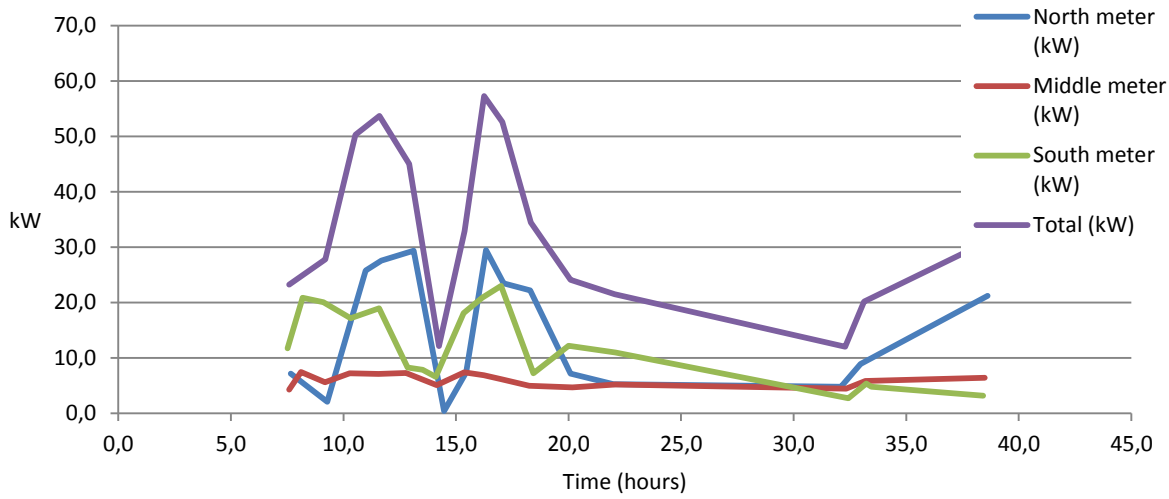

Figure 2.4 Hourly readings during the 27th and 28th of February (dry season). The 27th starts on hour 0, and the 28th on hour 24.

Readings from the south meter indicates that when the dam pump is running and filling the tank the power load is around 20kW. When the pump is used for irrigation purposes or not at all, electricity readings suggest that the average power load is around 5kW (as shown in figure 2.5)

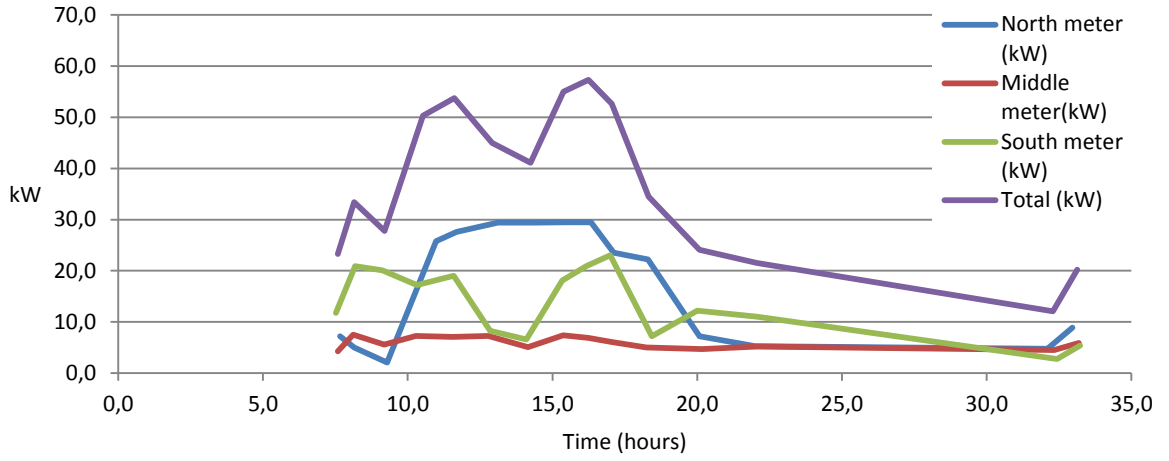

Figure 2.5 Hourly readings during the 27th and 28th of February with two corrected values. The 27th starts on hour 0, and the 28th on hour 24.

During both days, the dispensary was not in use except from a few light bulbs and a small refrigerator. The only consumed electricity in addition to the cooling room was therefore two refrigerators, a computed, some lights and hot water. Figure 2.5 also shows a dip

around 15hrs, but this is due to a lunch break giving reduced electricity consumption at the central meter.

2.5 The transformer at MCF Yatta

MCF Yatta is connected to the grid by a transformer, as shown in figure 2.6. The transformer only serves this property.

The transformer has the following properties:

- 200 kVA
- 11 kV high voltage
- 433V / 250 V low voltage
- 10.4-266.6 A rated current
- 50 Hz frequency

Figure 2.6The transformer at MCF Yatta Photo: R.Tjore

2.6 Consumption of hot water

Per today there are no solar heaters installed at MCF Yatta. An estimate is therefore carried out of the energy need if all the residents where to have hot showers every day, as there was a desire to establish such as system.

The following assumptions are made:

- Everyone showers 1,2 times/day (It is compulsory to shower every morning)
- Every shower lasts 5 – 10 min
- Water-saving shower with a capacity of 6-10 liters/min [26]
- Average ambient temperature is 20 degrees
- In total 410 residents (350 children, 60 staff members)
- Shower temperature is 37 degrees

Taking these assumptions into account the daily energy need for hot water is:

$$m = 1{,}2\ showers * (5-10)\frac{min}{shower} * \ 6-10\ l/\min = 14760-49200\ l/day$$

$$Q = m * C_p * \Delta T$$

$$Q = (14760-49200)kg * 4183 J/kg\ K * (40-20)K$$

$$Q = 292-972\frac{kWh}{day} = 107\text{-}355\ \text{MWh/year}$$

Because the number of showers per day, time per shower and the assumption that the water in the tank is never below 20° all are uncertain estimates, the total daily energy need for hot water is not very accurate. The study by Tutturen [18] estimated a yearly energy need from 45 MWh to 540 MWh for the same purpose. This shows the uncertainty linked to the data, and how the different variables affect the result.

3 Resource Assessment

Although irradiance incident on the Earth´s atmosphere is relatively constant, available sunlight at the ground varies. This is due to both the effect of the atmosphere, the latitude and the time of year. Also, sunlight that reaches the ground is both reflected and penetrates the ground where it is stored as heat.

The output of a photovoltaic system depends on the available amount of incoming irradiance at its location. With a temperature of almost 5800K, the sun is considered approximately a black body that emits electromagnetic light with different wavelengths. At the edge of the atmosphere the solar flux density is set by the solar constant [27]:

$$S = 1366 \pm 3\ W/m^2$$

The energy flux per unit time, the radiation flux, is called the irradiance. The most common unit is W/m^2. The irradiance integrated over a period of time is called the irradiation. A typical unit is $Wh\ m^{-2} day^{-1}$.

The i*nsolation* describes the average solar radiation energy received on a certain location and at a specific time. Normally, the energy is either given as annual energy in $kWh/\ m^2$ or average diurnal energy in $kWh/\ m^2$. Insolation maps also use hours per year/day, using the standard solar radiation of one sun [28].

3.1 Solar coordinate systems

Figure 3.1and 3.2 show the most important angles when working with two different solar coordinate systems, respectively the horizontal and the equatorial system. All angles are in degrees. The meridian is the circle connecting the zenith and the celestial North Pole. Both figures are based on Chen [27]

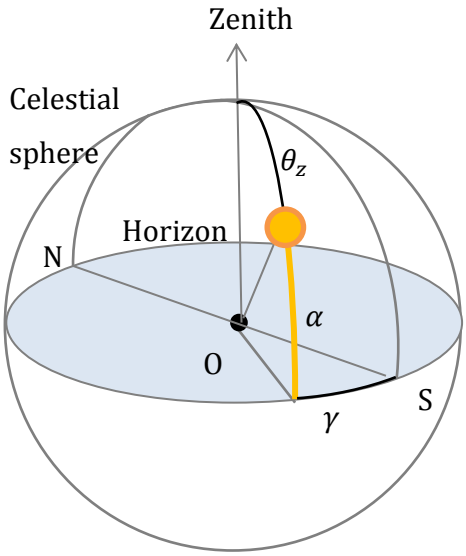

Figure 3.1 Horizon coordinate system with zenith angle θ_z, azimuth γ and elevation angle α.

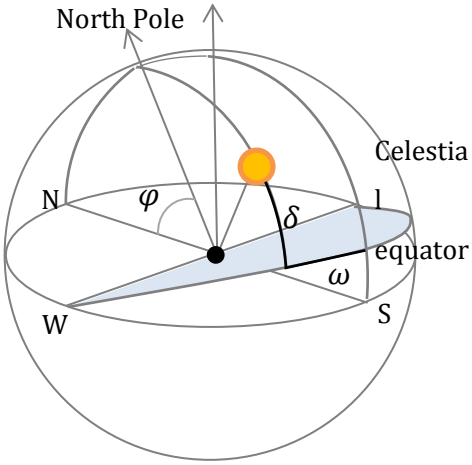

Figure 3.2 Equatorial coordinate system with declination angle δ, hour angle ω and latitude φ.

The horizon system defines a celestial body (here the sun), as perceived by the observer, O. The zenith is directly above the observer, and the angle between the incident sunlight and the zenith is known as the zenith angle, θ_z.

The azimuth γ, is the angle between the horizontal south and the suns position on the horizon. The azimuth is defined to have values between $-180 \leq \gamma \leq 180$,

The elevation angle, α, is the angular distance of the sun relative to the horizon [27]. The maximum elevation angle is found at solar noon, when the sun is positioned at its highest.

The equatorial system is defined by the celestial equator. The declination angle δ is the angle between the incoming rays of the sun and the plane of the equator. In the northern hemisphere the declination is greater than zero in summer, and less than zero during winter. The solar declination is assumed to be approximately constant during a day. It is usually assumed equal to its midday value [29]. The declination angle has values between $-23.45 \leq \delta \leq 23.45$.

The hour angle ω (HRA) is the angle between the meridian of the sun and the meridian of site. By definition, at solar noon the hour angle is 0° as this is the instant the sun crosses the north-south meridian. At solar noon the sun reaches its highest elevation. Each hour away from solar noon the hour angle changes with 15 ° because of the earth´s rotation. The shift is negative in the morning and positive in the afternoon [30]. The hour angle has values between $-180 \leq \omega \leq 180$.

3.2 Atmospheric effects

The irradiance incident on the Earth's surface is less than the solar constant due to interaction with the atmosphere. In general this is because of the absorption, reflection or scattering by aerosols, and the transmittance of incoming radiation [31]. Also local variations in the atmosphere, such as cloud cover and pollution will influence the irradiance.

The sunlight that reaches the earth directly in line from the sun is called *direct* or *beam radiation*, while the scattered and absorbed radiation that reaches the ground is called *diffuse radiation*. Radiation that is reflected from its surroundings depends on the albedo effect. The global radiation is the sum of these three components; the direct, the diffuse and the reflected radiation on a horizontal plane. This is illustrated in figure 3.3.

The reflected radiation can be found by multiplying the albedo with the sum of the direct and the diffuse radiation hitting the surface. An albedo of 1 indicates that all the radiation is reflected. An albedo of 0 indicates that all radiation is absorbed.

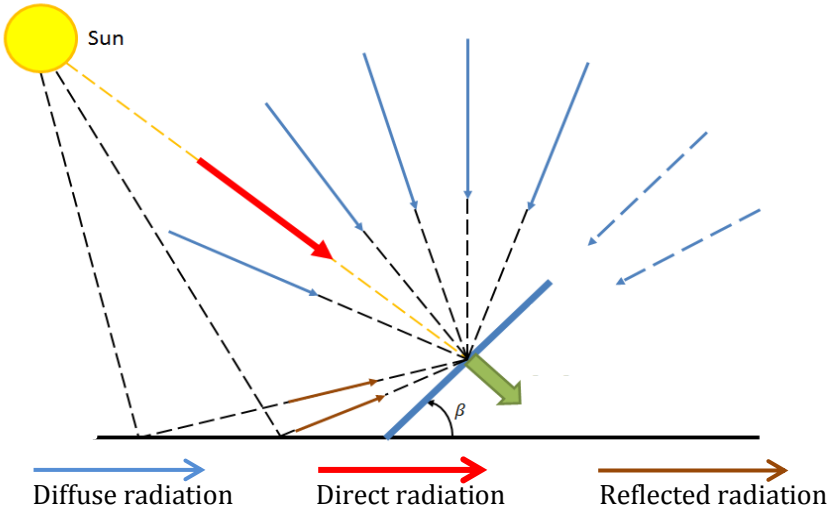

Figure 3.3 Radiation on an inclined surface: Diffuse, direct and reflected components

3.3 Air mass ratio

The air mass (AM) describes how far the incoming light waves have to travel through the Earth's atmosphere, expressed as a ratio relative to the length of the direct beam path at zenith. AM is defined as:

$$Air\ Mass = 1/\cos\theta_z \qquad \text{[Eq.1]}$$

Where θ_Z is the zenith angle, meaning the angle from the vertical. Air mass zero (AM0) describes the extraterrestrial spectrum, unaffected by the atmosphere. If the sun is situated directly overhead (at zenith), the air mass is 1 (AM1) [29].

When the angle between the position of the sun and zenith is 48,19°, the sunlight travels through one and a half time as much atmosphere as when the sun is positioned in zenith. AM1.5G (direct and diffuse radiation) and AM1.5D (direct radiation only) are chosen as the standard test condition for solar cells chosen by the American Society for Testing and Materials (ASTM) [27]. The power density for AM1.5G is about 1 kW/m^2, often reffered to as *one sun* or *standard solar radiation*.

3.4 Seasonal and latitudinal variation

Direct solar radiation varies both with time and location. The position of the sun relative to a fixed location on earth depends on both the time of day and the time of year. When the incoming rays are perpendicular to the surface, maximum power is achieved. As this angle changes, the power is also reduced.

Figure 3. 4 illustrates the seasonal variation in radiation with a period of one year because of the earth´s axial tilt. The tilt angle is 23.45°, giving an angle of declination of zero at the vernal and autumnal equinoxes and a maximum of $\pm$ 23.45°at respectively winter/summer solstice in the southern hemisphere[29].

The latitude determines the elevation of the sun through the year. At the equinoxes the solar noon angle equals 90° minus the latitude. During a year the elevation at a site varies with $\pm$23.5° from this angle.

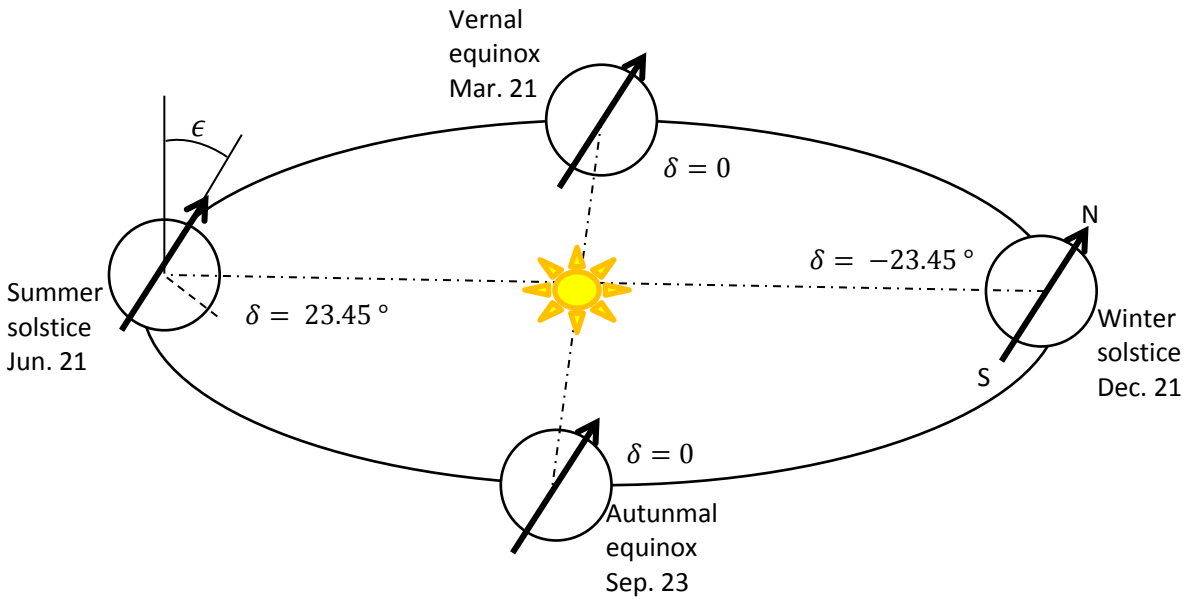

Figure 3.4 Equinoxes and Solstices.

3.5 Module angle and incident power on an inclined surface

The placement of the module is described using the plane azimuth and the tilt angle. The tilt angle β, is the angle between the horizontal plane and the module. The azimuth has different definitions, but in this paper the plane azimuth γ, is defined as the angle between the orientation of the collector plane and north (in the southern hemisphere). The angle is taken as negative towards east [32]. The azimuth and tilt angle for a solar collector plane located in the southern hemisphere is shown in figure 3.5.

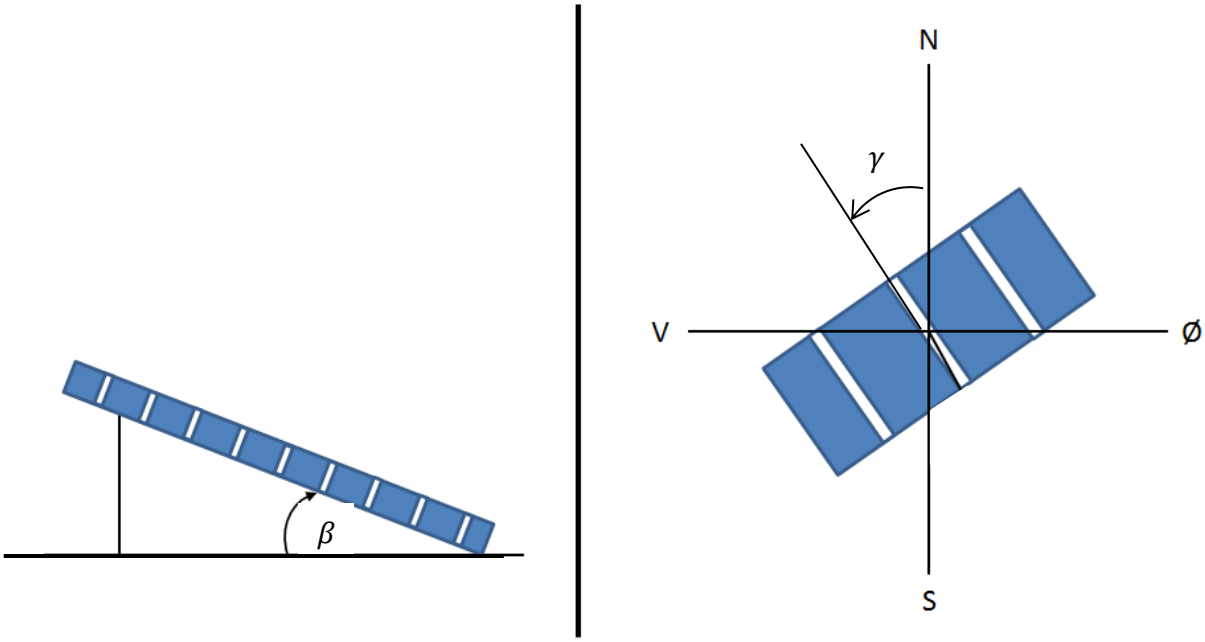

Figure 3.5 Azimuth and tilt angle for a solar collector plane located in the southern hemisphere. The azimuth, γ is the angle between the orientation of the collector plane and north. $\gamma < 0$ for towards east. The tilt, β is the angle between the horizontal and the module plane. Adopted from [7].

3.5.1 Optimal azimuth and tilt angle

Solar flux density always reaches its maximum when sunrays are perpendicular to the module as this allows for an optimized use of the direct beam radiation. Therefore, as a

general rule of thumb, the tilt angle is often equal or close to the latitude. The tilt angle is calculated to give the maximum yearly output, thus reducing the angle of incidence to its minimum. In general, tilting the module will also somewhat reduce the diffuse radiation on the module. Because of this, in humid areas, an incline less than the latitude can give a higher yield. Haberlin [7] recommends not having an inclination angle less than 20° so that dirt will easier slide off during rainfall, snow will fall off during winter and permanent layers of dirt (especially in the lower edges) will be smaller. When choosing the optimal inclination angle it is therefore important to also take into account practical implications due to local conditions.

Optimal azimuth is normally achieved by orienting the module towards the incoming sunlight at solar noon. In the northern hemisphere, an orientation towards south will increase the energy yield. Local weather conditions could also affect the module orientation. For instance, areas with thunderstorms in the summer afternoons can benefit from a small eastward orientation as irradiation will be higher in the morning [7].

3.5.2 Incident power

The insolation is obviously heavily dependent on the weather; therefore a *clearness index* is used to describe the average attenuation of solar radiation by the atmosphere. This is given as a ratio between the global irradiation at the surface on a horizontal plane, and the extraterrestrial irradiation on a horizontal plane during the same time period [33].

The total sum of the global irradiation arriving onto an inclined surface with an angle β relative to the horizontal is, as mentioned above, the sum of the direct beam radiation, diffuse radiation and ground reflection radiation [7].

When the sunlight is perpendicular to the module, maximum power is attained. For a tilted surface, the power is equal to that of the component perpendicular to the incident light [27].

3.6 Climatology of the humid tropics

The humid tropics are located between the Tropic of Cancer ($23.45\,°N$) and the Tropic of Capricorn ($23.45\,°S$). Located close to the equator, variation in day length is small throughout the year. Solar elevation is fairly high during the whole year, and assuming a clear sky, radiation is also relatively constant. However, wet and dry seasons are

normally defined periods causing considerable cloud cover, especially during the wet season. Heavy rainfall, often combined with thunderstorms is common in this area. As a result, the global solar irradiation in the humid tropics depends heavily on cloud cover during the different seasons.

In humid areas like this, the amount of diffuse irradiance is greater than in areas with clear sky conditions (such as the dry desert). According to [34] maximum diffuse radiation tends to occur during partially clouded weather, and reaches its highest when there is a thin, broken cloud. According to a study by Gu et al. [35] on cloud modelling of surface solar irradiance in southern Brazil, sunlit areas under a broken cloud can be even higher than during a clear sky due to the scattering and reflection from clouds. In addition, surface solar irradiance under broken cloud often (more than 1/5 of the time) exceeded clear sky values.

3.6.1 Kenya

Kenyas climate is tropical, located between 6˚S and 6˚N. Yatta is located in the central highlands, a region with a cooler climate than the warmer coast. Temperatures are stable year round, with a 2 degree decrease in during the coldest season. The precipitation is mainly driven by the migration of the Inter Tropical Convergence Zone (ITCZ)[1], triggering heavy, seasonal rains. Because of this, Kenya has to rainy seasons [36]

- "Short" rains from October to December
- "Long" rains from late March to early June

The monthly precipitation varies from location and from year to year, but generally the average lies around 50-200mm. Even though rainfall is high, it is often sunny part of the day.

The rest of the year can roughly be divided into two dry seasons

- Warm dry season from January to late March with light rainfall.
- Cool dry season from mid- June to early October

[1] Low pressure zone with heavy precipitation and cloud cover.

Average number of rainy days in January and February are 5 per month. Although the cool dry season is the driest of the seasons it often has high daily cloud cover and clear nights due to low-level moisture. The result is that the period with "short" rains often receives several daily hours of sunshine. Figure 3.6 shows the average monthly precipitation at Thika Meteorological Station (Thika met.). The two rainy seasons are clearly noticeable [37] [38].

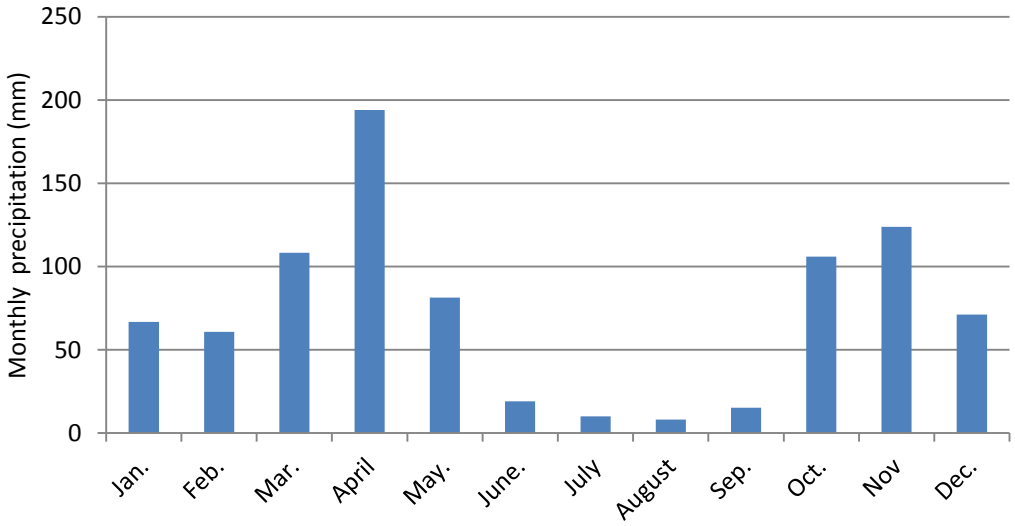

Figure 3.6Average total monthly precipitation from 2007-2011. Data from Thika Meteorological Station (S1.02, E37.10, 1574m)

The later years the country have started to experience some of the effects of climate change through periods with heavy rainfall, flooding and more frequent droughts. Relying heavily on hydropower these changes are well notes in the countries energy production [36].

4 Technology

If not otherwise cited the following sources are used in this chapter: [7, 34] [29] and [27].

4.1 Photovoltaic cells

The first usable solar cell was a silicon solar cell with 6% efficiency produced in 1954. But the first historical data of relevance for solar energy conversion was as early as 1839 when Bequerel discovered the photogalvanic effect. He observed that «electrical currents arose from certain light-induced chemical reactions» [29p.1]. The cost of solar electricity has decreased over the last decades making solar cells a more viable alternative.

Figure 4.1 show the connection of a PV cell, module, string and array. All solar cells have low individual voltages (about 0.5V). To achieve usable voltage levels, solar cells are connected in series. By connection cells and modules in series (a string) their voltage is added up. The current is given by the cell and module with the lowest current. Equally, the maximum voltage of an array is given by the lowest string voltage. The current from an array is the sum of the string currents [39].

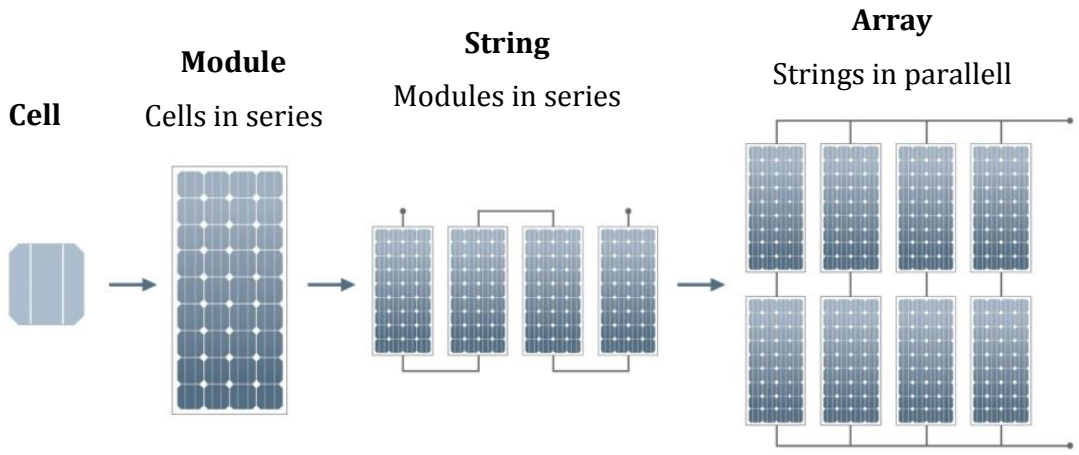

Figure 4.1 A PV cell, module, string and array. Figure adapted from [39]

4.1.1 Solar radiation

Radiation from the sun has a wave-particle duality. This means that it can be considered from two different points of view: as an electromagnetic wave and as a flow of photons. Photons have a wide range of energies ranging from roughly zero to four electron volts. The energy value of a photon is described by equation 2 [29]

$$\epsilon = hv = \frac{h \cdot c}{\lambda} \qquad \text{[Eq. 2]}$$

where $h = 4{,}14 \cdot 10^{-15} eVs$ is Plankc´s constant, v is the frequency of light $[s^{-1}]$, c is the speed of light $[3{,}00 \cdot 10^{8} m/s]$ and λ is the wavelength of the incoming photon.

When the electromagnetic wave from the sunlight interacts with an electron, which is also a wave, it transfers its energy to the electron in quants.

4.1.2 Generation of electricity

The generation of electricity in a solar cell depends on the potential of the semiconductor to convert sunlight into electrical power through the photovoltaic effect.

Most solar cells are made of semiconductors. Semiconductors consist of a relatively narrow band gap allowing electrons to be excited from one side of the gap, referred to as the valence band, to the other side, the conduction band. Sunlight, as a stream of photons interacts with a semiconductor. Photons with energy higher than the band gap of the semiconductor material can be absorbed, causing electrons to excite and create an *electron-hole pair a*s shown in figure 4.2.The pair can either recombine and emit a photon with energy roughly equal to that of the gap energy, or be separated by the pn-junction thus creating an electric current. The part of the photon energy that can be converted to electrical energy equals the band gap. A pn-junction is created by bringing together a p-type and a n-type semiconductor and thus establishing a built-in potential.

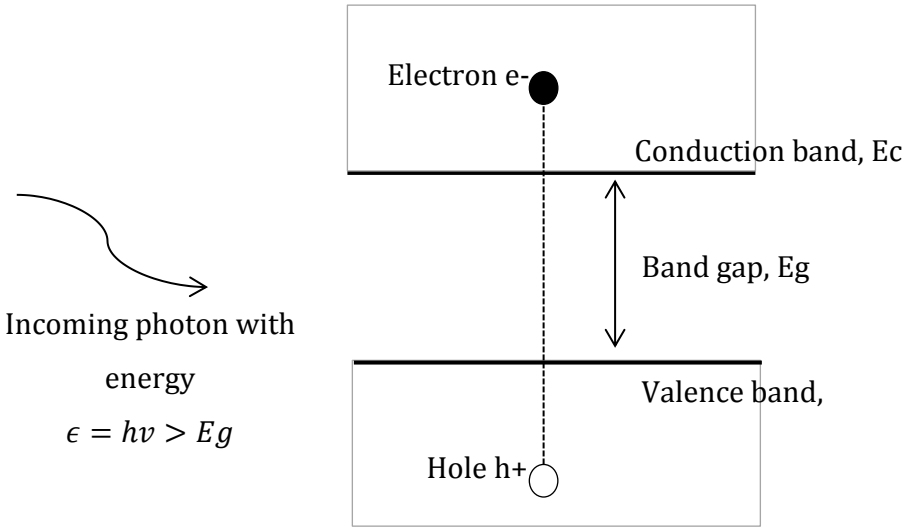

Figure 4.2Generation of an electron-hole pair. When a photon of incoming energy greater than that of the band gap reaches the semiconductor, an electron can be excited from the valence band to the conduction band. Excess energy is lost as heat.

Different semiconductors have different band gaps, thus the corresponding wavelength of light will vary. Normally, the energy gap corresponds to the photons of near-infrared or visible light. Band gaps close to the center of the solar spectrum generally have the best efficiencies. Typically the energy gap is less than a few electron volts. Figure 4.3 shows the equivalent circuit of a solar cell represented by a current source connected in parallel with a pn-junction diode. The current source is the photocurrent generated by the incoming sunlight. In a simplified circuit this equals the short circuit current.

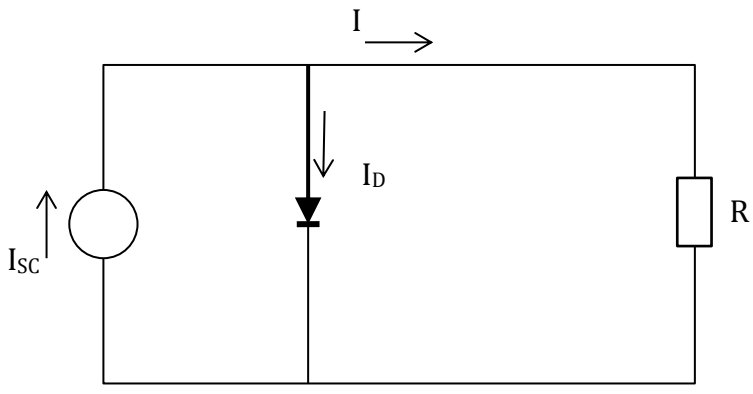

Figure 4.3Simplified equivalent circuit of a solar cell. Isc is the short circuit (light induced) current, I_D the diode current and I the output current. R is the load (R = ∞ = no load, R = 0 = shorted).

A solar cell can be well described using its electrical current-voltage (I-V) characteristics, as illustrated in figure 4.4. The point on the curve that represents the largest possible area of the rectangle is the maximum power point (MPP).

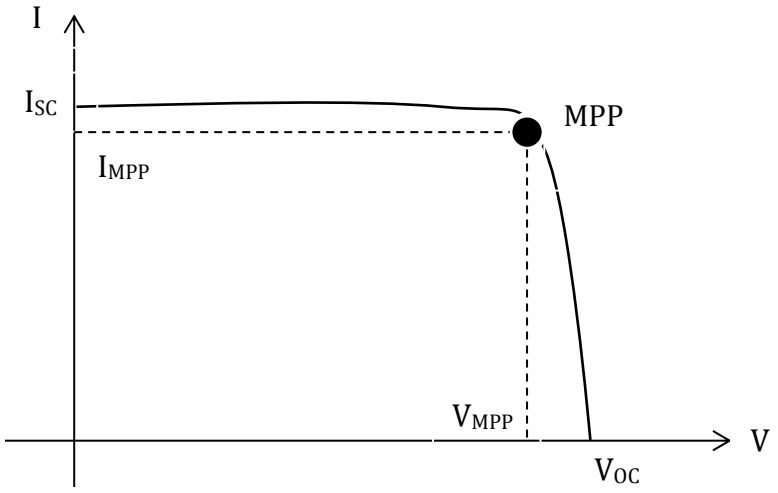

Figure 4.4 Characteristic curve I = f(V) for a solar cell with maximum power point (MPP). Isc is the short circuit current and Voc is the open circuit voltage. The MPP is the wanted operating point for a solar cell.

The fill factor (FF) is defined as the relation between Pmax and the product of the short-circuit current and the open-circuit voltage (the theoretical maximum power) [7]. The efficiency of a solar cell is described by its production at the MPP under STC divided by the incident radiation. I-V characteristics are often used to illustrate losses in a solar cell during operation.

4.1.3 Different types of solar cells

The most common solar cells are the group of crystalline silicon cells (c-Si). The cell with the highest efficiency is the monocrystalline silicon solar cell. In a monocrystalline cell the crystal structure is symmetrical. This gives high efficiencies, but also a production process that is energy intensive, slow and expensive. Polycrystalline silicon solar cells are easier and less energy intensive to produce and have efficiencies of about 13-15% [7]. All crystalline solar cells have indirect band gap, meaning that the top of the valence band

and the bottom of the conduction band are not aligned. Mediation by a photon is necessary, and a thicker substrate is required. The overall absorption coefficient is lower. c-Si solar cells exhibit light induced degradation (LID) of the solar cell´s performance [29].

Thin-Film solar cells are made of a very thin semiconductor layer and have direct band gaps, resulting in a higher absorption coefficient. Among the materials suited for thin-film cells are amorphous silicon (a-Si), cadmium telluride (CdTe), $CuInSe_2$ (CIS) and $Cu(In,Ga)Se_2$ (CIGS). Because of the reduced semiconductor need, the production of thin-film solar cells is less energy intensive. Thin-film modules have higher series resistance than crystalline modules.

A-Si cells have a more random structure than other silicon modules. The main drawback is its lack of stability/loss of efficiency when exposed to sunlight. After a period of time the efficiency stabilizes at a lower level. CdTe have a band gap close to the maximum theoretical efficiency and are less sensitive to degradation to light explosion compared to A-Si [7p. 118].

CIS cells absorbs almost all photons with hv>Eg. It is also stable under light, and have a high temperature tolerance[40] In a CIGS cell some of the indium is replaced by gallium, altering the band gap and producing a higher open-circuit voltage. A problem with CIS, CIGS and CdTe cells is the scarcity of indium, and that cadmium is highly toxic. Both CdTe, CIS and CIGS cells are commercially available.

4.1.4 Loss factors

Low irradiance

The irradiance level directly influences the output of the solar cell. The lower the irradiance level (compared to STC), the lower the efficiency of the system. This is illustrated in figure 4.5. The angle of incidence also affects losses mainly due to increased reflection from the solar cell coating at steeper angles of incidence.

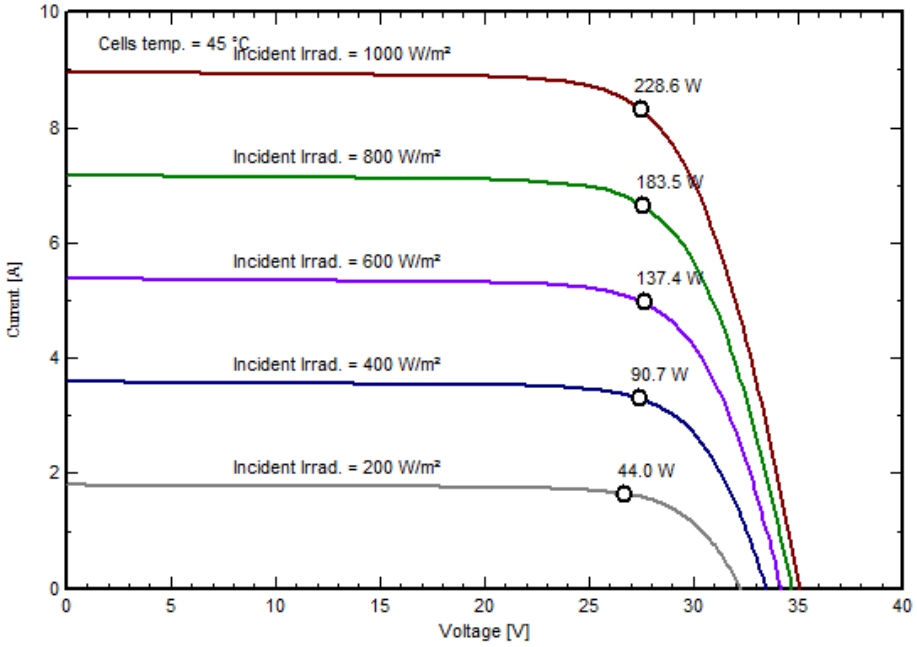

Figure 4.5 IV-curve dependence on incident irradiance for a polycrystalline module. Figure from PVsyst

Temperature

Increasing the temperature also increases the vibrations in the structure of the cell. Due to this the probability for recombination increases, thus reducing the efficiency of the cell. Figure 4.6 show the result of increasing the solar cell temperature on the IV-curve. A solar module is heated not only by the incident sunlight, but also by the operation of the module. At higher temperatures the internal energy losses are increased, and the diode threshold voltage decreases, resulting in a lower Voc and a slightly higher Isc [39]. The power temperature coefficient for a solar cell describes the loss in output maximum power per kelvin. Typical temperature coefficients are -0.4 - 0.5%/K for crystalline silicon solar cells [7p. 92]and around -0.1 to -0.3%/K for a-Si, -0.18 to -0.36 for CdTe and -0.33 to - -0.5 for CIGS cells [41]. Increased temperatures also decrease the lifetime of the panels because of increased stress due to thermal expansion.

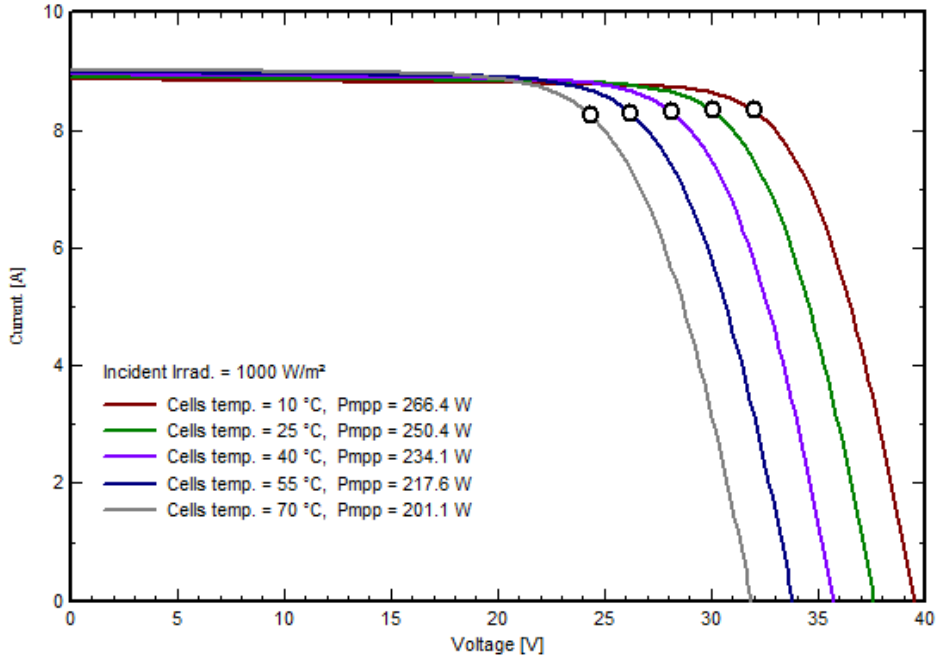

Figure 4.6 I-V characteristics dependence on cell temperature for a polycrystalline panel. Figure from PVsyst.

Cell temperature can be calculated using the following formula [28 p.280]

$$T_C = T_A + NOCT(°C) - 20°C \cdot \frac{G_{eff}}{G_{NOCT}} \qquad \text{[Eq.3]}$$

T_C is the cell temperature (°C), T_A is the ambient temperature (°C), NOCT is the nominal operating temperature, G_{NOCT} is 800 W/m^2 and G_{eff} is the irradiance. NOCT is given in the data sheet, and is defined at irradiance level of 800 W/m^2, an ambient temperature of $20°C$, wind speed is 1 m/s , solar spectral irradiance AM1.5 and open circuit.

Generally, the goal should be to keep the solar cell as cool as possible using measures such as ventilation, placement etc.

Mismatch losses

Mismatch losses occur when the characteristics of one cell is significantly different from the rest of the panel. Losses can occur for both cells connected in series and in parallel. Generally, the output of the panel is determined by the solar cell with the lowest output.

When solar cells are connected in series, this means that the production is given by the cell with the lowest production. For instance, if one cell is shaded, this will limit the current in the rest of the PV panel. This can be corrected by a parallel connection of a standard bypass diode to each solar cell [7]. Figure 4.7 shows how partial shading affects a module without diode[9].

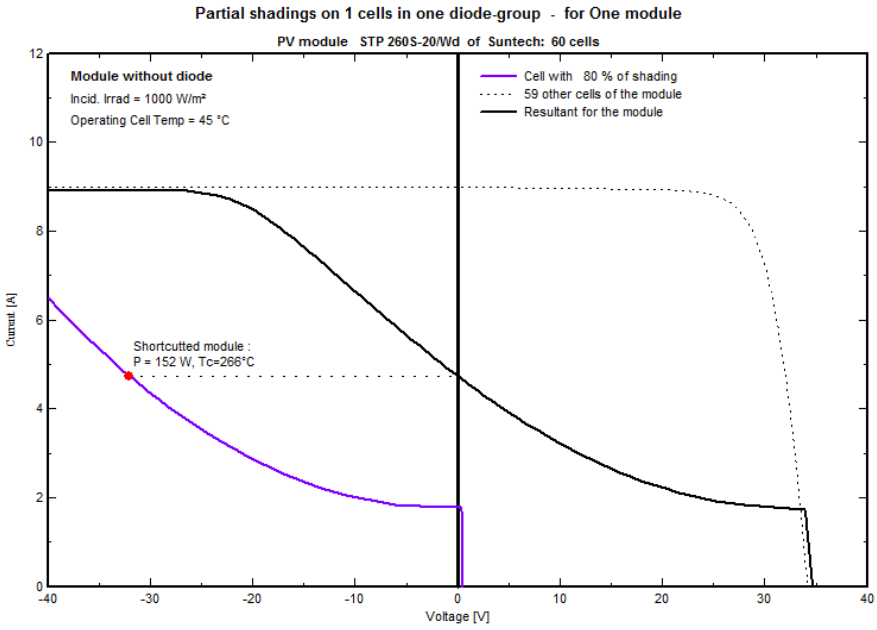

Figure 4.7 I-V curve for one module without diode that is partially shaded. From PVsyst.

Cells that are connected in series should always be of the same technology, type and manufacturer to avoid mismatch losses due to differences in the characteristic curves of each individual cell. When the characteristic curves of two cells are not matched, this results in power losses at the maximum power point (MPP).

4.2 Grid-connected PV systems

A PV system consists of a PV array, an inverter and other Balance of System (BoS) components such as a mounting system, charge controller, cables, transformer and suitable energy storage. The choice of components depends on the system and has to be selected individually for each project. Figure 4.8 shows an example of a grid-connected PV system.

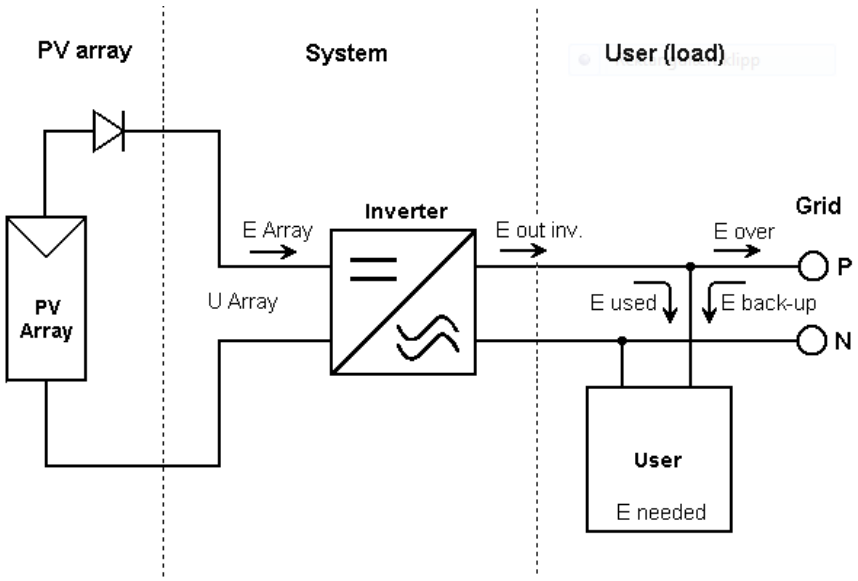

Figure 4.8 Example of a grid-connected PV system. From PVsyst.

4.2.1 Inverters

An inverter is used in order to change the generate direct current (DC) generated by the solar panels to alternating current (AC) for the loads. Today there are a number of inverters available on the market, both for grid-tied and battery based systems. Inverters have to be dimensioned to handle the expected power level, and be compatible with the conditions on the grid side. It also should be able to detect dangerous states, such as avoidance of undesired islanding. This implicates that when the grid is down the inverter should automatically shut down to avoid back-feeding electricity on to the local grid and potentially harm utility workers [33]. Grid- and battery inverters are very different in the way the function. Only grid-tied inverters will be studied in this paper. Inverters are made both with and without transformers. Transformerless inverters have higher

efficiencies because of transformer losses during operation. Inverters with transformers prevent DC current from reaching the grid. All inverters have high efficiencies, about 93-97% [39].

Most inverters have at least one Maximum Peak Power Tracking (MPPT) output. The MPPT applies the proper resistance to find the optimal maximum power point. With a MPPT the panel can operate at the optimal working range.

There are three different types of inverters; central, string and micro/module inverters. In a central inverter, several strings are connected in parallel on the DC side of the inverter in combiner boxes. This requires relatively extensive DC wiring, and the system is sensitive to losses from partial shading and mismatch losses, especially if the inverter only has one MPPT. On the plus side, central inverters generally have higher efficiencies, and it is generally cheaper to reduce the number of inverters in a PV system.

A string inverter is, as the name suggest, an inverter connected to one string. The advantage is that less wiring is required, and that system is less sensitive to partial shading. If string inverters are used, the strings need to be connected in parallel on the demand side. Despite the lower efficiencies, because of other reduced system losses string inverters often have system efficiencies at the same level or higher than central inverters. String inverters [7]. Multi-string inverters have, as the name suggests, input for multiple strings. They often have several MPPTs, and can be used for heterogeneus strings.

Micro/module inverters require little or no wiring and are not vulnerable to module shading and mismatch. With module inverters maximum power is supplied from each module regardless of the performance of the other modules in the array due to shading, mismatch, soiling losses or other damages to the cell. Using micro inverters also eliminates the risk of high DC voltages and extensive cabling and makes it easy to further expand the PV system. Each inverter has at least one MPPT [42]. Module inverters typically have sizes of about 100-500W.

Both string and micro inverters are mounted close to or on the modules. Because of the high operating temperatures of solar modules it is advisable to place the inverters isolated from the module so that its efficiency and life span is not reduced [8]. String and

module inverters are also subject to higher impacts from the elements compared to central inverters that are often placed indoors [43].

4.2.2 Other Balance of System (BoS) components

Other BoS components include mounting systems, cabling, switches, disconnects and system monitors. These components are not studied in any detail. The use of DC cables should be kept at minimum due to high ohmic losses and the cost [39] For central inverters it is also necessary to have a junction box between the array and the inverter for the fuses, overload voltage protections etc.

4.2.3 Energy back-up and storage

Depending on if the system is grid-connected or not, suitable energy storage should be considered. This subchapter gives possible alternatives for backup systems for grid-connected PV plants. If the PV system can operate when the grid is down this might reduce the fuel cost of the generator.

Grid-connected systems

In a grid-connected system the grid itself acts as an infinite energy storage where surplus power can be fed into the grid [3]

To continue to provide electricity from the solar panel in islanded mode, three options exist

- A battery based grid interactive system

  If a small battery bank, and a second, specialized inverter is added to the system, the second inverter can supply the grid-tie inverter with the necessary AC power for the grid-tie inverter to work. The capacity is limited by the capacity of the second inverter [44]. An example of a bimodal inverter is the Sunny Island from SMA [45] that work together with other SMA inverters. An option is to also tie the generator to the battery based inverter.

- Generator backup together with PV

The existing 48kWp generator at MCF Yatta is used during power outages. If electricity is supplied with the right voltage level and frequency, the PV system can possibly be run together with the generator. Due to lack of information regarding this alternative, it has not been studied any further. To investigate if this is a viable option the output power of the generator has to be compared to the required input of the inverter. It is also necessary to study how the generator will react to another AC source-

- Complete cut off with generator

Cheapest solution as there already is a generator available that is connected during outages. This does not reduce the consumption of fuel compared to today unless the generator is powered by biomass (as suggested by Tutturen [18]).

For a grid-connected system that is functioning when the grid is down, it is important that the power output of the inverter does not exceed the connected loads. If not, the inverter will shut of when it reaches its maximum allowed values for voltage or frequency [44].

5 Dimensioning and simulating a PV system

5.1 Meteorological data

To use PVsyst, and to investigate the potential yield of both PV systems and thermal solar systems, accurate global irradiation and temperature data are crucial. In PVsyst both wind velocity and diffuse radiation are optional. Irradiance data imported to PVsyst is checked for irregularities using PVsyst´s built in function for importing meteo data. If not otherwise stated, the information in this chapter is from the PVsyst contextual help manual [32].

5.1.1 Method for resource assessment

For the solar energy resource mapping an inquiry was made to the local meteorological institute. Meteorological data of monthly temperature from a ten year period was received, but unfortunately almost no data for solar irradiation was available. However, available online databases of climate data based on satellite measurements and ground interpolations have been used to map the solar energy resources for the area. The satellite data are from geostationary satellites, where global irradiation is estimated using a cloud index based on satellite pictures. Because of the lack of local climatic data, a comparison of ground and satellite data was not possible to carry out.

To execute simulations in PVsyst hourly data files are needed. If hourly values do not already exist, synthetic data files are constructed from monthly values. This is done using a stochastic model that generates a sequence of days, and then a sequence of hourly values during the day.

For irradiance generation, this is done using well known random algorithms presenting statistically probable data. To construct hourly temperature data, general models does not exist and the modelling are only adjusted to Swiss data and generalized for the rest of the world. Syntetic data in PVsyst is labeled with the year 1990.

According to a definition by Meteonorm in [32], the climatic distance between a station and a location is defined as

$$D_{climatic} = (Dist\ Hor^2 + (100 \cdot Diff\ Altit)^2)^{1/2} \quad \text{[Eq. 4]}$$

The vertical distance is weighed 100 times more than the horizontal. According to this standard, a site is thought to represent a certain location of the climatic distance does not exceed 20 km.

When analyzing climatic data the following factors should be considered [46]

- Uncertainty of ground measurements (measurement itself and long term variability of local climate data)
- Uncertainty of interpolation (interpolation of ground measurements and uncertainty of satellite)

The analyzed data are labeled low quality if the duration is less than 10 years, mid quality from 10-19 years and high quality for more than 20 years (definition also from Meteonorm [46]).

Temperature data

Monthly average daily maximum and minimum temperatures for the period 2007-2012 were received for Thika weather station. This is the weather station closest to the location, and its position is S1.02 E37.10, 1574m. The data has several missing values, and cover a relatively short time span and are therefore considered to be low quality data.

These temperature data have been compared with data monthly average temperatures from MeteoNorm V.6.1 and NASA SSE (both included in PVsyst, see closer description under "radiation data" below). According to PVsyst, the temperature data from Meteonorm have a mean bias error (MBE) of -0.58.

Radiation data

Estimated data from six different data bases were evaluated for the same coordinates. These are presented in table 5.1. Hourly values were only available from two of the six sources. Global horizontal and diffuse irradiance are evaluated. No ground values were

available for the location, but the data bases are compared with a Solar and Wind Energy Resource Assessment (SWERA) performed by (among others) DLR [8].

Table 5.1 Databases with meteorological data

Database	Region	Period	Source	Variables	Values
Meteonorm V.6.1	Worldwide	1961-1990, 1995-2005 (temp only)	Synthetic generation	GHI, DHI and wind vel.	Hourly
	Worldwide	1961-1990, 1995-2005 (averages)	1200 terrestrial stations (+ complement satellite) Interpolations	GHI, DHI, temp., and wind vel.,	Monthly
NASA-SSE	Worldwide	1983-2005 (averages)	Satellites $1°x\ 1°$ cells	GHI, temp.	Monthly
PVGIS-ESRA "classic"	Europe Africa South-West Asia	1985-2004	MeteoSat (Helioclim-1 database) 30 x 30 km	GHI, DHI No temp.	Monthly
PVGIS "Climate SAF"	Europe Africa $35\ °S - 58°N$ $15°W - 55°E$	1998-2011	MeteoSat and EuMetSat (first and second generation satellites)	GHI, DHI No temp.	Monthly
SoDa Helioclim-3	Europe Africa	Feb. 2004- Dec. 2005	MeteoSat	GHI No temp.	Hourly

Meteonorm V.6.1

The Meteonorm software provides monthly meteorological data for every location on earth. They also provide hourly data based on a synthetic generation using stochastic models. If there is not a station at the given location, Meteonorm uses interpolation between the 3 nearest stations. When ground data is poor, satellite data from five geostationary satellite is used as a supplement. 8 km horizontal resolution. The uncertainty of the ground measurements ranges between 1 and 10% (results from Meteonorm [46]), and for satellite data between 3 and 4% (low latitudes). For ground

interpolation, the uncertainty is 1% for a distance of 2 km, 6% at 100 km and 8% for distances greater than 2000 km. The diffuse horizontal irradiation is calculated using the Perez model for the separation of the global radiation into beam and diffuse components.

In Kenya there are stations in Garissa, Lamu, Nairobi, Mandera, Mombasa and Voi. The stations closest to the farm are Nairobi, Garissa and Voi. The Meteonorm software is included in PVsyst.

Nasa

The NASA SSE provides monthly data from 1983-2005 satellite measurements with a resolution of 111 km. The data are derived from several databases, and present average data for the area within a grid cells (111 km x 111 km). They therefore does not represent the microclimate within the cell, and cannot replace ground measurements.

Mean Bias Error (MBE) for monthly values on global horizontal insolation are 0.3%, and 6.86% on diffuse horizontal radiation. NASA SSE data are included in PVsyst [47].

PVGIS

"Classic"

PVGIS provides monthly data from the Helioclim-1 database, based on satellite images from Meteosat in the period 1985-2004. Resolution of roughly 30km x 30km (or 15 arc-minutes).

"Climate SAF"

This database are based on calculations from satellite images by CM-SAF, over a total of 12 years. The data are thought to be more representative of the last years climate than the classic PVGIS. The spatial resolution is 1.5 arc-minutes [48]. Because the number of measurement stations in Africa is very low (only 4 stations), it is difficult to comment on the accuracy of the database. According to a study [49], both databases ("climate SAF" and "classic) are assumed to do reasonably well. In Europe the new database is considered an improvement because of smaller errors when compared to ground data.

PVGIS data has to be imported to PVsyst from their website.

SoDa

Solar Data (SoDa) provides data from the HelioClim databases. Helioclim-3 has hourly values for the year 2005 for free for testing. The data are based on images from the Meteosat satellite and estimates hourly values for the horizontal global irradiance, and the normal beam irradiance. SoDa also provides a Nasa-SSE + HelioClim-1 database to get the best of the NASA SSE and HelioClim data bases. It provides data from the period 1983-2003, and automatically select the data with the highest quality. In the case of Kenya, the NASA-SSE + Helioclim-1 database only select data from NASA and are therefore not used.

5.2 Using PVsyst as a simulation tool

PVsyst is a software for analyzing the potential of a photovoltaic system (PV system) at a certain location. It contains both meteorological data and the possibility to select system components from various manufacturers. The system was chosen because of recommendation from earlier master student that had worked with similar projects, and because of its convenient student licenses. If not otherwise stated the information in this cubchapter is from the PVsyst contextual help manual

Table 5.2 lists the different input parameters for a base case scenario in PVsyst and their values. The base case is used to easier inspect the impact each parameter has on the result. Each input parameter, and the assumptions used in the base case, is described in detail below the table. The base case is used as a comparison during all simulations, and is assumed to be within the probable limits of the input data to PVsyst.

Table 5.2 Base case simulation input parameters for the simulation of a PV system at MCF Yatta using PVsyst.

Latitude 1.1°S, Longitude 37.3°E, Altitude 1318m

Input parameter	Value	Comment
PV Module	Polycrystalline S255P60	255 kWp
Inverter	Sunny Mini Central 4600	4,6 kWp
Meteorological data	PVGIS CM-SAF	
Array nominal power		About 10 kWp
Orientation	Tilt 25°C	
	Azimuth -100 °C	
Shading	Free horizon	
	No shadings	
Cell temperature	Absolute cell lower temperature	
	(for Voc at min temp) = 10°C	
	Minimum operating temperature	
	(for VmppMax design) = 18°C	
	Usual operating temperature under 1000	
	W/m = 60°C	
	Maximum cell temperature in operating	
	temperatures	
	(for VmppMin design) = 75°C	
Detailed losses	Default values	Kept constant
Array soiling losses	July-February: 3%	Kept constant
	March-June: 2%	
Albedo	0.25/0.25/0.20/0.20/0.20/0.20/	Monthly albedo values
	0.25/0.25/0.25/0.25/0.25/0.25	Kept constant

To inspect the impact of varying the different input parameters on the specific production, only *one* variable was varied at a time while the others were kept constant. New simulations were performed for each step to inspect the resulting deviation of the outcome, the specific production (kWh/kWp) of the PV plant.

5.2.1 Meteorological data set

The two datasets (see chapter 6.1) of climate data that were used in the simulations are

- PVGIS CM-SAF
  + Temperature data from Thika weather station
- Meteonorm

PVGIS CM-SAF is considered to give the highest probable yield, while Meteonorm gives the most conservative yield of the datasets studied. In addition, a third set from SWERA [8] was evaluated.

5.2.2 Sizing by power or area

PVsyst offers two options for the dimensioning of the PV system; to either size by planned power, or available area. Since area is abundant at Yatta, the system is dimensioned based on the electricity demand at Yatta, and existing policies regarding grid-connected solar.

To cover the total load, the system has to be dimensioned for the month with the lowest average insolation. Sizing a system to cover the total energy need will give a surplus of electricity for great periods of the year. Today there are no incentives for feeding excess energy to the grid for systems smaller than 500kW. Maximum nominal power was therefore chosen so that the probability of having surplus energy was considered low.

Based on the information on electricity demand in chapter 2.4, the average power load is about 30kW. Based on daily load curves it is not likely to drop below 20kW at any time during day or night. The system has been dimensioned so that the maximum power output will not exceed the minimum power load during the hours with sunlight. Due to uncertainties in the daily power load, the system is designed to be well below the daily load during sunlit hours, at 10 kWp. Also, the simulations give specific production rates and can easily be expanded to a system of a different dimension.

5.2.3 Orientation

The potential energy yield depends heavily on the angle of incidence of the incoming radiation, the season and local weather conditions. As a rule of thumb, the solar array receives a maximum amount of direct beam radiation if the angle of inclination is roughly the same as the latitude. In areas with a high portion of diffuse radiation, tilting the panel will somewhat reduce this irradiance. Close to the equator having a horizontal array will generally give the highest yield. It is also possible to use solar tracking devices that changes the azimuth and tilt angle throughout the year, but such systems are more costly and vulnerable to faults. One option is to manually change the tilt seasonally. The simulations in this thesis is performed with a fixed panel.

PVsyst has a built in optimizing tool for choosing the best orientation. The optimum depends on if the system is optimized over the whole year (as is normal for grid-connected systems), or if the aim is to have an optimization linked to the more critical periods (summer or winter optimization) or loads (for example cooling systems) for a stand-alone system. The optimizing tool was used to choose which orientations to study more in detail.

The transposition factor (FT) is the ratio of the incident irradiation, to the horizontal irradiation [32]. PVsyst uses hourly meteo data from one year to compute the FT for plane orientations and tilts up to 90°, both for the summer and winter season. FTs are studied for the two different climate data sets; Meteonorm and PVGIS CMSAF, to evaluate if the ratio of diffuse radiation has an impact on the preferred orientation.

Table 5.3 sums up the different orientations studied in more detail. For all system configurations it was studied how the change in orientation affected the specific production.

Table 5.3The different simulated orientations of the solar panels

Tilt [°]	Azimuth [°]
0	0
15, 20, 25 and 30	0(N)/180(S)/-90(E)/- 100/-110/-130/-150 /150/130/110/100/90(W)

In addition to the above mentioned parameters, a simulation was also carried out for a heterogeneous system with panels oriented in two different directions (East/West).

5.2.4 Cell temperature

PVsyst require design temperature inputs for the array voltage sizing ($V_{MPP\ max}$ and $V_{MPP\ min}$). The parameters are used for design purposes only and are not involved in the simulation.

Operating temperatures for the selected modules are found using equation 3 with climate data from chapter 6.1.1. Given the location close to the equator there are not notable difference in temperature between the different seasons. The lowest average temperature during the year is 17 °C, and the highest average is 24.4°C. Table 5.4 shows the cell temperature under different probable operating temperature and irradiance levels.

Table 5.4
Cell temperatures at different temperature and irradiance levels

		CIS, NOCT 47°C		Poly-si, NOCT 46 ± 2°C		Mono-si, NOCT 45 ± 2°C
Ambient temperature	Irradiation-level	Cell temperature [°C]				
15°C	100 W/m²	18,4	18,0	18,5	17,9	18,4
	200 W/m²	21,8	21,0	22,0	20,8	21,8
	400 W/m²	28,5	27,0	29,0	26,5	28,5
	600 W/m²	35,3	33,0	36,0	32,3	35,3
30°C	600 W/m²	50,3	48,0	51,0	47,3	50,3
	800 W/m²	57,0	54,0	58,0	53,0	57,0
	1000 W/m²	63,8	60,0	65,0	58,8	63,8
	1200 W/m²	70,5	66,0	72,0	64,5	70,5

Based on table 5.4 the following input parameters are used in PVsyst:

Absolute cell lower temperature (for Voc at min temp)= 10°C
Minimum operating temperature(for VmppMax design) = 18°C
Usual operating temperature under 1000 W/m = 60°C
Maximum cell temperature in operating temperatures (for VmppMin design) = 75°C

Based on maximum and minimum average daily values from Thika met. Station (See appendix A), the maximum operating temperature is set to 75 °C to assure that the array voltage stays within the range of the MPPT of the inverter.

The absolute lower temperature is set at 10°C as a safety measure to be sure the array operating voltage stays below the absolute maximum inverter´s in put at all times, and the maximum allowed system voltage for the PV module.

The cell temperature is normally about 20-40 °C above ambient temperature at 1kW/m^2 (depending on wind, module design and mounting system) When electricity is drawn from the panel the cell temperature will be lower than at open or short circuit [7].

The output power´s dependency on temperature for the chosen modules is presented in the table below.

Table 5.5 Temperature coefficients for four different types of PV modules

Model	Type	Temperature coefficient of Pmax [-%/K]
Centro Solar S-Class professional S250P60/S255P60	Polycrystalline	-0,43
Suntech STP250S/ STP260S	Monocrystalline	-0,44
Solar Frontier SF165-S	CIS	-0,31
First Solar FS395	CdT	-0,25

5.2.5 Choosing Inverter and Array

According to a report by Georg Hille et al. [6], the PV equipment requirements can be divided between two fields, safety and performance. The selected modules should meet current standards with respect to both areas.

Array

Crystalline silicon is an obvious choice. It is the most commonly used material in solar cells, and used in two of the existing grid-connected plants in Kenya. A CIS and CdT module was simulated for comparison.

The modules were chosen based on reports on already existing systems in Kenya (see chapter 1.2), and also had to meet the following criteria

- Be well known, mature technologies
- Meet the International Standards for photovoltaic modules, IEC 61215 (design qualification and type approval for crystalline silicon modules), IEC 61646 (for thin film modules), and IEC61730 (Safety qualification). The international Standards set down IEC requirements for long-term operation in general open-air climates [50].

Table 5.6 lists the selected modules. Datasheets can be found online at [40, 51-53]

Table 5.6 PV modules used during simulations. Performance at STC.

Model	Technology	Nominal power [Wp]	Efficiency [%]
Centro Solar S-Class professional S250P60/S255P60	Polycrystalline	250/255	15,2/15,5
Suntech STP250S/ STP260S	Monocrystalline	250/260	15,4/16,0
Solar Frontier SF165-S	CIS	165	13,4
First Solar FS395	CdT	95	N/A

Given the authors limited knowledge on different PV modules, there might be more adequate modules available, both with respect to efficiency, suitability and availability in Kenya. The main reason for choosing four different modules was to compare the performance of different types of well known, commercial solar cells.

Inverter

The simulation of the inverters was performed using one inverter of each type. The chosen technologies also had to meet the following criteria:

- Be well known, mature technologies
- Meet the International Standards for photovoltaic modules, IEC 62109-1, and IEC 62109-2 (Safety of power converts for use in photovoltaic power systems- Part 1: General requirements and Part 2: Particular requirements for inverters).

According to the report by Hille[6] "modern inverters fully comply with the Kenyan Grid Code, and from the inverter side, no serious obstacles can be expected"

Table 5.7 lists the selected inverters. Information from datasheets that can be found online at [54-56].

Table 5.7 Inverters used during simulations

Model	Technology	Maximum efficiency [%]	Nominal AC power [kW]	Max DC power (input)	Comment
(Multiple) String	Sunny Boy 5000 TL-21	97	4,6	4,8	2 MMPT inputs; 2 strings per input
(Multiple) String	Sunny Boy 4000 TL-21	97	4,0	4,2	2 MMPT inputs; 2 strings per input
Mini Central	Sunny Mini Central 4600 A-11/9000 TLRP	96,1/98	10,0/9	10,3/9,3	1 MMPT; 4 strings per input/1 MMPT; 5 strings per input
Module	APS YC500	95,4	0,5	0,6	2 MMPT inputs; 1 module per input

When an inverter have multiple MPPT inputs, PVsyst divide the operating power between the inputs. Two inputs = half the nominal power at each input. It is not possible to share the power unequally between each MPPT input.

5.2.6 Matching array and inverter

PVsyst has a built in system that matches the number of inverters with the number of strings based on the theory below. It also proposes a number of modules in each series, and the number of strings based on the sizing parameter. This is to assure that all requirements regarding current, voltage and power levels are met. Faults in the design give warning messages in the program. If not otherwise mentioned, theory in presented below is from [32, 39]

Current

Maximum output DC current of the array must not exceed maximum input current of the inverter. The maximal output DC current is defined by the short-circuit current Isc.

Power

The nominal power ratio describes the ratio of the nominal power of the inverter array with respect to the inverter. The Pnom of the inverter is defined as the output AC power. The Pnom of the array is the DC output power. PVsyst proposes a Pnom of 1.25, while most manufacturers suggest (or require) values about 1.0-1.1. This is because the Pnom of the array is defined at STC, conditions that are rarely met. In addition, cabling losses reduces the Pnom of the array before it reaches the inverter. An increase in cell temperature also causes the PMPP of the array to decrease (as defined by the temperature coefficient in chapter 4.1.4).

Also, many inverters accept overload for short periods (specified by the Pmax of the inverter).

Oversizing the inverter may lead the inverter to operate more often in its low power range, with reduced efficiency. When choosing an inverter, all the above conditions should be considered. In addition, the economy of the system should be taken into account. Some overload loss may be acceptable if this can be balanced by the decrease in inverter price. In PVsyst, overload losses up to 3% are considered acceptable.

Voltage

Maximum array operating output voltage in worst case scenario (i.e. at min. module operating temperature 18°C) should be lower than the max. V_{MPPT} of the inverter.

Minimum array operating output voltage in worst case scenario (i.e at max. module operating temperature 70°C) should be higher than the min. V_{MPPT} of the inverter.

The absolute maximum array voltage in open circuit (i.e Voc at 10°C) should stay below the absolute maximum inverter´s input voltage. The absolute maximum module voltage is found using the following equation

$$V_{module} = V_{OC\ STD} + \Delta T_{CELL} \cdot Vc \qquad \text{[Eq. 5]}$$

where Voc is the open circuit voltage at STC, ΔT_{CELL} is the temperature difference between and minimum operating temperature and temperature at STC [25°C]. Vc is the voltage temperature coefficient of the module [V/°C]. This formula can also be used to find the maximum and minimum array operating voltages, replacing $V_{OC\ STD}$ with $V_{MPPTSTD}$, the voltage MPPT at STC. All values are given by PVsyst.

The absolute maximum array voltage should stay below the absolute maximum system voltage of the PV module.

The above limits are set to keep the inverter operating within its MPPT range.

When matching array and inverter it is important to consider the type of inverter. For a string inverter the number of string has to match the number of “string” inputs. This is found in the inverter´s datasheet.

The maximum and minimum number of modules in a string can be calculated using formula 6 and 7.

$$N_{max,string} = \frac{0{,}95 \cdot V_{max,DC}}{V_{max,module}} \qquad \text{[Eq. 6]}$$

$$N_{min,string} = \frac{1{,}1 \cdot V_{min,DC}}{0{,}99 \cdot V_{min,module}} \qquad \text{[Eq. 7]}$$

$V_{min,DC}$ and $V_{max,DC}$ are minimum and maximum inverter input voltages. $V_{min,module}$ and $V_{max,module}$ are minimum and maximum module voltages. For the maximum number of strings the number is reduced 5% as a safety margin. For the minimum number, the minimum module voltage is reduced with 1% due to cabling losses, and the minimum input of the inverter is increased with 10% as a safety margin.

The above formulas (5-7) are used together with the numbers proposed by PVsyst to set design the configurations in table 5.8. The inclination and orientation of the modules within each string must be identical.

Table 5.8 Simulated Array/Inverter combinations

Polycrystalline CENTROSOLAR 255 Wp								
Type	System number	# Mod. in series	# Strings	Pnom Array [kWp]	# Inv.	MPPT inputs/ Strings per input	Pnom Inv. [kWp]	Pnom Ratio Array/ Inv.
SMA SB 5000 TL-21 Multi-string	1	10	4	10,2	2	2/2	9,2	1,11
SMA SB 4000 TL-21 Multi-string	2	10	4	10,2	2	2/2	8	1,28
SB2000HF-30 String	3	10	4	10,2	4	1/2	8	1,28
APS YC500 Module	4	1	40	10,2	20	2/1	10	1,02
SMA mini central 9000 TLRP	5	14	3	10,7	1	1/5	9	1,19

5.2.7 Shading

In PVsyst, shadings are treated in three different manners; near shadings & sheds, and far shading (horizon profile).

Near shading

The simulated PV system is assumed to have no near shadings. This is because the placement of the system is not decided and makes it difficult to construct a near shading

scene for the system. Also, it is possible to remove eventual trees or objects that will cause near shading. As the farm owns most of the surrounding land, this will not cause any conflict of interest.

Mutual shadings can be computed in two different ways in PVsyst. In the "Orientation" parameter option it is possible to define general parameters for each shed (several identical planes in a row), and their azimuth and tilt angle. This method computes a simplified estimate of the shading effect where losses are assumed to be "linear". This means that the electrical cell effect is neglected and that the sheds have an unlimited length, thus neglecting edge effects. The first shed is not shaded.

The system row layout and the parameters used with the "Orientation" option is defined in figure 5.1. Panel size is found in the module data sheets.

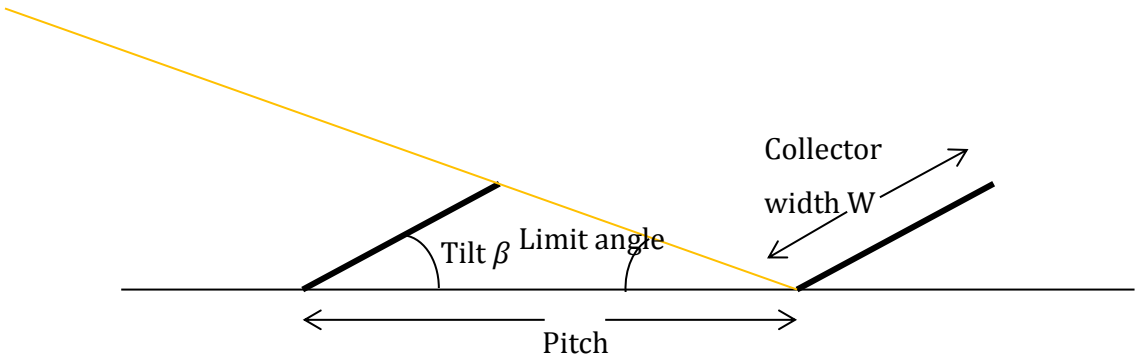

Figure 5.1 Representation of a row arrangement

The other option is to include the PV panels in the 3D constructed near shading scene. This computation will include shed edges and electrical effects can also be estimated. The electrical effect depends on the "weakest link" of the PV panel, as described in chapter 4.1.4. This means that the current of the whole panel is limited by the current of the shaded cell.

For this system the first option is used, and is expected that estimated losses due to near shadings effects are somewhat lower than the actual shading losses. The size of the polycrystalline module is 1660mm x 990 mm [51].

Far shading

According to the PVsyst project design tutorial [32], the horizon profile is suited for objects with a distance of more than 10 times the PV system size. When the sun is behind the horizon the beam component is equal to zero. However, the diffuse component is not much affected. The horizon profile was not recorded on-site, but the surrounding area is mostly flat highland. By studying the map of the farm (chapter 2.3), a possible location for the PV system can be on an elevated part of the area.

Figure 5.2 shows the sun paths and example of horizon profiles for MCF Yatta, and Bergen, Norway (latitude roughly 60°N) for comparison. This shows that far shadings will have a small impact on low latitude locations where the average sun height is greater.

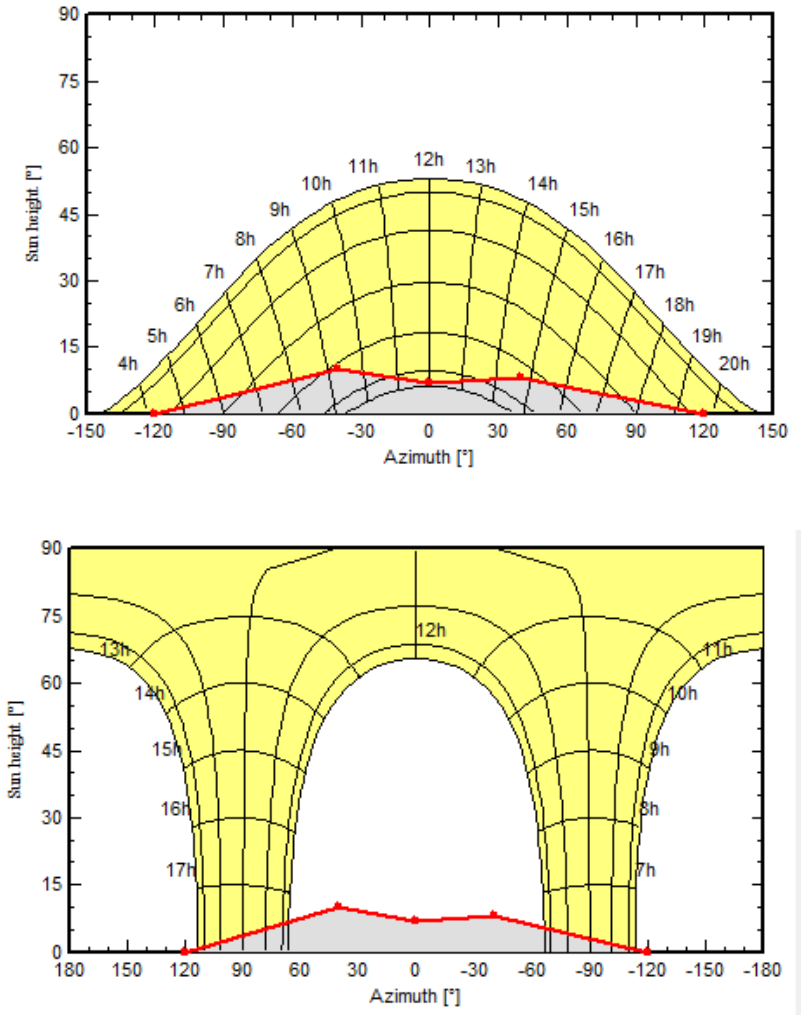

Figure 5.2 Identical horizon line drawings for the sun path graphs at Yatta and Bergen, Norway. From PVsyst

From this, it is assumed that far shadings will have a minimal impact on the system and are excluded from this study.

5.2.8 Albedo

If not changed, PVsyst uses a default albedo value of 0.2. This is a common standard adapted when simulating PV systems unless conditions like snow, sand etc. suggest otherwise. Figure 5.3 is a picture of a typical soil ground at MCF Yatta.

Soil albedo depends on the surface color and on the moisture content. Albedo values for dry soil vary from 0.14 (clay) to 0.37 (dune sand), between 0.16-0.26 for grass, and agricultural crops has albedos between 0.18-0.25. In general, the albedo will be somewhat lower during the rainy season as the ground will be wet. On the other hand, dry sand has high albedo [32].

During the rainy season, between March and May the albedo is set to 0.20. For the rest of the year it is assumed to be slightly higher, at 0.25.

Figure 5.3Typical ground at MCF Yatta. Photo: R. Tjore

5.2.9 Soiling losses

Soiling losses are caused by dirt on the module, and has a potential high effect on the system performance if not treated. This is a uncertainty the depends on local conditions such as rain, bird droppings, agricultural activity, local climate (wind and rain), etc. Periodical cleaning of rain gives lower soiling losses during the heavy rains. During dry periods cleaning of the panels are of high importance for the system performance. If dust, dirt or mosses is accumulated along the frames this can cause partial shading on the cells. Also, pollution of this type are not removed by rainfall.

Due to its location and required low tilt angles, the panels tend to accumulate higher levels of dust and dirt deposition. An option would be to use frameless modules to reduce the accumulation of dirt. Weekly cleaning is also recommended, especially during the dryer seasons [57]. Higher tilt angles should also be considered.

Due to the periodical seasons in Kenya, the soiling losses are assumed to be somewhat lower during rainy season. The monthly values used are listed in table 5.2.

5.2.10 Detailed losses

Six addition detailed losses are used with the default values set by PVsyst. These losses are kept constant during all simulations.

Thermal losses due to the instantaneous operating temperature of the cell is dependent on the thermal balance off the cell. For a module with complete free air circulation around the collectors the heat loss factors is set to Uc = 29W/m^{2}K (avoiding heat loss due to wind).

Wiring ohmic resistance losses between the modules and the terminal of the array are definind by a default global wiring loss fraction of 1.5% with respect to STC.

The module efficiency loss proposes the mod quality with respect to the manufacturer´s specification. This is defined from modules specifications.

Mismatch losses (as described in chapter 4.1.4) due to different cell characteristics. Power loss at MPP is set to 1.0% (for a polycrystalline module). The mismatch losses are

generally lower for thin-film modules. These losses are calculated by PVsyst based on module performance.

Light Induced Degradation (LID) loss factor of crystalline silicon modules in their first working hours is set to the default value of 2.0%.

The Incidence Angle Modifier (IAM) is set to its default value of 0.05. The IAM losses are due to reflections, i.e the lower reflection at higher incidence angles. The diffuse component is assumed to be isotropic, and the IAM factor of the diffuse irradiance is computed using an integral over all directions.

The yearly unavailability for the PVsystem due to maintenance, power outings, etc. is set to its default value of 2.0%. Power outings are discussed in more detail in the results.

5.3 Cost benefit analysis

The net present value is the sum of the present value of the future cash flows of the system. The NPV can be calculated using formula [58]

$$NPV = I_0 + \sum_{t=1}^{T} \frac{R_t}{(1+r)^t} \quad \text{[Eq. 8]}$$

WhereI_o is the initial investments cost, r is the discount rate, T is the system lifetime and R_t is the net cash flow.

The levelized cost of energy (LCOE) is used to evaluate the economic feasibility of the project. LCOE is the levelized cost of electricity per unit [kWh] over a time period t [58]. With the LCOE the PV plant can be compared to other electricity generating technologies. In Kenya, it is relevant to compare the LCOE to current electricity prices. Grid parity is the condition when the LCOE of solar PV is comparable to the grid electrical price.

The major cost of solar PV is the upfront investment cost, making the LCOE dependent on the financing method. As mentioned in chapter 2.1, solar panels are exempted from VAT (16%).

The LCOE is calculated using equation 9. The LCOE model used in this thesis is based on [12] and [6].

Equation 9:

$$\mathbf{LCOE} = \frac{\mathbf{I_0} + \sum_{\mathbf{t=1}}^{\mathbf{T}} \frac{\mathbf{O_t} + \mathbf{D_t} + \mathbf{M_t}}{(\mathbf{1}+\mathbf{r})^{\mathbf{t}}}}{\sum_{\mathbf{t=0}}^{\mathbf{T}} \frac{\mathbf{S_{t=0}}(\mathbf{1}-\mathbf{d})^{\mathbf{t}}}{(\mathbf{1}+\mathbf{r})^{\mathbf{t}}}}$$

where T is the economic lifetime of the project, t is the year of operation (t=0 is the installation and startup year), I_o is the initial investments cost, O_t is the operation and maintenance costs, D_t stands for decommissioning costs, M_t are the interest and loan payments, r is the discount rate, $S_{t=0}$ is the energy output of the system in year 0 and d is the annual degradation factor of the module. It is worth nothing that $I_0 + \sum_{t=1}^{T} \frac{O_t+D_t}{(1+r)^t}$ is the same as the net present value costs. It may look like the energy is being discounted for, but this is just a result of the rearranging of the equation.

Table 5.9 presents the different input variables used for the base case of the LCOE analysis. The table is based on the study by Ondraczek [12]. The parameters are discussed in detail below the table. A sensitivity analysis is then carried out to study the impact the different input variables has on the result. Only one parameter is varied at the time so that its impact on the LCOE can be evaluated.

Table 5.9 Input parameters and values for the base case of a solar PV system at MCF Yatta, Kenya

Input parameter	Value	Unit
Plant lifetime	20	Years
Installed capacity	10,2	kWp
Investment cost	1500	euro/kWp
Operating cost	2	%
Discount rate (real)	10	%
Degradation factor	0,5	%
Debt share	80	%
Inflation rate	5	%
Interest rate	9,5	%
Loan terms	15	Years
Production	1522,05	kWh/kWp per year

Installed capacity

Installed capacity is set to 10,2 kW (base case used in PVsyst). Capacities of 30, 40 and 50 kWp are also evaluated.

Plant lifetime

Average lifetime for the base case is set to 20 years based on the study by [6], Branker et al. [58] suggest lifetimes often well beyond 25 years, even for older technologies (See also Ondraczek [12]). Manufacturer´s life time is often between 20-25 years. Plant lifetime values of 25 and 30 years are evaluated.

Financing and incentives

The debt share of the initial investment cost is assumed to be 80%. The project is assumed to either have part equity or being donor-suported. The internal rate of the equity share has been left out of the study. Debt shares of 0%, 50% and 100% are also calculated.

Discount rate

The discount rate is the interest rate used in discounted cash flow analysis. The discount rate determine the net present value, and takes into account the risk and uncertainty of the future cash flows in addition to the future value of the money. The more risk there is linked to a project, the higher the discount rate. The discount rate is set to 10% based on studies by[6, 15]. Values of 8% [12] and 15% are also studied.

Operation cost

A great deal of the operation and maintenance (O&M) costs of solar PV are due to the replacement of inverters every 10 years, cleaning and repairs of the electrical system [58]. O&M are set to 2% of installation cost [6, 15]. The inflation rate for maintenance costs is based on the study by Hille[6] and is set to 5%. Maintenance costs of 1.5% as suggested by [12] are also used.

Installation cost

Table 5.10 sums up installation costs based on various sources. All prices are for high quality modules. In this analysis a set system cost based on literature has been uses. Due to this the installation cost is a rough estimate that does not take into consideration the type of panel, inverter or other BoS components used. Installation cost is for a system without backup power during blackout.

Table 5.10 Installation cost for a PV system

Source	Year of data	Small PV system (about 5kWp)	Large PV system (up to 50 kWp)
[6]	2011	2698 euro/kWp	2526 euro/kWp
[12]	2011	2566 USD/kWp	
[15]	2011	2100 USD/kWp	
[59]	2013	1300-1800 euro/kWp	1000-1700 euro/kWp

Estimated value of the installation cost today is calculated assuming a 10% yearly cost reduction [6]. Prices are excluding VAT. For the base case scenario an installation cost of 1500euro/kWp is used based on the above mentioned studies.

Yearly system output

System outputs are based on results from chapter 6.2

One conservative and one best possible value is used in addition to the base case production for the simulated PV system.

Degradation factor

0.5% based on [6, 12]. The study by Branker[58] concludes based on various studies of crystalline silicon cells that a degradation rate of 0.2-0.5% is a reasonable assumption.

Power tariffs for comparison

The electricity price in Kenya is roughly divided between a fixed charge, a rate per kWh, a fuel cost and an inflation rate. The fuel cost is dependent on the fraction of the production that is produced by conventional power plants. This again, depends on the hydro production. Due to this, the power tariff is sensitive to changes in the imported oil price. Prices based on estimates from electricity bills at MCF Yatta show prices between 13-23 KES/kWh. The expected annual increase is 5% (incl. inflation) [6] In 2014 the energy charge of sept is 14.00 KES/kWh, a foreign exchange cost at 20 cents/kWh and fuel cost of 500 cent/kWh. The inflation is set to 20 cents/kWh [60]. Based on this today´s power tariff is assumed to be 20 KES/kWh.

Loan payment

The base case loan is assumed to be an annuity loan with a 15 year loan term. The intern rate is set to 9,5% based on data from Central Bank of Kenya [61]. The annual loan and interest is found in excel using the PMT function in Excel (the function calculates the payment for a loan based on constant payments).

In the above calculations exchange rates of 112 euro and 90 USD are used [62].

6 Results and discussion

In this chapter the results are presented and discussed. At the end of each subchapter, the results are compared.

6.1 Meteorological data

To carry out a simulation in PVsyst the minimum data required are monthly global horizontal irradiation and monthly average ambient temperature. Optional data includes monthly diffuse horizontal irradiation and wind velocity. A comparison of the different databases presented in chapter 5.1.1 is presented and discussed in this chapter.

6.1.1 Results

Temperature data

The monthly temperatures from Thika and Yatta are identical in datasets from both Meteonorm and Nasa. Together with data for Thika meteorological station these are illustrated in figure 6.1. The temperature data can be found in Appendix A.

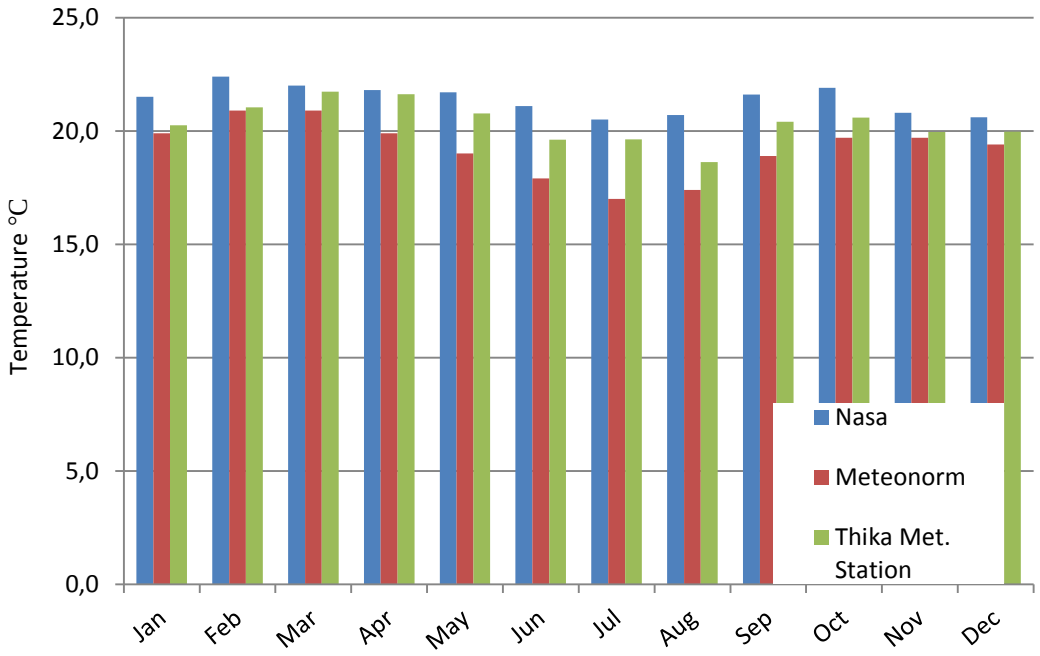

Figure 6.1 Monthly daily average temperature from NASA, Meteonorm and Thika Met. Station.

Yearly average temperature for Yatta is 21.4°C, 19.2°C and 20.4°C for NASA, Meteonorm and Thika Met. Station respectively. Figure 6.1 illustrates well the month-to-month correspondence between the different data.

The average maximum temperature at Thika Met. Station is 26.2 °C (See Appendix A). Thika is positioned 1.02°S 37.10°E, with an altitude of 1574m, while Yatta has coordinates 1.1°S, Longitude 37.3°E, and altitude 1318m. It is reasonable to assume that the temperature at Yatta may be 1-2°C higher due to the difference in altitude. It is important to stress that this is an assumption that ignores local climatic variations that might affect the temperature data more than the difference in altitude. Still, if this is correct, than the data from Meteonorm probably yield temperatures that are too low. According to equation 4, the climatic difference between Yatta and Thika is almost 66 km, and is therefore by definition not a good representation of the location. But, given the uncertainties of the satellite data, the temperatures from Thika is the only available ground data and is a good comparison and validation of the satellite data.

Radiation data

Five different databases are compared to evaluate the potential solar resources at MCF Yatta. The databases are Meteonorm, NASA, PVGIS, PVGIS CM-SAF and Helioclim-3. The data are compared in figure 6.2 and figure 6.3.

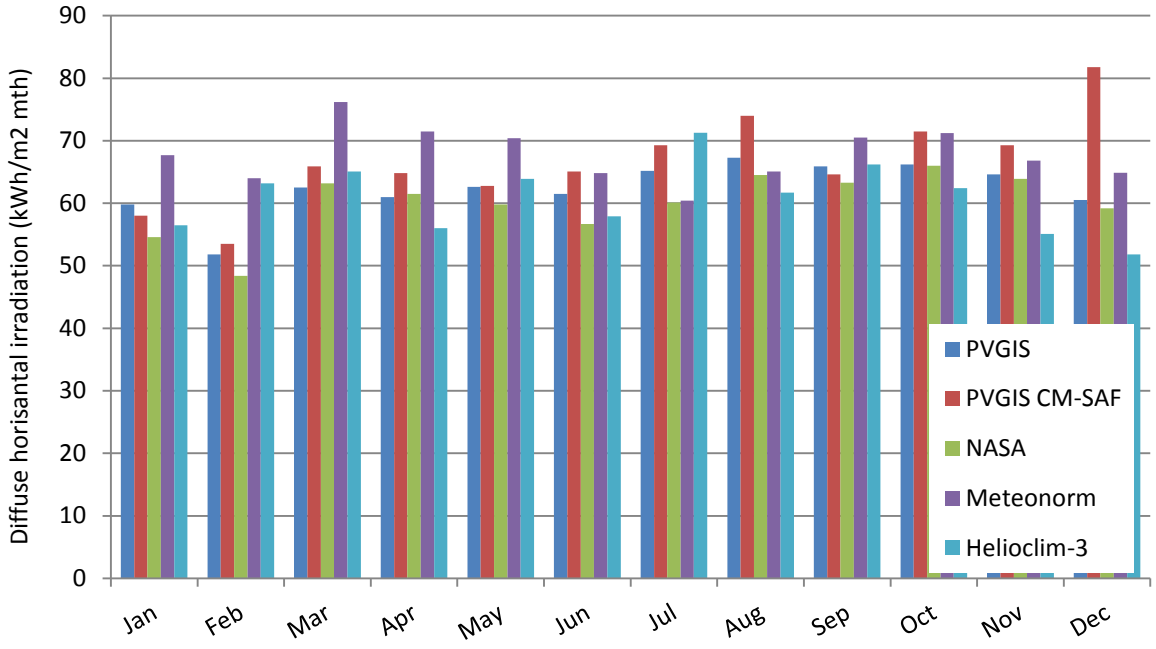

Figure 6.2 Diffuse horizontal irradiation, Yatta for five different databases

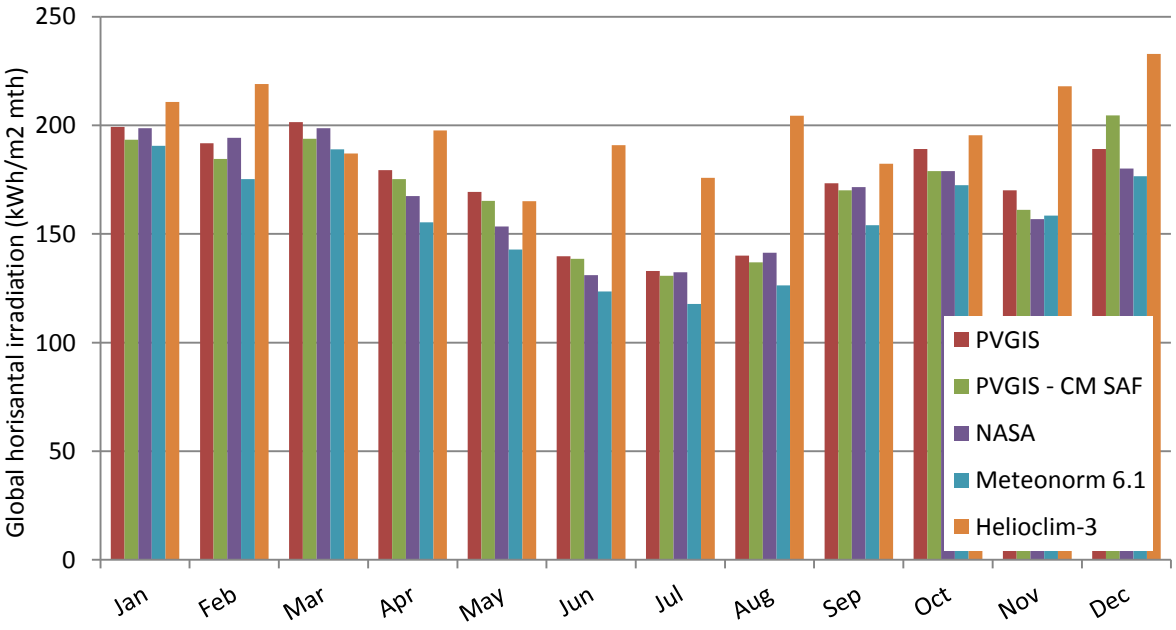

Figure 6.3 Global horizontal irradiation, Yatta for five different databases

The associated numbers for monthly global irradiation are found in App. A. Because of the relatively short distance between Thika and Yatta, all satellite derived values show approximately the same values for both locations. Only PVGIS gives different estimates between Yatta and Thika. The difference is between 1.8-3.2%. Figure 6.3 (when not considering the Helioclim database) correspond well with the climatic description of the

location (chapter 3.6). During the cool dry season (Jun-Oct), especially the first three months, the irradiation is notably lower. Both the "short rains" (Oct-Dec) and the "long rains" (Mar-Jun) are expected to have a relatively high number of sunshine hours despite the rainfall. The warm dry season (Jan-Mar) have high levels of solar radiation.

Figure 6.4 and table 6.1 compare the yearly global and diffuse irradiation. Since the diffuse components have a greater impact on panels with low tilts, the share of diffuse irradiation is expected to have an impact on the yearly production. The monthly variation in diffuse radiation is presented in table 6.2.

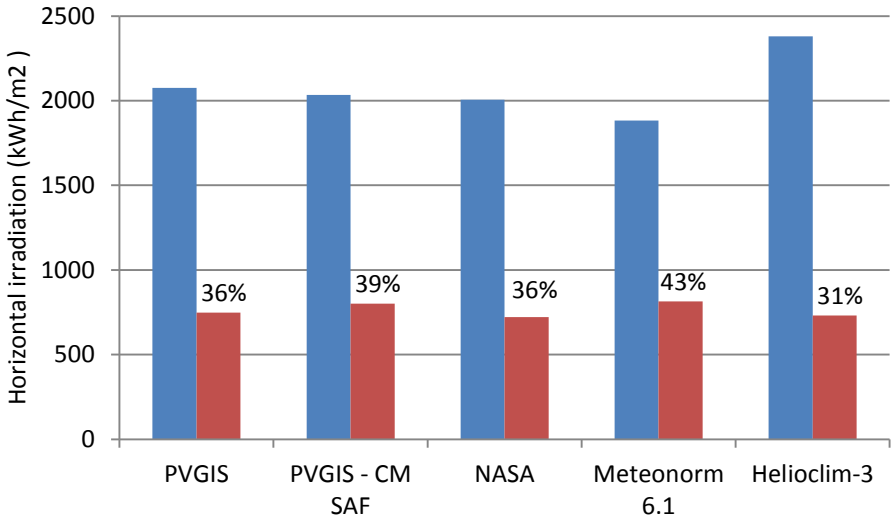

Figure 6.4 Yearly global (in blue) and diffuse (in red) horizontal irradiation at Yatta. The diffuse irradiation is labeled with its percentage of the total global irradiation.

Table 6.1Yearly global and diffuse horizontal irradiation [kWh/m²]

	PVGIS	PVGIS - CM SAF	NASA	Meteonorm 6.1	Helioclim-3
Global horizontal irradiance [kWh/m2 yr]	2076	2033	2005	1882	2379
Diffuse horizontal irradiance [kWh/m2 yr]	749	801	721	814	731

The monthly ratios for diffuse irradiation are given in Appendix A. The numbers show that the share of diffuse irradiation is highest from April/May to November for all databases except Helioclim. This is due to the lower irradiance levels during these months, while the diffuse irradiance is more or less the same throughout the year (see figure 6.2 and 6.3). Meteonorm have the highest yearly diffuse irradiation, while NASA has the lowest.

It is difficult to determine which data set gives the most realistic picture. A comparison done by PVsyst (found in the contextual help [32]) for several location north to south in Europe sums up that:

- Meteonorm tends to give lower values than the average, thus leading to conservative simulation results
- PVGIS is the sources most compatible with Meteonorm data.
- The Helioclim data response seems to be chaotic. Especially the 2005 values (Helioclim-3 hourly file) are very high over the other data, by a factor which is not always compatible with the 2005 irradiance

The Helioclim-3 data in figure 6.3 are considerably higher than the rest. Due to this and the comparison by PVsyst, they are therefore considered to give an unrealistic high yield at the location and are not used in the simulation.

6.1.2 Comparison with similar studies

Data from the UNEP SWERA study are used for comparison with the selected datasets [8, 36]. The SWERA data is based on images from Meteosat 7, and calculated for the years 2000, 2001 and 2002. The geostastionary Meteosat 7 is located at an orbit of 0° latitude and 0°longitude and scans a 5km x 5 km area every 30 mins. For Thika hourly time series of GHI and DNI high resolution data are made available by DLR. The same method is used for deriving GHI as with the Meteonorm data (the Perez model), using cloud information. Monthly averages from this study are presented in figure 6.5. The data from year 2000 was not possible to import to PVsyst, so only the years 2001 and 2002 have been studied. The data are open access and are imported to PVsyst using Kenya_Sitename_Lat_Lon_Z_Year from [63].

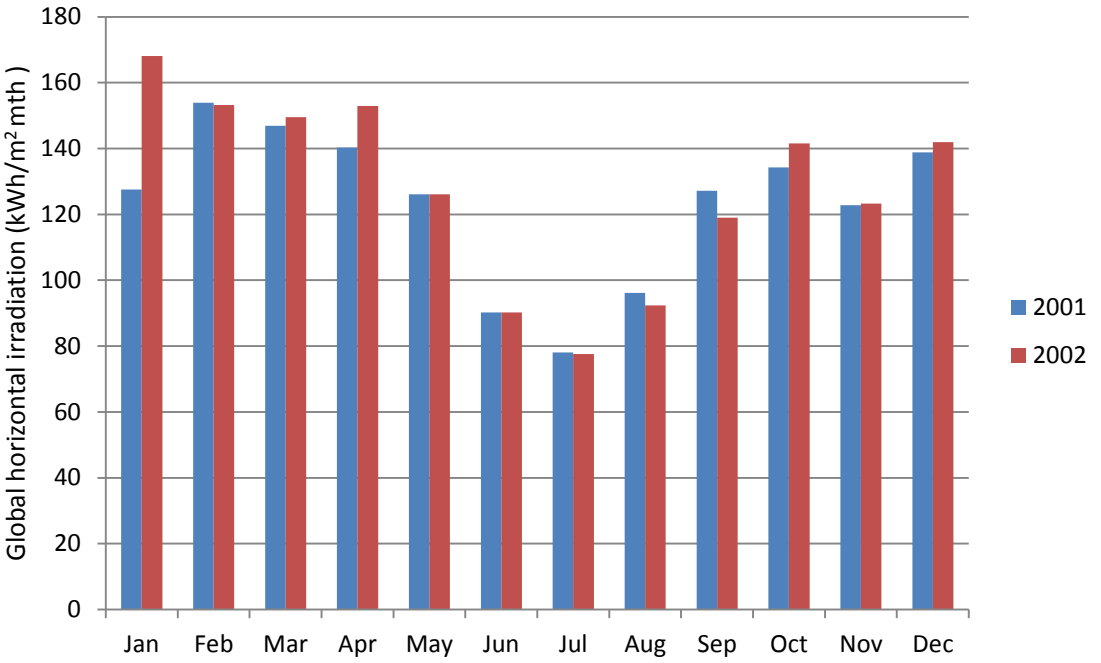

Figure 6.5 Monthly global horizontal irradiation at Thika, from SWERA. Data in Appendix A.

Compared to the data in figure 6.3, the data from SWERA gives a considerable lower yearly global irradiation. The 2001 data gives a yearly global of 1482 kWh/m2, while the data from 2002 is slightly higher, at 1536 kWh/m2. This gives a daily average irradiation of 3.8 and 4.2 kWh/m2.

6.1.3 Discussion

The meteorological data have several uncertainties. On the plus side, being situated almost on the equator several of the satellites are situated almost directly above the location. This should improve the result of the data. One of the main issues is the lack of ground data to verify/compare with satellite data. This being said, short data series with ground data also contain errors both due to human handling, and because of erroneously equipment. Also, data should be measured over a period of several years to be sure that they do not represent extreme values that will seldom occur.

The data from SWERA has the highest resolution, but also yield the lowest result. This could mean that the SWERA data are the best estimate of the actual irradiation at Yatta, or at least that the correct data are the once with the most conservative estimates. The

percentage difference between the SWERA and the PVGIS CM-SAF data is 27.1%, and the difference between the PVGIS CM-SAF dat and Metonorm is 7.4%. The problem with the data, despite its high resolution is its short time span (only one year). The data can therefore show values from extreme years, and does not represent a good picture of the average conditions. This is illustrated by the relatively high variation between the years 2001 and 2002 (3.5%). This makes it difficult to conclude on which dataset is the most probable, and several sets are used during the simulations.

Meteonorm is chosen as the most conservative estimate for the energy potential at Yatta. PVGIS yields considerably higher values than the other sources, and is used as a best case scenario. Because of the good experience and smaller errors with the PVGIS CM-SAF data in Europe (see chapter 5.1.1), this data set is used. As for the temperature data the real, measured values from Thika agromet station are chosen.

The average daily yields from PVGIS (highest GHI) and Meteonorm (lowest GHI) are 5.7 and 5.2 kWh/m2 respectively (calculated using daily values from synthetic data sets produced in PVsyst).

6.2 PVsyst

Figure 6.6 shows the normalized monthly energy production of the simulated base case. The yearly system production is 17067 kWh/yr, and the specific yearly production is 1521 kWh/kWp/yr. The overall performance ratio is 0.792.

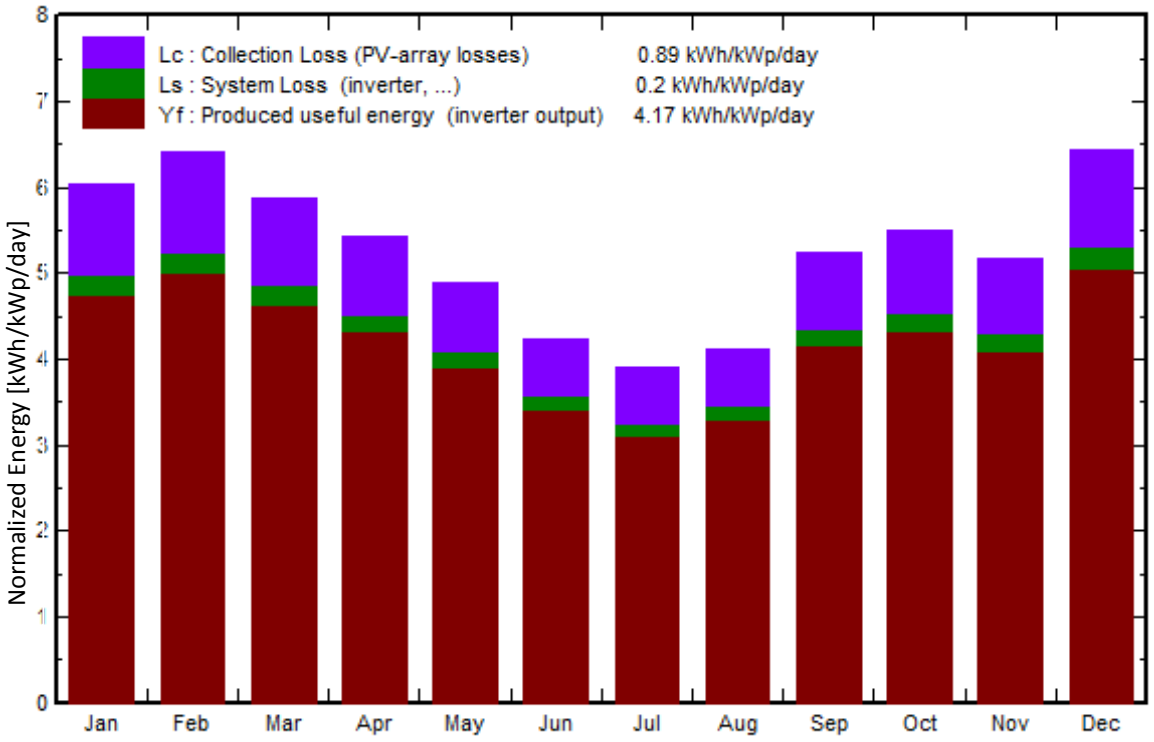

Figure 6.6 Monthly normalized energy production for the base case simulation

6.2.1 Meteorological data set

Simulation with Meteonorm show a yearly system production of 15932 kWh/yr, and the specific yearly production is 1420 kWh/kWp/yr. The overall performance ratio is 0.785 and the normalized production is 3.89 kWh/kWp/day.

The result from the simulation with data from SWERA yield a yearly system production of 14795 kWh/yr, and the specific yearly production is 1319 kWh/kWp/yr. The overall performance ratio is 0.751 and the normalized production is 3.61 kWh/kWp/day. It is important to note that the simulation using the SWERA data is for Thika.

6.2.2 Orientation

The transposition factors for Yatta for the summer (defined in PVsyst as October – March), winter (April – September) and the whole year are given in Appendix A. The graphs are found using the optimization tool in PVsyst, together with the data set PVGIS CM-SAF.

As expected, year round, a horizontal panel will give the highest yearly yield. During summer, the highest yield is achieved having a tilt of about 15°, oriented towards south. The same tilt is optimal during winter, but oriented northwards. Due to the higher irradiance levels from August – April/May, if a tilt is used, the panels should be oriented southwards. The higher irradiance levels when the sun is located south of the equator is due to local climatic effects such as morning fog or evening storms. According to theory in chapter 3.5 a tilt should have an angle of at least 20° to reduce soiling losses.

Table 6.2 Transposition Factors for Yatta for a whole year. Higher FTs are circled

Azimuth / Tilt	-180°	-150°	-120°	-90°	-60°	-30°	0°	30°	60°	90°	120°	150°	180°
90°	0.38	0.42	0.49	0.51	0.47	0.39	0.35	0.39	0.47	0.51	0.49	0.41	0.38
80°	0.46	0.49	0.56	0.59	0.55	0.47	0.42	0.46	0.54	0.58	0.56	0.49	0.46
70°	0.55	0.58	0.64	0.66	0.62	0.55	0.50	0.55	0.62	0.65	0.64	0.58	0.55
60°	0.65	0.68	0.72	0.73	0.70	0.65	0.61	0.64	0.70	0.73	0.71	0.67	0.65
50°	0.75	0.77	0.79	0.80	0.78	0.74	0.71	0.73	0.77	0.80	0.79	0.76	0.75
40°	0.84	0.85	0.86	0.86	0.85	0.82	0.81	0.82	0.84	0.86	0.86	0.85	0.84
30°	0.91	0.91	0.92	0.92	0.91	0.89	0.88	0.89	0.90	0.91	0.92	0.91	0.91
20°	0.96	0.96	0.96	0.96	0.95	0.95	0.94	0.95	0.95	0.96	0.96	0.96	0.96
10°	0.99	0.99	0.99	0.99	0.99	0.98	0.98	0.98	0.99	0.99	0.99	0.99	0.99
0°	1.00	1.00	1.00	1.00	1.00	1.00	1.00	1.00	1.00	1.00	1.00	1.00	1.00

Based on the transposition factors in table 6.2, azimuth values between $-90 \leq \gamma \leq 90$ (from west towards east, southbound) are selected for further investigation. With low tilts ($\leq 20°$), the FT does not change notably for any orientation. The results are presented in table 6.3.

Table 6.3 Yearly system production [kWh] and normalized daily production [kWh/kWp/day] due to different tilt and azimuth angles.

Azimuth [°]	Tilt [°]							
	15		20		25		30	
	kWh/ yr	kWh/ kWp/day	kWh/ yr	kWh/ kWp/day	kWh/ yr	kWh/ kWp/day	kWh/ yr	kWh/ kWp/day
0 (N)	17418	4.25	17031	4.16	16544	4.04	15968	3.90
-90 (E)	17648	4.31	17397	4.25	17050	4.16	16654	4.07
-100	17664	4.31	17413	4.25	17067	4.17	16675	4.07
-110	17674	4.32	17417	4.25	17074	4.17	16672	4.07
-130	17679	4.32	17407	4.25	17042	4.16	16610	4.06
-150	17672	4.32	17381	4.24	16999	4.15	16525	4.04
-180 (S)	17647	4.31	17334	4.23	16922	4.13	16418	4.01
150	17591	4.30	17278	4.22	16876	4.12	16385	4.00
130	17560	4.29	17258	4.21	16866	4.12	16406	4.01
110	17534	4.28	17239	4.21	16859	4.12	16431	4.01
100	17518	4.28	17226	4.21	16842	4.11	16427	4.01
90 (W)	17500	4.27	17207	4.20	16821	4.11	16404	4.01

The yearly system production for a horizontal system is 17673 kWh/yr, and the specific yearly production is 1607 kWh/kWp/yr. The overall performance ratio is 0.790, and the normalized production is 4.40 kWh/kWp/day.

According to table 6.3 even though the sun will be behind the panel part of the day it is still beneficial to have the panels towards east or south-east for an optimal yearly production. The higher the tilt, the higher the impact from changes in azimuth angle.

To compare the result, transposition factors for the data set from Meteonorm was also analyzed. The Meteonorm data have a slightly higher ratio of diffuse irradiation, and are global values are lower during all months. According to theory, diffuse irradiance is decreased with increased tilt. For Meteonorm, the highest yield is achieved having a tilt of nearly 5° during summer, oriented towards east. During winter, the optimal tilt and azimuth have not changed notably from the optimal for PVGIS. For a year round optimal a horizontal panel still give the highest yield.

From the data in table 6.4 it is likely to assume that the orientation of the panel does not have a high impact on the yearly production of the system. However, the orientation of the panel does have an impact on the variation in daily production. Orientating the panel towards east will give a higher production in the morning. As discussed earlier, the aim is that the maximum power output will not exceed the minimum power load during the hours with sunlight. By placing half of the panels facing east, and half of the panels facing the daily production curve will be evened out, and a larger PV system can be installed without "loosing" excess energy to the grid. Figure 6.7 and 6.8 illustrates the yearly system output power distribution for a system orientated in respectively one, and two directions. The average output for a two faced system is lower, and the distribution of the output power is more even. The same effect is illustrated in figure 6.9, but using the power output during a day (24h).

For a heterogeneous PV system (with a 25° tilt angle) the nominal daily production is 4.14 kWh/kWp. An identical system with all modules facing east yields a normalized energy production of 4.16 kWh/kWp.

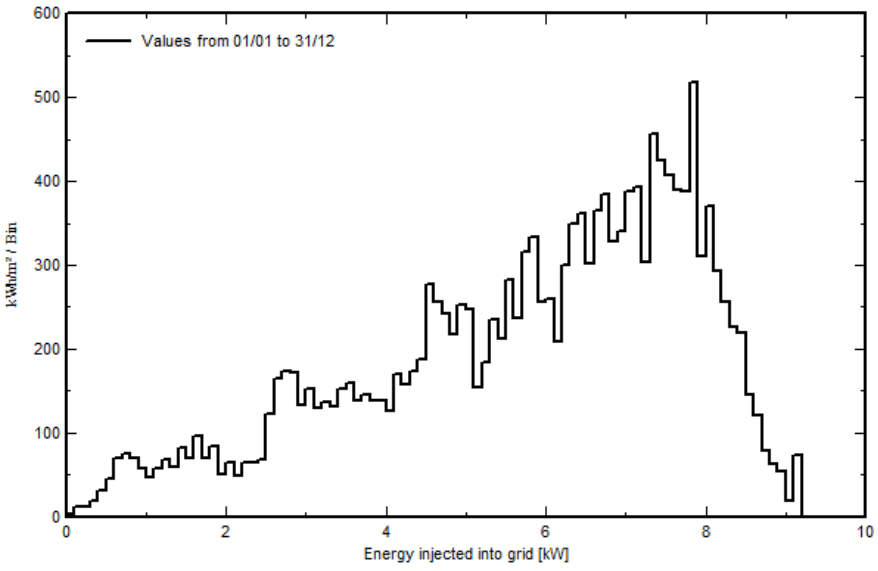

Figure 6.7 System output power distribution for panels facing one direction (E) with a 25° tilt angle

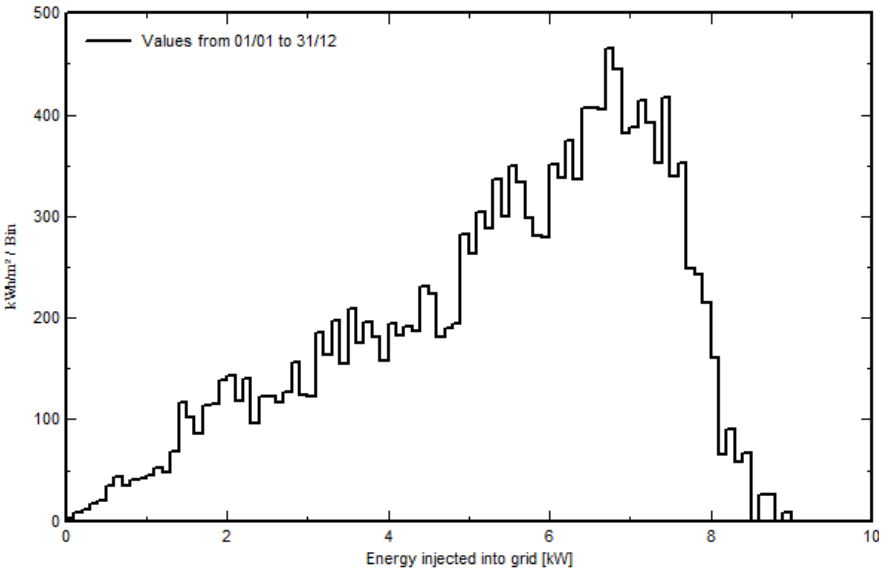

Figure 6.8 System output power distribution for four identical strings with different orientation (E-W) and a 25° tilt angle. Figures from PVsyst.

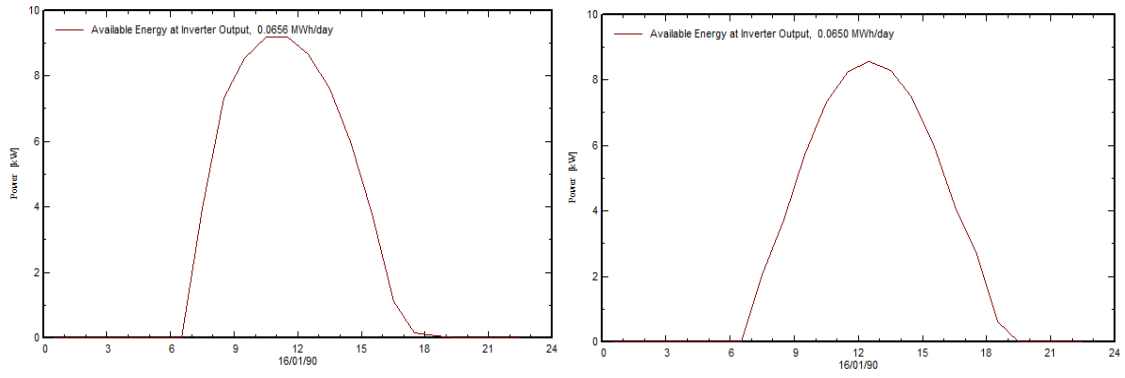

Figure 6.9 Daily system output power distribution for a PV system facing East/West (to the left), and East (to the right) for the 16th of January. Figures from PVsyst

6.2.3 Array and inverter

The choice of array and inverter is important both because of internal system losses both also due to mismatch losses between array and inverter. The different type of inverter also impacts the sensitivity of the system to reduced module performance due to for instance shading.

Fixed inverters and varying module

All simulated systems had a nominal power as close to 10kW as possible. The normalized daily production is listed in table 6.4, and the system losses are presented in figure 6.10. The monthly normalized array production can be found in Appendix B. Surprisingly, the CIS module has the highest normalized array production, even though the efficiency is higher for the crystalline modules. This is due to the much lower array losses for the thin-film modules, and their higher performance ratios. Detailed losses are studied in chapter 6.2.5. Even though system production is higher for thin-film modules, their production/m2 is lower and they require more space.

Table 6.4 Normalized array production, system production and performance ratio

	Normalized array production kWh/kWp/day	Normalized system production kWh/kWp/day	Performance Ratio
CIS	4,68	4,43	84,30
cdT	4,54	4,34	82,40
mono	4,41	4,20	79,90
poly	4,38	4,17	79,40

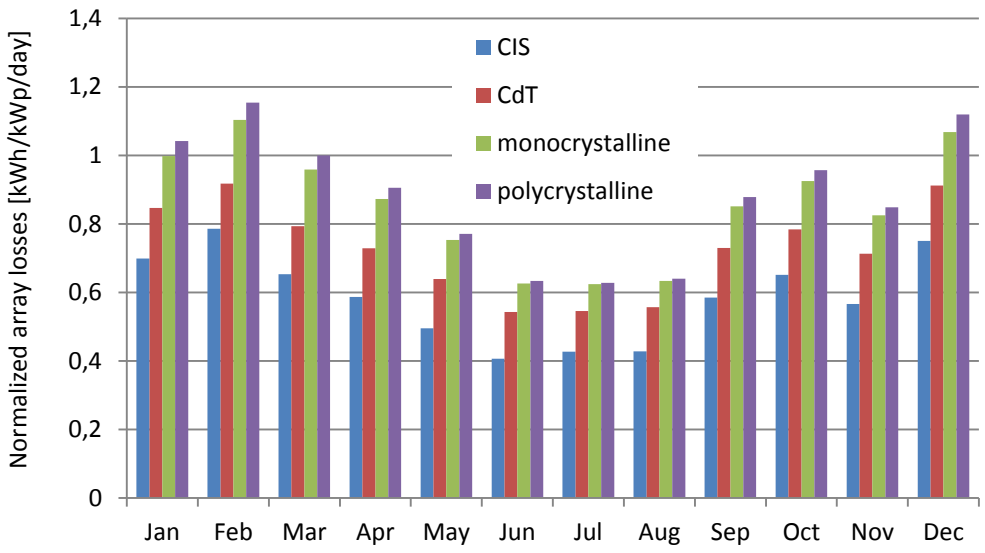

Figure 6.10 Normalized array losses for four different types of modules

Keeping the module fixed and varying the inverter

Table 6.5 presents the different array/inverter configurations simulated. The nominal power (Pnom) of the array is kept around 10kWp. Simulations are performed with both module, string, multi-string and a central inverter. For the multi-string inverter, the impact of changing the Pnom ratio array/inverter, i.e. over- or undersizing the inverter was investigated. Most simulations are performed for a polycrystalline module (as in the base case).

Table 6.5 Comparison of different array/inverter configurations and their corresponding normalized production and inverter losses

Polycrystalline CENTROSOLAR 255 Wp									Production	
Type	System number	# Strings	Pnom Array [kWp]	# Inv.	MPPT inputs/ Strings per input	Pnom Inv. [kWp]	Pnom Ratio Array/ Inv.	Inv. losses [kWh/ yr]	[kWh/ Yr]	[kWh/ kWp/ day]
SMA SB 5000 TL-21 Multi-string	1	4	10,2	2	2/2	9,2	1,11	577,3	15695	4,22
SMA SB 4000 TL-21 Multi-string	2	4	10,2	2	2/2	8	1,28	588,5	15683	4,21
SB2000HF-30 String	3	4	10,2	4	1/2	8	1,28	804,7	15467	4,15
APS YC500 Module	4	40	10,2	20	2/1	10	1,02	972,	15299	4,11
SMA mini central 9000 TLRP	5	3	10,7	1	1/5	9	1,19	498,6	16587	4,24

Simulations with a normal sized and undersized multiple- string inverter from SMA show that the inverter losses are nearly identical. Inverter losses during operation are about 3.7% for the normal sized, and 3.6% for the undersized inverter, but there is also a 0.1% loss over nominal power for the undersized inverter. The central inverter has operational losses of about 3.0%, and the module inverter of about 6.4% (the percentages are calculated from the detailed inverter losses found in appendix B).

The detailed losses show that most losses are due to the efficiency of the inverter, while the other losses are negligible.

Ohmic losses are assumed to be constant for these simulations, but in general module inverters require less DC wiring than both central and string inverters, and the ohmic losses will be lower.

What these simulations show is that the choice of inverter has an impact on the yearly production. Sizing the inverter so that it works within its ideal operating range will increase the output. Sizing the inverter slightly smaller than the Pnom of the array does not seem to decrease the energy production significantly. Today, there are many inverters on the marked that cover the specific technical needs for the location (Hz, voltage). Choosing a slightly undersized inverter can reduce the total cost of the system without experiencing significant overload losses. Generally, having multiple inverters increase the global inverter losses and the price of the system, but reduces the vulnerability of the system.

6.2.4 Shading

The panel used during the simulations has dimensions of 1660mm x 990 mm, and the pitch is set at twice the width of the panel (3320mm). Table 6.6 show the loss due to mutual shading with a shading limiting angle of 21.1°. To achieve a smaller limiting angle, a larger pitch is required. This is a question of the available area for the solar PV system. Shading should be avoided if possible.

Table 6.6 also illustrates how losses are reduced when using module instead of string inverters. This will not only apply to losses due to shading, but also other losses such as dirt on the panels.

Table 6.6 The effect of mutual shed shading on an array of polycrystalline modules with string, module or mini central inverters.

Polycrystalline CENTROSOLAR 255 Wp	Inverter		
	Sunny mini central 4600	SB 4000 TL-21	APS YC500
# Modules in series	11	10	1
# Strings	4	4	40
# Rows/Sheds	4	4	10
Tilt°	25	25	25
Azimuth °	-100	-100	-100
Shading limiting angle °	21,1	21,1	21,1
Yearly production without shading [kWh/yr]	17067	15683	15299
Yearly production with shading [kWh/yr]	16646	15301	15226
Loss in percentage [%]	2,5	2,4	0,5
Normalized production with shading [kWh/kWp/day]	4,06	4,11	4,09

6.2.5 Detailed losses

The losses set at their default values will not be discussed in any detail.

As discussed earlier, the efficiency of a solar cell decreases with increasing temperature. From the simulation results, the detailed system losses (in Appendic C) due to temperature are found to be -3.8% for CdT modules, -6.7% for monocrystalline modules, -6.3% for polycrystalline modules and -4.8% for CIS modules. The ambient temperatures used in the simulation are the temperatures from Thika Met. Station.

The temperature coefficients for the different modules (table 5.2, chapter 5.2.4), show that crystalline solar cells have higher sensitivity to temperature, and that the CdT is least

affected by higher temperatures. Both crystalline modules also have light induced degradation (LID) losses of 2%. It is also worth noting that monocrystalline modules are also more sensitive to changes in irradiance level. Only the CdT module experience loss in module quality.

The average normalized array losses are presented in table 6.7. To reduce losses due to temperature different cooling systems should be considered. Reducing the temperature with 2°C, will increase the output power of a polycrystalline array with 0,86%.

Table 6.7 Average normalized array losses for four different PV modules

	Average normalized array losses [kWh/kWp/day]
CIS	0,56
CdT	0,72
Monocrystalline	0,85
Polycrystalline	0,88

When studying the different losses by module type, inverter loss is of less importance since all simulations have been performed with the same inverters. Difference in inverter loss during operation are explained earlier in this thesis.

6.2.6 Discussion

The results from chapter 6.2.1-6.2.5 are summed up in table 6.8. All results are found through simulations in PVsyst. The table summarizes how the different input parameters changes the energy output of the inverter, and show a variation in normalized system production from 3.61-4.44 kWh/kWp/day. This is a difference of 18.7%.

The case study by Silva et al. [15] show a normalized production of 4.6 kWh/kWp/day, while the report by Georg Hille et al. [6] estimates a specific production of 1389 kWh/kWp/year, giving a normalized production of about 3.8 kWh/kWp/day. The

evaluated PV systems in both studies are located in Nairobi. Nairobi as a location, although with a higher altitude (1811m), is assumed to have similar radiation and weather conditions as the investigated location. Irradiation levels are expected to be slighter higher due to the increase in altitudes. Also, the reduced temperature will ha a positive impact on the system production. When comparing the Meteonorm data for Nairobi they show a yearly GHI of 1932 kWh/m2, within the range of the investigated databases for Yatta, but 2.6% higher than the Meteonorm data for Yatta. Temperatures are on average 0.2°C lower [12].

The table shows that the PV system is most sensitive to changing the radiation data. As a number two is the type of module, and the tilt and orientation of the system. The module that shows the highest production is the CIS module. This is probably mainly because of reduced array losses with increased temperature compared to the other modules.

As long as a tilt of minimum 20° is set as a requirement for the system, the changes in azimuth does not affect the production on a yearly basis much as long as the panels are not oriented northwards.

The choice of inverter does not affect the nominal production much, but when the PV system is subject to losses from for partial shading the type of inverter plays an important role. If several smaller inverters (either string or module) are chosen instead of one central inverter, it is also easier to expand the system. The multiple-string inverter can be a good choice for systems of this size. Reducing the number of inverters compared to using module and string inverters, but with multiple MPPT trackers [54] to increase production.

Table 6.8 Base case and system simulations for different input parameters and their corresponding normalized production. The percentage change is when compared to the base case simulation

1. Base Case		Normalized production [kWh/kWp/day]	Percentage change [%]
(as described in chapter 5.2) PVGIS CMSAF		4,17	
2. Meteorological data			
SWERA		3,61	-13,4
Meteonorm		3,89	-6,7
3. Orientation			
Tilt 0°		4,40	5,5
Tilt 20°	Azimuth 0° (N)	4,16	-0,2
	Max value, Azimuth -100° – -110°	4,25	1,9
	Azimuth 90°	4,20	0,7
Tilt 25°	Azimuth 0° (N)	4,04	-3,1
	Max value, Azimuth -100° – -110°	4,17	0,0
	Azimuth 90°	4,11	-1,4
Tilt 30°	Azimuth 0° (N)	3,90	-6,5
	Max value, Azimuth -100° – -110°	4,07	-2,4
	Azimuth 90°	4,01	-3,8
Tilt 25°	Heterogeneous orientation facing East/West	4,14	-0,7
4. Array			
Monocrystalline		4,20	0,7
Polycrystalline		4,17	0,0
CdT		4,34	4,1
CIS		4,44	6,5
5. Inverter			
Multi-string	Pnom array/inverter: 1,11	4,22	0,7
	Pnom array/inverter: 1,28	4,21	1,0
String	Pnom array/inverter: 1,28	4,14	-0,7
Module	Pnom array/inverter: 1,02	4,11	-1,4
Mini central	One mini central inverter. Pnom array/inverter: 1,19	4,24	1,7
	Two mini central inverters (base case). Pnom array/inverter: 1,22	4,17	0,0
6. Shading			
With mutual shading from shed		4,06	-2,6

For a potential PV system at MCF Yatta there are several factors to consider

- The size of the system
- Its location and orientation
- Its use for educational purposes
- Potential backup during power outings

As long as no FITs for systems of this size exists, feeding electricity to the grid is not an option. The simulations done in PVsyst can easily be multiplied up, although larger systems are assumed to have higher system efficiencies [6].

Given the average power load of 30kW, and studying the daily load curve (figure 2.6), it is likely to assume that the power during daytime (between 7AM and 7PM) will drop below 20kW. A typical daily PV production curve (example in figure 6.9) reaches its maximum around solar noon. The daily load curve also has a maximum of about 50kWp. If the system is placed in two directions, east and west, this will further even out the power production from the PV system as discussed earlier. Sizing a system to at least 30kWp, and maximum 50kWp, should not produce peak load excess energy. A 50kWp PV system will have a minimum production of 65.9 MWh and a maximum of 81.0 MWh.

If excess energy is produced, there are several possibilities for "energy storage" at Yatta. There is a 15kW pump that pumps water from the dam to a reservoir/tank. The dip in the daily load curve is for a period when the pump is not running. For a 50kWp system, potential excess energy can be stored by pumping water from the dam to the tank. Another option is two use the excess energy for the heating of water. According to estimates in chapter 2.6, the yearly energy need is at least 100MWh.

The monthly highest production (January-March) also corresponds well when the need for irrigation is at its highest.

The system can be located both on ground and as a rooftop installation. Because the solar PV system at MCF Yatta also will be used for educational and training purposes, a ground mounted system is considered most adequate. Also, due to its low tilt, the panels ought to be cleaned regularly to avoid soiling losses. This is easier for a ground based system. Framless modules should be considered if available to reduce soiling losses. Because of

the high losses due to temperature, a location that is well ventilated will give higher yields. If the system is placed on a roof, the roof should be flat, and the PV system mounted with free circulation of air. To reduce heat transfer from the roof to the panels, the roof (if black) could be painted white to reduce absorption.

According to the head of the agricultural depertment at MCF Yatta, Joshua Nyalia, the grid is relatively stable, and power outages are estimated to occur maximum once a week, lasting 8 hours as a worst case scenario. If one assumes half of the outages occur during daytime, the PV system will be down about 2.4% of the time. Today there is a diesel generator that starts up when the grid is down. The average yearly fuel use of this generator is 1400 l. With a backup system (as described in chapter 4.2.3), both the fuel cost for the generator and the down time for the PV system would be reduced.

6.3 Economic analysis

6.3.1 Results

The results from the sensitivity analysis and the base case are presented in table 6.9. The corresponding EXCEL spreadsheets are found in appendix C. The net present value has also been calculated in excel assuming a yearly increase in electricity price of 5% (see chapter 5.3). For the base case the net present value is -350000 KES. To achieve a positive NPV the discount rate has to be reduced from 10% to 8%.

The LCOE sensitivity analysis display values between 18.3 – 36.3 KES/kWh.

Table 6.9 LCOE values and sensitivity analysis for a simulated PV system at Yatta with an installed capacity of 10,2 kWp

Parameter	KES/ kWh	Change in % compared to Base Case	USD/ kWh	euro/ kWh
1. Base Case				
(as described) Data from PVGIS CM-SAF	27,3		0,30	0,24
2. Plant lifetime (years)				
15	29,7	9,0	0,33	0,27
25	26,1	-4,2	0,29	0,23
30	25,6	-6,3	0,28	0,23
3. Investment cost (euro/kWp)				
€ 1 000	18,3	-33,0	0,20	0,16
€ 1 800	32,7	19,8	0,36	0,29
€ 2 000	36,3	33,1	0,40	0,32
4. Operating cost (percent)				
1 %	25,6	-6,0	0,28	0,23
1,5 %	26,5	-3,0	0,29	0,24
5. Discount rate (percent)				
5 %	22,7	-16,8	0,25	0,20
8 %	25,4	-6,9	0,28	0,23
15 %	32,3	18,2	0,36	0,29
6. Degradation factor (percent)				
0,20 %	26,8	-1,9	0,30	0,24
1,50 %	29,1	6,5	0,32	0,26
7. Production				
16220 kWh /kWp per year	25,5	-6,6	0,28	0,23
13177 kWh /kWp per year	31,5	15,4	0,35	0,28
9. Loan share				
0 %	16,8	-38,5	0,19	0,15
50 %	23,3	-14,4	0,26	0,21
100 %	29,9	9,6	0,33	0,27
10. Interest rate on loan				
5 %	24,7	-9,5	0,27	0,22
15 %	30,8	13,1	0,34	0,28

6.3.1.1 Discussion

The results in table 6.9 display that the investment cost, and the method for financing is the determining factors for the LCOE of the system. Of second most importance is the discount rate and the estimated production. According to the report by Hille [6], the electricity yield is the dominant determing factor for the deviation of the LCOE. Nr two is the associated investment cost.

Compared to current electricity tariffs in Kenya of 20KES/kWh, the simulated base case yield higher electricity prices for the PV system than purchasing the electricity directly from the grid. Georg Hille et al. [6] suggest that electricity prices will increase with 5% every year. If this is correct, prices will exceed 30 KES/kWh in less than ten years and the system will reach grid parity.

The article by Georg Hille et al. [6] suggest LCOE of about 32.1 KES/kWh in Nairobi in 2011 (with an exchange rate similar to that of today), and the study by Ondraczek [12] suggest a LCOE ranging from USD 0.17–0.30/kWh. In his study, Ondrazcek suggest that solar PV LCOE is lower than expected, and when compared to other peak load technologies it might already be competitive.

For the system to be sustainable in the long term, the running O&M costs should be covered by the income of the system, i.e. the reduced electricity purchase. The running cost of the system is lower than the saved electricity cost for the base case at all times (see Excel spreadsheet in appendix C). The high upfront installation and the corresponding discount rate is what make this project unprofitable.

7 Conclusions

For the yearly production of the system the evaluation of the meteorological data are of uttermost importance. Changes in the radiation data are the one factor that influences the system output most. There are high uncertainties linked to the data, and a difference from 1482 kWh/m^2 per year for the 2001 SWERA data to 2033 kWh/m^2 per year for the PVGIS CM-SAF data. This yields a difference of 27% from the best to the most conservative yield. Eliminating the SWERA data due to its short measured time period (only one year per set), the data from Meteonorm is considered the most conservative estimate, at 1882 kWh/m^2 per year. In general, it is difficult to conclude on which meteorological data set that is the most probable for Yatta.

The simulated irradiation data yield a normalized system production of between 3.89 – 4.17 kWh/kWp per day. The case study by Silva et al. [15] on the energy performance of a 10kWp plant in Nairobi show a normalized system production of 4.6 kWh/kWp per day, based on actual system measurements. Even though Nairobi is assumed to have somewhat higher values than Yatta (about 2.6% in the Meteonorm database), this still give a normalized production higher than the simulated (4.48 kWh/kWp per day). The report by Georg Hille et al. [6] uses a normalized production of about 3.8 kWh/kWp/day in their report.

The PV system should have an optimal orientation somewhere between east, south and west, depending on the input irradiation data. Generally, the system should have a low tilt, but not below 20° due to soiling losses. If possible, the system should avoid partial shading.

The economic analysis of a potential system show that the LCOE for a large system (i.e. lower module prices) is from 18.3 KES/kWh to 27.3 KES/kWh. With today´s electricity price of 20KES the profitability of the system is dependent on installation costs. Medium installation costs (1500 euro/kWp), and a loan share of 50% results in a LCOE of 23.3 KES/kWh. This is a value relatively close to today´s tariff. There are several uncertainties linked to the economic analysis and the choice of variables. To better estimate the actual system cost, exact installation values should be collected from Kenyan companies specializing in the installation of small commercial PV systems instead of the average

values used in this study. It is assumed that a net-metering system soon will be put in place. This will also alter the economic viability of the project.

Hard to quantify, and not included in the economic analysis is the potential environmental benefit of a solar PV system. About a fourth of the country´s electricity production today is from fossil-fuel power plants. By increasing the share of renewable energy in, the production from these plants will be reduced (as it is today with increased hydropower production). The reduced fuel use is not only an environmental benefit. Renewable energy systems also increases the energy self-sufficiency and reduce transmission line costs due to the decentralized energy production.

The aim of the project being to "enable replication of 'Best Practices' in the area of renewable energy", a PV system can be used for educational purposes, and for training operating personnel within the photovoltaic field. As summarized in the study by Hirmer and Cruickshank [23] (in chapter 2.2.1) common barriers for the implementation of rural energy systems are financial (high upfront cost, dependency on subsidies), technical (low technical skill levels) and social (lack of ownership). This project is being development in corporation with, and as a response to an inquiry by MCF to estimate the potential for use of solar energy. Therefore it can be claimed that the implementation of a system maintain local ownership. The training center will develop the required skills for the operation and maintenance of a solar PV system.

When considering the final system, all of the above factors should be taken into account.

7.1 Recommendation for further work

When the final size of the system is decided, a more detailed system design should be carried out for the selected sizing. Losses due to temperature should be analyzed more closely, and also how these be decreased.

Also, one should further explore the possibility for adding a suitable back up system so that the system can work during the (somewhat) frequent power outages experienced at MCF Yatta.

References

1. International Energy Agency (IEA). (2013). *World energy outlook - Executive summary*. Paris: OECD.

2. Shikha, S. & Ravindranath, N. H. (2007). Decentralized energy planning; modeling and application—a review. *Renewable and Sustainable Energy Reviews*, 11 (5): 729-752.

3. Kaundinya, D. P., Balachandra, P. & Ravindranath, N. H. (2009). Grid-connected versus stand-alone energy systems for decentralized power—A review of literature. *Renewable and Sustainable Energy Reviews*, 13 (8): 2041-2050.

4. Clancy, J. (2011, 2011). *Small-scale energy systems on a large-scale in developing countries*. First International Engineering Symposium, The impact of engineering in regional development. 14 pp.

5. REN21. (2014). Renewables 2014 Global Status Report. In Secretariat, R. (ed.). Paris.

6. Georg Hille et al. (2011). Technical and Economical Assessment of Net-Metering in Kenya. In Franz, M. (ed.): Deutsche Gesellschaft für Internationale Zusammenarbeit (GIZ).

7. Haberlin, H. (2012). *Photovoltaics : system design and practice*. Chichester, West Sussex: John Wiley & Sons Ltd. xxix, 701 p. pp.

8. Schillings, C., Meyer, R. & Trieb, F. (2004). High resolution Solar Radiation Assesment for Kenya. In Deutsches Zentrum für Luft- und Raumfahrt (DLR) (ed.). SWERA/UNEP.

9. IEA. & OECD iLibrary. (2014). *Solar Photovoltaic Energy*. IEA Technology Roadmaps,. Paris: OECD Publishing,.

10. Kammen, D. M. Case study 5: The Commercial Dissemination of Photovoltaic Systems in Kenya: IPCC.

11. Meza, E. (2013). Special Report Africa: Kenya. *pv magazine*.

12. Ondraczek, J. (2014). Are we there yet? Improving solar PV economics and power planning in developing countries: The case of Kenya. *Renewable and Sustainable Energy Reviews*, 30 (0): 604-615.

13. National Renewable Energy Laboratory (NREL). Solar and Wind Energy Resource Assesment (SWERA). In *United Nations Environment Programme (UNEP)*.

14. Gichungi, H. (2012). *Workshop paper: Progress report on use of Renewable Energy in off-grid areas*

15. Silva, I. D., Ronoh, G. & Ndegwa, J. (2013). *Energy Performance of Grid Connected Solar PV Systems in Kenya- Case Study:Technical, economical and policy analysis of the Strathmore University 10 kW PV System*.

16. Deutsche Gesellschaft für Internationale Zusammenarbeit (GIZ). *Pioneering grid-connected solar PV systems in Kenya – SOS Children's Village Mombasa goes green with German technology*

17. Hansen, U. E., Pedersen, M. B. & Nygaard, I. (2013). *Review of Solar PV market development in East Africa*. UNEP Risø Centre Working PaperSeries no. 12 ed.: UNEP Risø Centre Technical University of Denmark. 22 pp.

18. Tutturen, K. A. (2013). *Industrial charcoal production with power generation at Mully Children's Family Yatta, Kenya*. Norwegian University of Life Sciences, Dept. of Mathematical Sciences and Technology (IMT).

19. Observ'ER. (2013). Chapter 3: Electricity production from renewable sources: details per region and per country (3.10.6. Kenya). In Observ'ER (ed.). *Worldwide electricity production from renewable energy sources*

20. Ministry of Energy. (2012: 2nd revision). *Feed-i tariffs policy for wind, biomass, small-hydro, geothermal, biogas and solar generated electricity*. Ministry of Energy: Republic of Kenya.

21. Ministry of Energy. (2012: Third draft). *National Energy Policy*. Energy, M. o.: Republic of Kenya.

22. Ulsrud, K., Winther, T., Palit, D., Rohracher, H. & Sandgren, J. (2011). The Solar Transitions research on solar mini-grids in India: Learning from local cases of innovative socio-technical systems. *Energy for Sustainable Development*, 15 (3): 293-303.

23. Hirmer, S. & Cruickshank, H. (2014). The user-value of rural electrification: An analysis and adoption of existing models and theories. *Renewable and Sustainable Energy Reviews*, 34 (0): 145-154.

24. Müggenburg, H., Tillmans, A., Schweizer-Ries, P., Raabe, T. & Adelmann, P. (2012). Social acceptance of PicoPV systems as a means of rural electrification — A socio-technical case study in Ethiopia. *Energy for Sustainable Development*, 16 (1): 90-97.

25. Mully Children's Family. *About Mully Children's Family* [homepage]. Available at: http://www.mullychildrensfamily.org/about/view/about_mcf (accessed: 15.08).

26. enok.no. *Enøkguiden*. http://www.enok.no/enokguiden/07_2.html (accessed: 22.08).

27. Chen, C. J. (2011). *Physics of solar energy*. Hoboken, N.J.: John Wiley & Sons. xxvi, 326 p., 16 p. of plates pp.

28. Paulescu, M., Gravila, P., Badescu, V., Paulescu, E. & SpringerLink (Online service). (2013). *Weather Modeling and Forecasting of PV Systems Operation*. Green Energy and Technology. London: Springer London : Imprint: Springer. XVIII, 355 s. 166 illus. pp.

29. Markvart, T. (2000). *Solar electricity*. 2nd ed. Energy engineering learning package. Chichester ; New York: Wiley. xiv, 280 p. pp.

30. Badescu, V. (2008). *Modeling solar radiation at the earth's surface : recent advances*. Berlin: Springer. xxxiii, 517 p. pp.

31. Fu, W. Q. (2006). 4 - Radiative Transfer. In Wallace, J. M. & Hobbs, P. V. (eds) *Atmospheric Science (Second Edition)*, pp. 113-152. San Diego: Academic Press.

32. PVsyst. *PVsyst contextual help (built-in software)*. http://files.pvsyst.com/help/index.html.

33. McEvoy, A. J., Markvart, T. & Castañer, L. (2012). *Practical handbook of photovoltaics : fundamentals and applications*. 2nd ed. Waltham, MA: Academic Press. xxiv, 1244 p. pp.

34. Markvart, T. & Castañer, L. (2003). *Practical handbook of photovoltaics : fundamentals and applications*. New York: Elsevier Advanced Technology. xiv, 984 p. pp.

35. Gu, L., Fuentes, J. D., Garstang, M., Silva, J. T. d., Heitz, R., Sigler, J. & Shugart, H. H. (2001). Cloud modulation of surface solar irradiance at a pasture site in southern Brazil. *Agricultural and Forest Meteorology*, 106 (2): 117-129.

36. UNEP. (2008). *SWERA country report: Kenya*. In UNEP (ed.). http://en.openei.org/datasets/files/864/pub/kenya_swera-country_reportsmall.pdf.

37. United Nations Office at Nairobi (UNON). *Climate in Kenya*. http://dcs.unon.org/index.php?option=com_content&view=article&id=124&Itemid=171&lang=en.

38. McSweeney, C., New, M. & Lizcano, G. (2010). *UNDP Climate Change Country Profiles: Kenya* http://country-profiles.geog.ox.ac.uk/ (accessed: 01.10.2014).

39. Stapleton, G. & Neill, S. (2012). *Grid-connected solar electric systems the Earthscan expert handbook for planning, design and installation*. Earthscan expert series. London: Earthscan. xx, 235 s. pp.

40. Solar Frontier. *Product overview: SF150-170-S Series*. http://www.solar-frontier.eu/fileadmin/content/downloads/modules/en/20141030/EN_Productoverview_S-SF145-170.pdf (accessed: 01.06).

41. Virtuani, A., Pavanello, D. & Friesen, G. *Overview of temperature coefficients of different thin film photovoltaic technologies*.

42. Altenergy Power System (APS). *APS M1P-SAA Single-phase Micro-inverter Installation and User Manual* http://s3.amazonaws.com/acsolar/attachments/242/downloads/APS%20M1P-SAA%20%20Datasheet_REV4.0.pdf?1384128283 (accessed: 05.12).

43. Sher, H. A. & Addoweesh, K. E. (2012). Micro-inverters — Promising solutions in solar photovoltaics. *Energy for Sustainable Development*, 16 (4): 389-400.

44. OutBack Power Technologies. (2013). *Adding the battery back-up power option to existing grid-tied PV/solar systems* http://hespv.ca/hesproductspecs/technical-bulletins/outback/outback-whitepaper.pdf (accessed: 07.12).

45. *Datahseet: SMA SUNNY ISLAND 3.0M/4.4M*. http://www.sma.de/en/products/battery-inverters/sunny-island-30m-44m.html (accessed: 07.12).

46. Meteonorm. (2014). *Handbook part II: Theory*. Global Meteorological Database. http://meteonorm.com/images/uploads/downloads/mn71_theory.pdf.

47. NASA Langley ASDC. (2013). *Surface meteorology and Solar EnergyA renewable energy resource web site* https://eosweb.larc.nasa.gov/sse/ (accessed: 22.11.2014).

48. European Commission, J. R. C. & Institute for Energy, R. E. U. (2012). *Photovoltaic Geographical Information System (PVGIS),*. http://re.jrc.ec.europa.eu/pvgis/.

49. European Commission, J. R. C. & Institute for Energy, R. E. U. *PVGIS radiation databases,*. http://re.jrc.ec.europa.eu/pvgis/apps4/databasehelp_en.html.

50. pvresources.com. *Standards*. http://www.pvresources.com/Standards.aspx (accessed: 01.06).

51. Centrosolar. *S-Class Professional: 245-260Wp*. http://www.centrosolar.de/fileadmin/user_upload/downloads/product_info/td_s-class_p60_professional_EN_20140624.pdf (accessed: 01.06).

52. First Solar. *Data sheet: FS Series 3*. http://www.firstsolar.com/~/media/documents/data-sheets/module%20data%20sheet/pd-5-401-03_series3black-4.ashx (accessed: 01.06).

53. Suntech. *Datasheet: STP250S/260S-20/Wd*. http://de.krannich-solar.com/fileadmin/content/data_sheets/solar_modules/STP245S-260S_Wd_Mono_EN_AD_Free.pdf (accessed: 01.06).

54. SMA. *Datasheet: Sunny Boy 3000TL / 3600TL / 4000TL / 5000TL* http://files.sma.de/dl/15330/SB5000TL-21-DEN134924W.pdf (accessed: 02.06).

55. SMA. *Datasheet: Sunny mini central 9000TL*. http://files.sma.de/dl/5710/SMC11000TL-DEN102330.pdf (accessed: 01.06).

56. SMA. *Datashett: Sunny mini central 4600A/5000A/6000A*. http://files.sma.de/dl/16191/SMC6000A-11-DEN123112w.pdf (accessed: 02.06).

57. Mani, M. & Pillai, R. (2010). Impact of dust on solar photovoltaic (PV) performance: Research status, challenges and recommendations. *Renewable and Sustainable Energy Reviews*, 14 (9): 3124-3131.

58. Branker, K., Pathak, M. J. M. & Pearce, J. M. (2011). A review of solar photovoltaic levelized cost of electricity. *Renewable and Sustainable Energy Reviews*, 15 (9): 4470-4482.

59. Kost, C., Mayer, J. N., Thomsen, J., Hartmann, N., Senkpiel, C., Philipps, S., Nold, S., Lude, S., Saad, N. & Schlegl, T. (2013). Levelized Cost Of Electricity Renewable Energy Technologies. In Fraunhofer Insitute for Solar Energy Systems ISE (ed.).

60. Kenya Power. (2014). *FERFA summary December 2014*. http://www.kplc.co.ke/index.php/content/item/571/FERFA-Summary-December-2014 (accessed: 20.12).

61. Central Bank of Kenya. (2014). *Central Bank Rate (CBR)*. https://www.centralbank.go.ke/index.php/interest-rates/central-bank-rate (accessed: 18.12.2014).

62. XE currency converter. (2014). *Currency converter*. http://www.xe.com/currencyconverter/ (accessed: 20.12).

63. UNEP. *Datsets*. http://en.openei.org/datasets/dataset?tags=SWERA (accessed: 15.06).

Appendices

A Meteorological Data

Data from SWERA

Thika (Lat. 1.0°S, long.37.1°E, alt.1574m) Thika imported ASCIIfile 2001 and 2002: Meteo for Thika (from SWERA) Data recorded from 01.01.2002 to 31.12.2002, and 01.01.2001 to 31.12.2001		
	GlobHor kWh/m².mth	
	2002	2001
Jan	168	128
Feb	153	154
Mar	150	147
Apr	153	140
May	126	126
Jun	90	90
Jul	78	78
Aug	92	96
Sep	119	127
Oct	142	134
Nov	123	123
Dec	142	139
Year	1536	1482

Comparison of different meteorological databases for temperature and irradiation

	Avarage external temperature		
Month	Nasa	Meteonorm 6.1	Thika met. Station
January	21,5	19,9	20,3
February	22,4	20,9	21,0
March	22,0	20,9	21,7
April	21,8	19,9	21,6
May	21,7	19	20,8
June	21,1	17,9	19,6
July	20,5	17	19,6
August	20,7	17,4	18,6
September	21,6	18,9	20,4
October	21,9	19,7	20,6
November	20,8	19,7	20,0
December	20,6	19,4	20,0

	Horizontal global irradiation (kWh/m^2 mth)					Diffuse horizontal irradiation (kWh/m^2 mth)				
	PVGIS	PVGIS - CM SAF	NASA	Meteonorm 6.1	Helioclim-3	PVGIS	PVGIS-SAF	**NASA**	Meteonorm	Helioclim-3
January	199,3	193,4	198,7	190,6	210,8	59,8	58	54,6	67,7	56,5
February	191,8	184,5	194,3	175,3	219	51,8	53,5	48,4	64	63,2
March	201,5	193,8	198,7	189	187,1	62,5	65,9	63,2	76,2	65,1
April	179,4	175,2	167,4	155,4	197,7	61	64,8	61,5	71,5	56
May	169,3	165,2	153,4	142,9	165,1	62,6	62,8	59,8	70,4	63,9
June	139,8	138,6	131,1	123,5	190,9	61,5	65,1	56,7	64,8	57,9
July	133	130,8	132,4	117,8	175,8	65,2	69,3	60,1	60,4	71,3
August	140,1	137	141,4	126,3	204,4	67,3	74	64,5	65,1	61,7
September	173,4	170,1	171,6	154	182,3	65,9	64,6	63,3	70,5	66,2
October	189,1	178,9	178,9	172,5	195,5	66,2	71,5	66	71,2	62,4
November	170,1	161,1	156,9	158,4	217,9	64,6	69,3	63,9	66,8	55,1
December	189,1	204,6	180,1	176,5	232,9	60,5	81,8	59,2	64,9	51,8
	2075,9	**2033,2**	**2004,9**	**1882,2**	**2379,4**	**748,9**	**800,6**	**721,2**	**813,5**	**731,1**

	THIKA AGROMET STATION 9137048												
	Year	Jan	Feb	Mar	April	May	June	July	August	Sep	Oct	Nov	Dec
Temperature; daily av. max	2007	25,6	28,3	27,8	26,3	25,5	25	23	23,3	26,3	26,8	22	22,9
Temperature; daily av. min	2007	15	14	14,8	16,1	16	14,1	13,5	13,9	13,4	13,3	14,2	13,5
Temperature; daily av. max	2008	26,9	27,3	28,2	25,8	25,3	23,7	23,1				22,9	23,7
Temperature; daily av. min	2008	13,6	13,3	15,8	15,8	15	13,5	13,3				14,7	14,6
Temperature; daily av. max	2009	28,6	29,2	30,4	28,2	26,6	28	25,4	25,2	28,6	26,9	24,7	25,05
Temperature; daily av. min	2009	12,9	13,9	14,7	16,5	15,8	14	11,5	12,9	14,1	14,7	15,25	14,5
Temperature; daily av. max	2010	26,4	27,3	26,6	26,7	25,5	24	23,3	23,6	26,7	28	24,8	26,5
Temperature; daily av. min	2010	14,2	16,4	15,5	17	16,15	14,3	12,7	12,8	12,9	15,3	15,6	13,9
Temperature; daily av. max	2011	27,9	29,2	29,1	26,9	26	25,3	25,75	23,8	26,4	26,5	25,5	26,05
Temperature; daily av. min	2011	12,25	12,05	13,8	16,75	15,95	14,3	11,7	13,5	14,2	15,7	16,1	14,9
Temperature; daily av. max	2012	28,2	29,3	30,3	26,6	25,8	24,1	32,2					
Temperature; daily av. min	2012	10,8	11,9	13,4	16,2	15,4	14	24,5					
Average daily maximum	2007-2012	27,3	28,4	28,7	26,8	25,8	25,0	25,5	24,0	27,0	27,1	24,0	24,8
Average daily minimum		13,1	13,6	14,7	16,4	15,7	14,0	14,5	13,3	13,7	14,8	15,2	14,3

Transposition Factors for simulation at Yatta

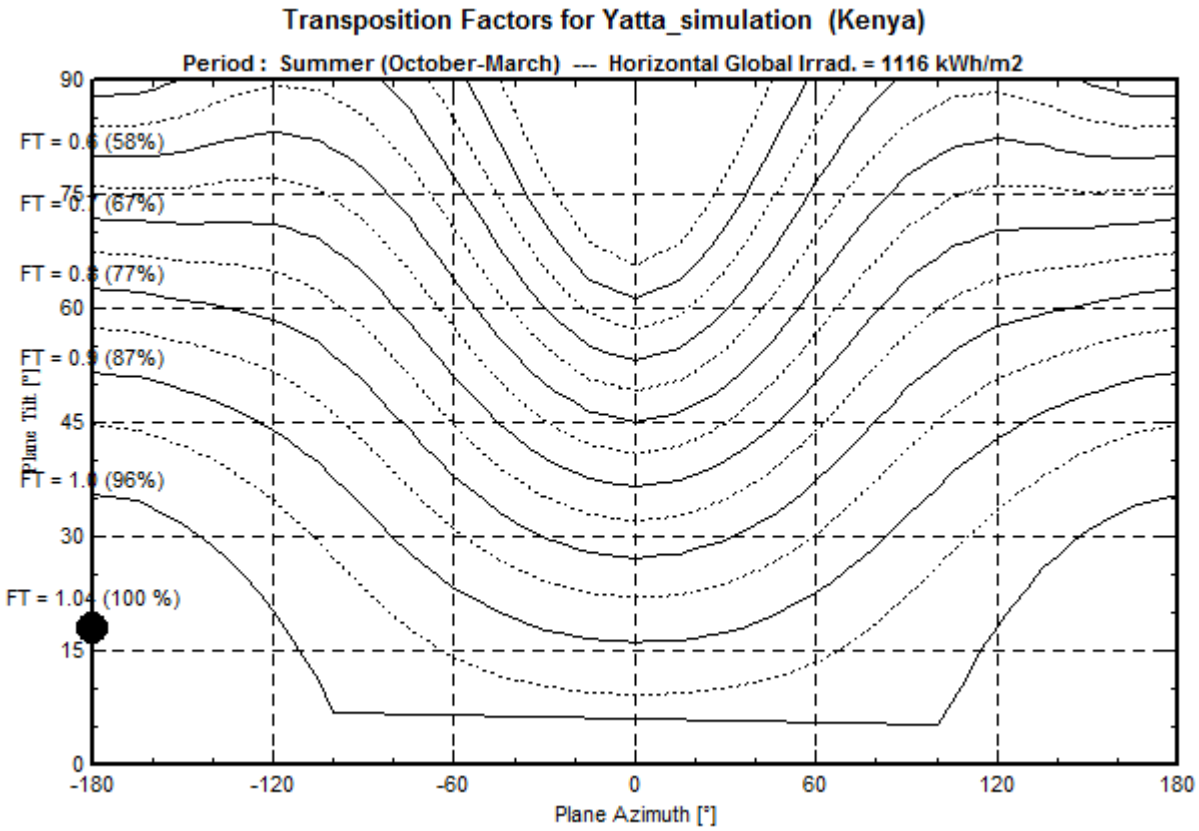

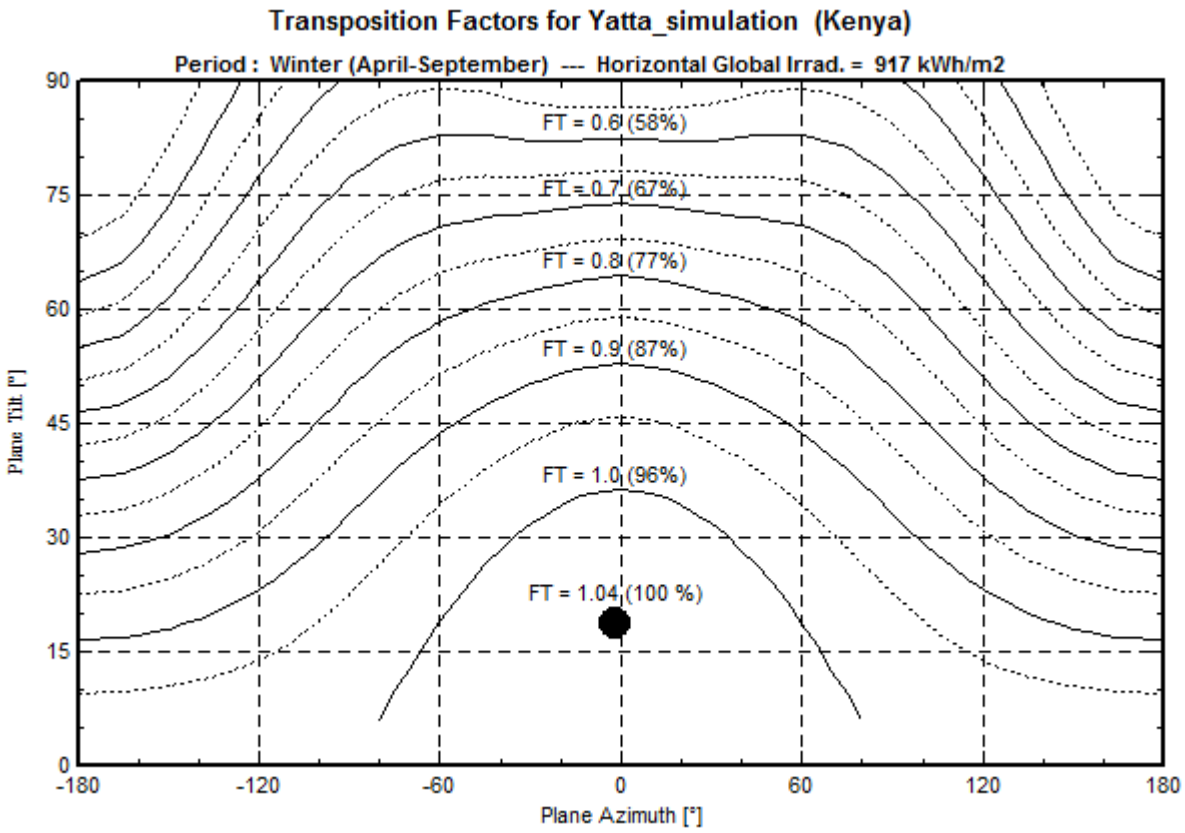
Transposition Factors for Yatta_simulation (Kenya)
Period : Winter (April-September) --- Horizontal Global Irrad. = 917 kWh/m2
FT = 0.6 (58%)
FT = 0.7 (67%)
FT = 0.8 (77%)
FT = 0.9 (87%)
FT = 1.0 (96%)
FT = 1.04 (100 %)
Plane Tilt [°]
Plane Azimuth [°]
90
75
60
45
30
15
0
-180
-120
-60
0
60
120
180

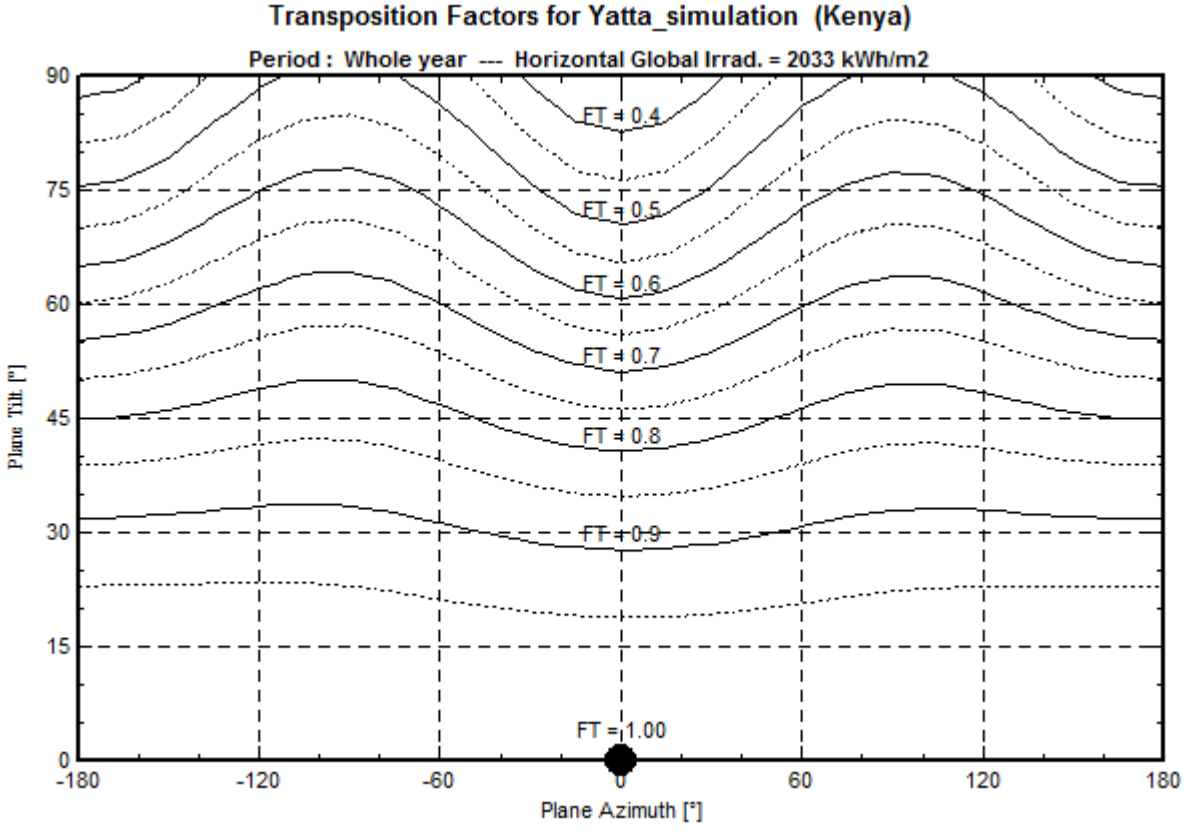
Transposition Factors for Yatta_simulation (Kenya)
Period : Whole year --- Horizontal Global Irrad. = 2033 kWh/m2
FT = 0.4
FT = 0.5
FT = 0.6
FT = 0.7
FT = 0.8
FT = 0.9
FT = 1.00
Plane Tilt [°]
Plane Azimuth [°]
90
75
60
45
30
15
0
-180
-120
-60
0
60
120
180

Monthly ratios for the diffuse to global irradiation

	Ratio diffuse/global irradiation				
	PVGIS	PVGIS – CMSAF	NASA	Meteonorm	Helioclim
January	30,0	30,0	27,5	35,5	26,8
February	27,0	29,0	24,9	36,5	28,9
March	31,0	34,0	31,8	40,3	34,8
April	34,0	37,0	36,7	46,0	28,3
May	37,0	38,0	39,0	49,3	38,7
June	44,0	47,0	43,2	52,5	30,3
July	49,0	53,0	45,4	51,3	40,6
August	48,0	54,0	45,6	51,5	30,2
September	38,0	38,0	36,9	45,8	36,3
October	35,0	40,0	36,9	41,3	31,9
November	38,0	43,0	40,7	42,2	25,3
December	32,0	40,0	32,9	36,8	22,2

B Simulation results from PVsyst

Normalized array production for the four different modules simulated

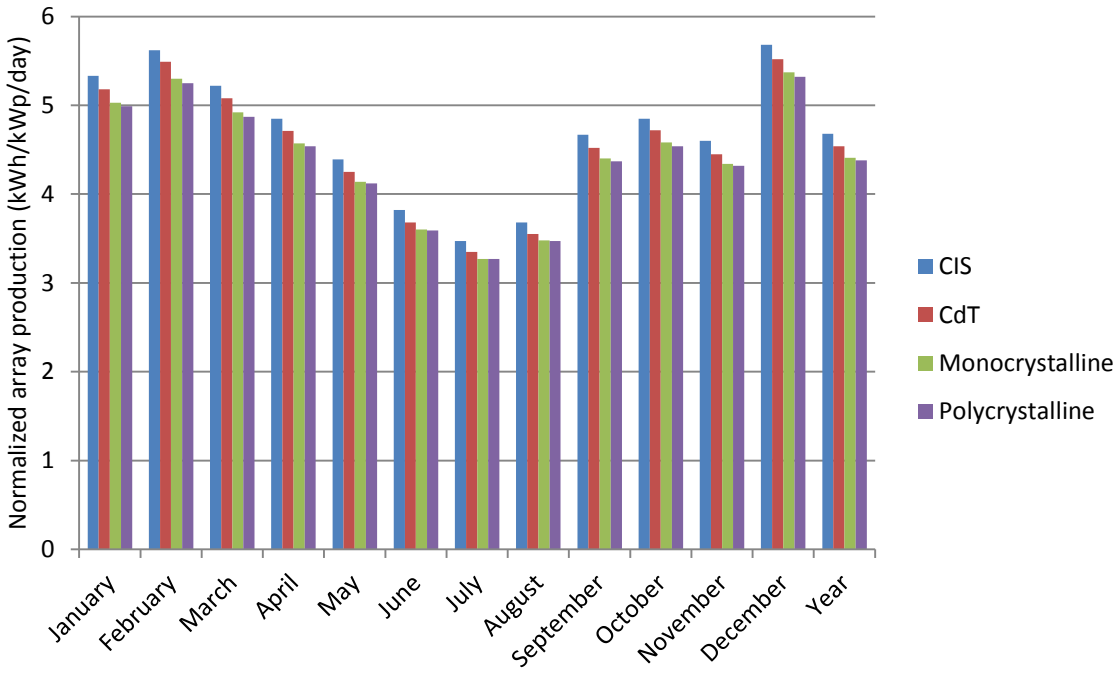

For the tables below the following definitions are used

Detailed inverter losses

EOutInv = Available energy at inverter output

EffInvR = Inverter efficiency (operating)

InvLoss = Global inverter losses

IL Oper = Inverter loss during operation (efficiency)

IL Pmin = Inverter loss due to power threshold

IL Pmax = Inverter loss over nominal inv. power

IL Vmin = Inverter loss due to voltage threshold

IL Vmax = Inverter loss over nominal inv. voltage

Detailed losses for polycrystalline modules with module inverters and a Pnom ratio of 1.02

Yatta_poly_micro

Detailed Inverter losses

	EOutInv	EffInvR	InvLoss	IL Oper	IL Pmin	IL Pmax	IL Vmin	IL Vmax
	kWh	%	kWh	kWh	kWh	kWh	kWh	kWh
January	1486	94.4	88.54	88.54	0.000	0.000	0.000	0.000
February	1415	94.4	83.61	83.61	0.000	0.000	0.000	0.000
March	1451	94.3	87.63	87.63	0.000	0.000	0.000	0.000
April	1304	94.2	80.25	80.25	0.000	0.000	0.000	0.000
May	1219	94.0	78.34	78.34	0.000	0.000	0.000	0.000
June	1024	93.5	71.02	71.02	0.000	0.000	0.000	0.000
July	958	93.1	71.12	71.12	0.000	0.000	0.000	0.000
August	1020	93.3	72.96	72.96	0.000	0.000	0.000	0.000
September	1255	94.0	79.81	79.81	0.000	0.000	0.000	0.000
October	1347	94.0	86.28	86.28	0.000	0.000	0.000	0.000
November	1236	93.8	81.14	81.14	0.000	0.000	0.000	0.000
December	1585	94.5	92.23	92.23	0.000	0.000	0.000	0.000
Year	15299	94.0	972.93	972.93	0.000	0.000	0.000	0.000

Detailed losses for polycrystalline modules with string inverters and a Pnom ratio of 1.11

Yatta_poly

Detailed Inverter losses

	EOutInv	EffInvR	InvLoss	IL Oper	IL Pmin	IL Pmax	IL Vmin	IL Vmax
	kWh	%	kWh	kWh	kWh	kWh	kWh	kWh
January	1519	96.5	55.61	55.61	0.000	0.000	0.000	0.000
February	1445	96.5	52.95	52.95	0.000	0.000	0.000	0.000
March	1484	96.5	54.44	54.44	0.000	0.000	0.000	0.000
April	1336	96.5	48.22	48.22	0.000	0.000	0.000	0.000
May	1252	96.5	45.72	45.72	0.000	0.000	0.000	0.000
June	1055	96.4	39.56	39.56	0.000	0.000	0.000	0.000
July	991	96.3	38.17	38.17	0.000	0.000	0.000	0.000
August	1053	96.4	39.65	39.65	0.000	0.000	0.000	0.000
September	1288	96.5	47.16	47.16	0.000	0.000	0.000	0.000
October	1382	96.4	51.28	51.28	0.000	0.000	0.000	0.000
November	1270	96.4	47.02	47.02	0.000	0.000	0.000	0.000
December	1620	96.6	57.51	57.51	0.000	0.000	0.000	0.000
Year	15695	96.5	577.30	577.30	0.000	0.000	0.000	0.000

Detailed losses for polycrystalline modules with string inverters and a Pnom ratio of 1.28

Yatta_poly_undersized

Detailed Inverter losses

	EOutInv	EffInvR	InvLoss	IL Oper	IL Pmin	IL Pmax	IL Vmin	IL Vmax
	kWh	%	kWh	kWh	kWh	kWh	kWh	kWh
January	1516	96.5	58.18	55.22	0.000	2.964	0.000	0.000
February	1437	96.5	61.54	52.45	0.000	9.085	0.000	0.000
March	1483	96.5	55.63	54.08	0.000	1.547	0.000	0.000
April	1336	96.5	48.02	47.82	0.000	0.198	0.000	0.000
May	1253	96.5	44.86	44.86	0.000	0.000	0.000	0.000
June	1056	96.5	38.58	38.58	0.000	0.000	0.000	0.000
July	992	96.4	37.14	37.14	0.000	0.000	0.000	0.000
August	1054	96.5	38.69	38.69	0.000	0.000	0.000	0.000
September	1288	96.5	46.53	46.52	0.000	0.010	0.000	0.000
October	1379	96.5	54.19	50.43	0.000	3.762	0.000	0.000
November	1271	96.5	46.14	46.10	0.000	0.039	0.000	0.000
December	1618	96.6	59.03	57.34	0.000	1.687	0.000	0.000
Year	15683	96.5	588.52	569.22	0.000	19.292	0.000	0.000

Detailed losses for polycrystalline modules with a central inverter and a Pnom ratio of 1.19

Yatta_poly

Detailed Inverter losses

	EOutInv	EffInvR	InvLoss	IL Oper	IL Pmin	IL Pmax	IL Vmin	IL Vmax
	kWh	%	kWh	kWh	kWh	kWh	kWh	kWh
January	1602	97.0	50.93	49.25	1.141	0.540	0.000	0.000
February	1523	96.9	49.71	47.73	0.642	1.338	0.000	0.000
March	1567	97.0	48.25	47.28	0.968	0.000	0.000	0.000
April	1412	97.2	41.08	41.08	0.000	0.000	0.000	0.000
May	1324	97.2	38.01	38.01	0.000	0.000	0.000	0.000
June	1117	97.2	32.35	32.15	0.196	0.000	0.000	0.000
July	1050	97.2	30.81	30.72	0.084	0.000	0.000	0.000
August	1116	97.2	31.98	31.87	0.111	0.000	0.000	0.000
September	1361	97.1	40.14	39.83	0.313	0.000	0.000	0.000
October	1460	97.0	44.75	44.14	0.273	0.338	0.000	0.000
November	1343	97.1	39.75	39.75	0.000	0.000	0.000	0.000
December	1710	97.1	50.79	50.79	0.000	0.000	0.000	0.000
Year	16587	97.1	498.57	492.62	3.728	2.216	0.000	0.000

Yearly system production with two different climate datasets and two different inverters

	PVGIS-CMSAF		Meteonorm	
Inverter	APS YC500	SMA 9000	APS YC500	SMA 9000
Nominal power Array	10,2 kWp	10,7 kWp	10,2 kWp	10,7 kWp
January	1538 kWh	1657 kWh	1523 kWh	1638 kWh
February	1448 kWh	1558 kWh	1391 kWh	1494 kWh
March	1481 kWh	1599 kWh	1455 kWh	1563 kWh
April	1320 kWh	1429 kWh	1198 kWh	1296 kWh
May	1226 kWh	1332 kWh	1070 kWh	1166 kWh
June	1028 kWh	1121 kWh	906 kWh	993 kWh
July	964 kWh	1056 kWh	878 kWh	964 kWh
August	1030 kWh	1126 kWh	945 kWh	1035 kWh
September	1282 kWh	1389 kWh	1155 kWh	1252 kWh
October	1383 kWh	1498 kWh	1342 kWh	1448 kWh
November	1278 kWh	1388 kWh	1255 kWh	1354 kWh
December	1643 kWh	1771 kWh	1437 kWh	1545 kWh
Yearly energy Production [kWh]	**15620**	**16925**	**14555**	**15748**

Loss diagram over the whole year for simulations with CdT modules (left) and monocrystalline modules (right). Figure from PVsyst

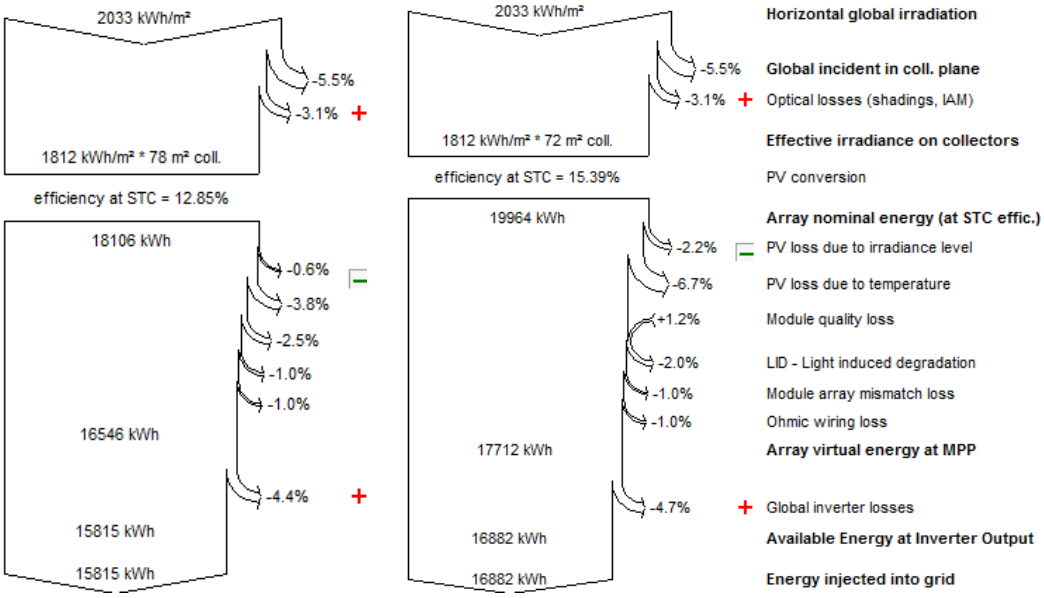

Loss diagram over the whole year for simulations with CIS modules(left) and polycrystalline modules (right). Figure from PVsyst

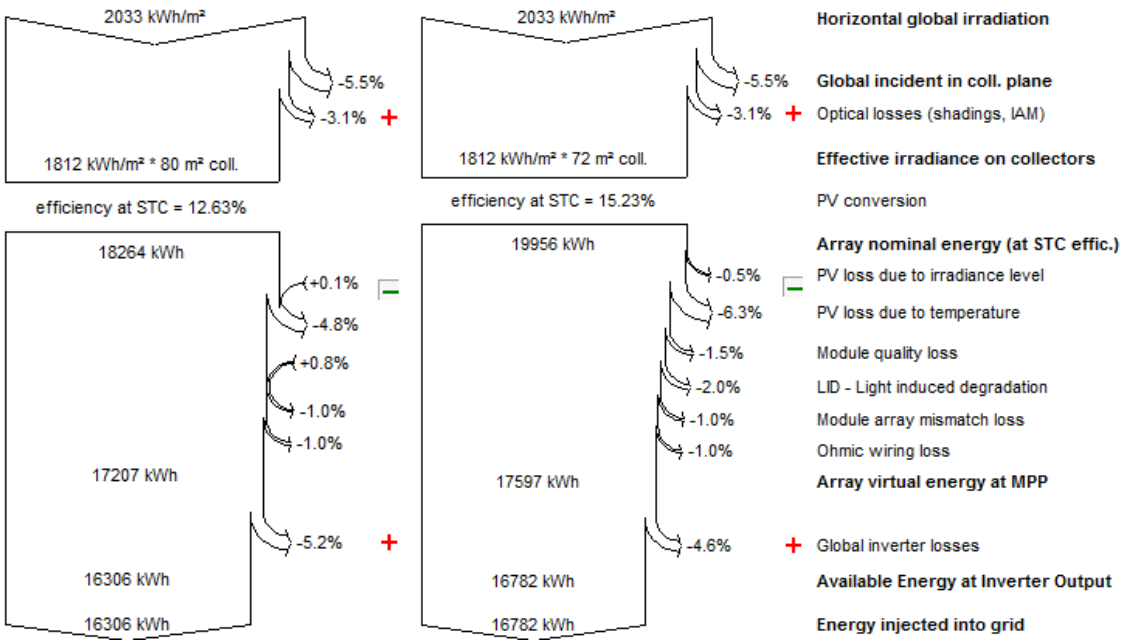

C Economical analysis

System Inputs		Direct Purchase Inputs		Direct Purchase Inputs	Small	Large
Discount rate	10,0 %	Price per Wp module	168	Subsidies	0 %	
Annual Degradation	0,50 %	Installed capacity (Wp)	10200	Purchase price (in euro)	1500	
Scrap value	0	other BoS per Wp	1,5	Exchange rate (KES/euro)	112	
Inflation rate	5 %	O&M per Wp/yr	0,025	Purchase price (in KES/kWp)	168000	
Production/kWp	1,52205	O&M (%)	2 %	Exchange rate (KES/USD)	90,3	
Interest rate	9,5 %	Investment cost	1728900	Purchase price (in UDS)	0	
Electrisity cost	20,0			Purchase price (in KES/kWp)	0	
				Sum	168000	

Year	Production (kWh)	Direct Purchase Cost ($)	O&M Cost (%)	Interest & down payment	Rate per year	NPV production	NPV cost (%)	LCOE	Saved el. Cost	Electricity price increase	Cost	Cash flow	Saved cost
0		1728900			1		1728900						
1	15 525		34578,0	220856,1	1,1	14113,6	232212,8	138,9524	310498	20	255434	55064	5,6388
2	15 447		36306,9	220856,1	1,2	12766,4	212531,4	80,8650	324393	21	257163	67230	4,8251
3	15 370		38122,2	220856,1	1,3	11547,7	194574,2	61,6280	338910	22	258978	79931	4,2400
4	15 293		40028,4	220856,1	1,5	10445,5	178187,6	52,1024	354076	23	260884	93191	3,7994
5	15 217		42029,8	220856,1	1,6	9448,4	163231,4	46,4603	369921	24	262886	107035	3,4561
6	15 141		44131,3	220856,1	1,8	8546,5	149578,4	42,7591	386475	26	264987	121487	3,1812
7	15 065		46337,8	220856,1	1,9	7730,7	137112,7	40,1660	403769	27	267194	136575	2,9564
8	14 990		48654,7	220856,1	2,1	6992,8	125728,8	38,2645	421838	28	269511	152327	2,7693
9	14 915		51087,5	220856,1	2,4	6325,3	115330,6	36,8233	440715	30	271944	168772	2,6113
10	14 840		53641,8	220856,1	2,6	5721,5	105830,8	35,7036	460437	31	274498	185939	2,4763
11	14 766		56323,9	220856,1	2,9	5175,4	97149,9	34,8167	481042	33	277180	203862	2,3596
12	14 692		59140,1	220856,1	3,1	4681,3	89215,4	34,1039	502569	34	279996	222572	2,2580
13	14 619		62097,1	220856,1	3,5	4234,5	81961,5	33,5242	525058	36	282953	242105	2,1687
14	14 546		65202,0	220856,1	3,8	3830,3	75328,0	33,0484	548555	38	286058	262497	2,0898
15	14 473		68462,1	220856,1	4,2	3464,7	69260,5	32,6551	573103	40	289318	283784	2,0195
16	14 400		71885,2	0,0	4,6	3134,0	15644,3	31,9214	598749	42	71885	526864	1,1364
17	14 328		75479,4	0,0	5,1	2834,8	14933,2	31,2969	625543	44	75479	550064	1,1372
18	14 257		79253,4	0,0	5,6	2564,2	14254,4	30,7628	653536	46	79253	574283	1,1380
19	14 185		83216,1	0,0	6,1	2319,4	13606,5	30,3040	682782	48	83216	599566	1,1388
20	14 115		87376,9	0,0	6,7	2098,0	12988,0	29,9087	713336	51	87377	700348	1,0185
21	14 044		91745,7	0,0	7,4	1897,8	12397,7	29,5671	745258	53	91746	732860	1,0169
22	13 974		96333,0	0,0	8,1	1716,6	11834,1	29,2713	778608	56	96333	766774	1,0154
23	13 904		101149,7	0,0	9,0	1552,8	11296,2	29,0148	813451	59	101150	802155	1,0141
24	13 834		106207,1	0,0	9,8	1404,5	10782,7	28,7921	849853	61	106207	839070	1,0129
25	13 765		111517,5	0,0	10,8	1270,5	10292,6	28,5985	887884	65	111518	877591	1,0117
26	13 696		117093,4	0,0	11,9	1149,2	9824,8	28,4303	927617	68	117093	917792	
27	13 628		122948,1	0,0	13,1	1039,5	9378,2	28,2841	969128	71	122948	959749	
28	13 560		129095,5	0,0	14,4	940,3	8951,9	28,1571	1012496	75	129095	1003544	
29	13 492		135550,2	0,0	15,9	850,5	8545,0	28,0469	1057805	78	135550	1049260	
30	13 425		142327,7	0,0	17,4	769,3	8156,6	27,9515	1105142	82	142328	1096985	

Tidspunkt (år)	0	1	2	3	4	20	21	25	30
Kontantstrøm	-1 728 900	85 659,1	97 218	109 284	121 881	610 537	638 227	762 104	951 225
Diskonteringssats	10 %								

BEREGNING AV N(NPV)

Netto nåverdi (EXCEL-funksjonen NNV)	660 601

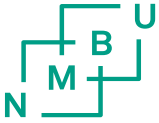

Norwegian University
of Life Sciences

Postboks 5003
NO-1432 Ås, Norway
+47 67 23 00 00
www.nmbu.no